



NTNU – Trondheim
Norwegian University of
Science and Technology

Probabilistic Damage Stability

Maximizing the Attained Index by Analyzing
the Effects of Changes in the Arrangement
for Offshore Vessels

Ole Martin Djupvik

Marine Technology

Submission date: June 2015

Supervisor: Svein Aanond Aanonsen, IMT

Co-supervisor: Bjørn Egil Asbjørnslett, IMT

Norwegian University of Science and Technology
Department of Marine Technology



MASTER THESIS IN MARINE RESOURCES AND AQUACULTURE

SPRING 2015

Probabilistic Damage Stability

Maximizing the attained index by analyzing the effects of changes in the arrangement for offshore vessels

Background

Naval Architects are in most cases prone to time pressure when designing a vessel. Design companies are working on the so called “no cure, no pay” agreements, which entails them to run many projects simultaneously. Designing a vessel is complicated and it is difficult to comprehend the results for stability calculations beforehand. Stability regulations are one of the factors that determines how the vessels are designed, and the calculations are time demanding. Naval Architects wants to do few iterations in the design process to save time. In order to cut down on the iterations, the ship designer has to rely on previous experience in the early stages of the design process, to know whether the vessel will fulfill the damage stability regulations. If the designer could know how the placement of certain bulkheads affects the attained index, it would limit the amount of iterations in the design process.

Probabilistic damage stability calculations requires details in order to calculate whether a ship fulfills the requirements. In general, ship designers follow a top-down based design approach, meaning they start off with the main dimensions and the design gets more detailed further on in the process. The damage stability calculations are done at a late stage of the design process and that's when the designer can confirm if the ship has sufficient stability to fulfill the damage stability regulations. As almost every vessel is different, small modifications of the arrangement can impact the attained index for offshore vessels. In order to minimize iterations in the design process, it is helpful for designers to know more about how the damage stability properties of a ship varies according to internal watertight arrangement. When designing according to the deterministic damage stability regulations, the damage extents are defining where to place certain bulkheads. Since there are no damage extents in the probabilistic damage stability requirements, it leaves more freedom for the designer when placing bulkheads, but how can the designers take advantage of this freedom?

Primary objective

The longitudinal wing tank bulkhead in the mid-ship section of a vessel is a bulkhead that applies for all offshore vessels. Placing this bulkhead at the correct distance from the hull, in regards to maximizing the attained index, has been a subject of discussion in Wärtsilä Ship Design. Is it possible to maximize the attained index by moving the longitudinal wing tank bulkhead? How will the attained index change when the longitudinal bulkhead is moved and will the attained index change equally for different ship sizes? Introducing U-tanks is common practice to maximize the attained index, but how much will it influence the final attained index?



Scope of work and main activities

- Learn how to use NAPA to calculate PDS for different bulkhead placements
- Do PDS calculations on four different ships with multiple variations of bulkhead placement
- Review ways to analyze damage cases in order to explain how different changes will affect the total attained index
- Analyze the results and explain why the index changes according to the changes in the arrangement as well as the movement of the longitudinal bulkhead.
- Document each step in the process

Modus operandi

The thesis will not use any kind of optimization software, as these tools are expensive and requires the user to be familiar with computer programming. The thesis is going to analyze how the attained index changes when the transverse position of the longitudinal wing tank bulkhead is changed. In order to find out if the attained index changes proportionally for different ship sizes, the study will determine if there is a correlation between the placement of the longitudinal bulkhead and the attained index for four different vessel sizes. To reveal how the attained index develops for different arrangement configurations, the four vessels will have two different arrangements. One arrangement with U-tanks and one with longitudinal bulkheads in the double bottom with normal wing tanks. Since it is common practice to include U-tanks to maximize the attained index, the report will also find out how much the attained index increases when U-tanks are introduced. Wärtsilä Ship Design will supply me with the needed software to run the calculations as well as guidance on how to model the ships in order to minimize uncertainties. I will follow the guidelines given by NTNU and submit the report at the time agreed upon with my supervisor.

Wärtsilä Ship Design contact: Ketil Fykse

Primary supervisor:

Svein Aanond Aanonsen

Secondary supervisor:

Bjørn Egil Asbjørnslett

Preface

This dissertation is the master thesis in my 10th semester of MSc in Naval Architecture. The work has been carried out in the spring of 2015 as the mandatory part of the Master of Science program at the Norwegian University of Science and Technology (NTNU). The thesis intends to give Naval Architects insight in how the attained index is affected by changes in the arrangement for offshore vessels.

The dissertation has been written by one author, Ole Martin Djupvik, fifth year student of Marin Technology, NTNU. I would like to thank my primary supervisor Svein Aa. Aanonsen and my secondary supervisor Professor Asbjørnslett for their guidance, feedback and support. I would also like to thank Inge Skaar and Ketil Fykse at Wärtsilä Ship Design, for their proposal of the subject of the thesis and their guidance throughout the writing process. Vedran Vickovic at Wärtsilä Ship Design, for his guidance when designing the vessels in AutoCAD. Ulf Ottesen at Wärtsilä Ship Design, for his help with modeling the hulls in NAPA. Dino Ivkovic at Wärtsilä Ship Design and Olli Puustinen at NAPA help desk, for valuable assistance with questions related to NAPA. Odd Olufsen, Gunnar Hjort and Inge Seglem at DNV GL for their help with interpreting the SOLAS requirements. I also acknowledge the help from Sigurd Underhaug at Wärtsilä Ship Design who arranged with the computer and software needed for writing the thesis.

It should be noted to the reader that the references are done in a different style for some of the paragraphs where only one source is used. In these cases, the reference will appear after the final period at the end of the paragraph, as opposed to referencing every sentence with the same reference. This was done to increase the readability of the thesis.

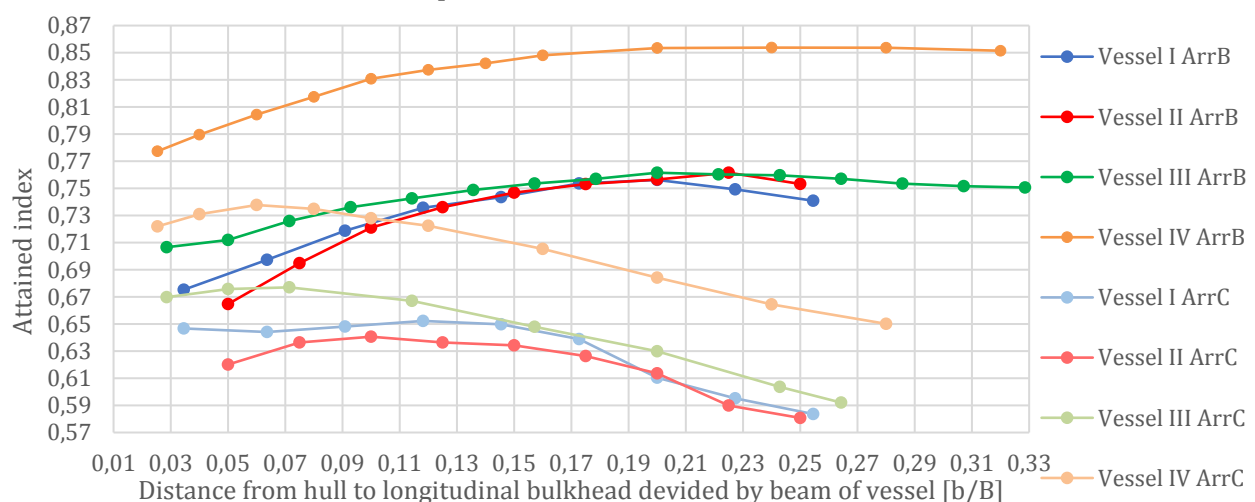

Ole Martin Djupvik, 09.06.15

Abstract

Probabilistic damage stability calculations are time demanding and are conducted at a late stage of the design process. A detailed arrangement is required to calculate whether a ship fulfills the requirements. To minimize the amount of iterations in the design process Naval Architects have to know how the attained index is affected by the watertight arrangement. The longitudinal wing tank bulkhead in the mid-ship section of a vessel, is a bulkhead that applies for all offshore vessels. The placement of this bulkhead, in regards to maximizing the attained index, has been a subject of discussion in Wärtsilä Ship Design. The objective of this dissertation has been to analyze how the attained index is affected by the transverse position of the longitudinal wing tank bulkhead. This information can be used to maximize the attained index for offshore vessels. To find out if the attained index changes proportionally for different ship sizes, the study determines if there is a correlation between the placement of the bulkhead and the attained index for four different vessel sizes.

To reveal how the attained index develops for different arrangement configurations, the four vessels had two different arrangements. One arrangement had U-tanks, arrangement B, and the other arrangement had two longitudinal bulkheads in the double bottom without U-tanks, arrangement C. Since it is common practice to include U-tanks to maximize the attained index, the report also studies how much the attained index increases when U-tanks are introduced.

The results of the attained index for the four vessels with different placements of the longitudinal wing tank bulkhead, can be seen in the graph below. There is not a correlation of the attained index and the placement of the longitudinal bulkhead, for all vessels with different arrangement configurations. It was therefore not possible to develop a formula for the optimal placement of the bulkhead that applies for all vessel types and sizes. By analyzing the development of the attained index, as the longitudinal bulkhead was relocated, we found out which parameters that affected the attained index.

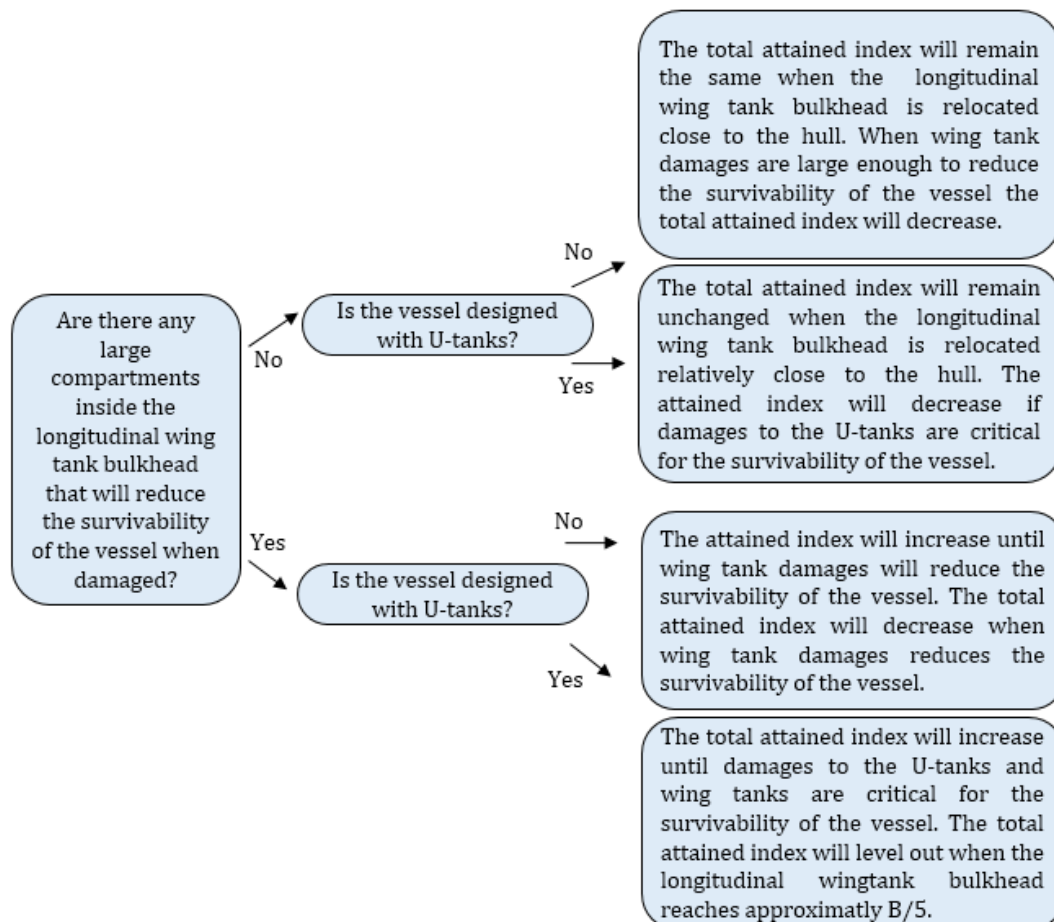


As seen from the results, the attained index increases as the longitudinal bulkhead is moved towards the centerline for all vessels with U-tank arrangement. The development of the total attained index levels out when U-tank damages are critical for the survivability of the vessel.

For vessels without U-tanks the development of the total attained index did not correspond for all vessels. The attained indexes increases for Vessel II, III and IV until damages to the wing tanks are critical for the survivability of these vessels. The common denominator for all vessels with U-tanks are that the total attained index decreases when damages to the wing tanks are critical for the survivability of the vessels.

The total attained index for the two arrangement with and without U-tanks were compared. It was found that the effect of introducing wing tanks is approximately 7%, when the longitudinal wing tank bulkhead is placed at B/20. The effect of introducing U-tanks increases as the distance between the hull and the longitudinal wing tank bulkhead increases.

Is it possible to maximize the attained index by evaluating the placement of the longitudinal bulkhead? The effect of changing the position of the bulkhead changes according to the arrangement configuration. As different vessel types have different arrangement configurations it is difficult to predict the effect of relocating the longitudinal bulkhead. The flowchart below can be used by designers as a tool to help them maximize the attained index when placing the longitudinal wing tank bulkhead.



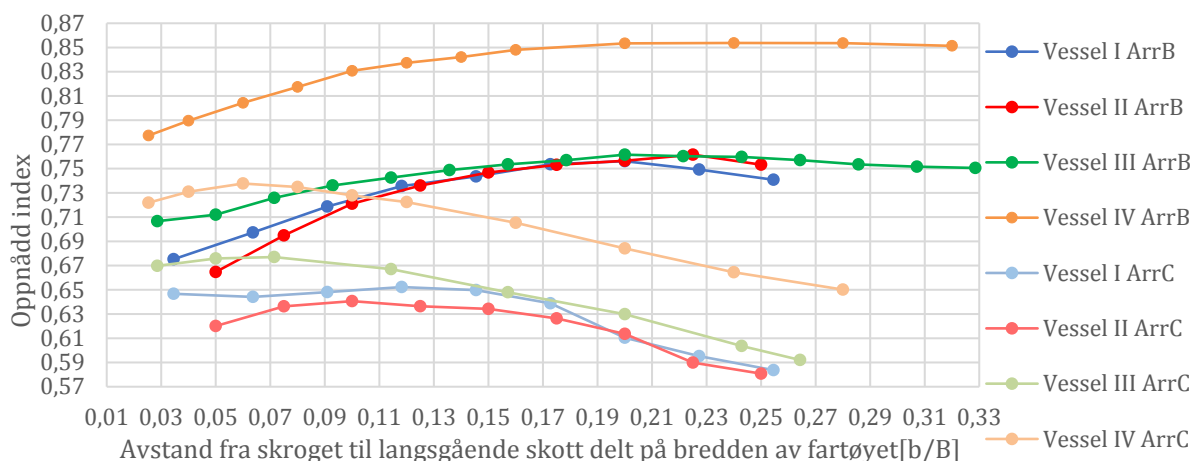
Sammendrag

Probabilistisk skadestabilitetsberegninger er tidskrevende og gjennomføres på et sent stadium i designprosessen. Detaljerte arrangements tegninger er nødvendig for å beregne om et skip oppfyller kravene for skadestabilitet. For å minimere antallet iterasjoner i designprosessen, må skipsdesignere vite hvordan den oppnådde indeksen blir påvirket av den vanntette inndelingen i arrangementet.

De langsgående vingtankskottene i midtskipet i et fartøy, er skott som er vanlige å se i offshorefartøy. Å finne den beste plasseringen av dette skottet, med tanke på å maksimere den oppnådde indeksen, har blitt diskutert i Wärtsilä Ship Design. Formålet med denne avhandlingen har vært å analysere hvordan den oppnådde indeksen påvirkes av plasseringen av det langsgående vingtankskottet. Denne informasjonen kan brukes til å maksimere den oppnådde indeksen for offshorefartøy. For å finne ut om den oppnådde indeksen endres proporsjonalt for forskjellige skipsstørrelser, vil studiet undersøke om det er en sammenheng mellom plassering av skottet og den oppnådde indeksen for fire forskjellige skipsstørrelser.

For å se hvordan den oppnådde indeksen utvikler seg for ulike arrangement konfigurasjoner, hadde de fire fartøyene to forskjellige arrangement. Det ene arrangementer hadde U-tanker, arrangement B, og det andre hadde to langskipsskott i dobbeltbunnen uten U-tanker, arrangement C. Siden det er vanlig praksis å designe U-tanker for å maksimere den oppnådde indeksen, undersøker studiet i tillegg hvor mye den oppnådde indeksen øker ved å tegne inn U-tanker.

Resultatene av den oppnådde indeksen for de fire fartøy, med forskjellige plasseringer av de langsgående vingtankskottene, kan sees i grafen nedenfor. Det var ikke en korrelasjon av den oppnådde indeksen og plassering av det langsgående skott, for alle fartøyer med alle arrangement konfigurasjoner. Det var derfor ikke mulig å utvikle en formel for optimal plassering av skottet som gjelder for alle skipstyper og størrelser. Ved å undersøke utviklingen av den oppnådd indeksen, når det langsgående skottet ble flyttet, har vi funnet ut hvilke parametere som påvirket den oppnådde indeksen.



Som det fremgår av resultatene, økte den oppnådde indeksen når det langsgående skottet ble flyttet mot senterlinjen for alle fartøy med U-tank arrangement. Utviklingen av den oppnådde indeksen flatet ut når U-tank skader ble kritiske for overlevelsessevnen til fartøyet. For fartøy uten U-tanker utviklet ikke den oppnådde indeksen seg i samsvarer for alle skipene. Den oppnådde indeksen økte for fartøy II, III og IV helt til skader på vingtankene ble kritiske for overlevelsessevnen til disse fartøyene. Fellesnevneren for alle fartøy med U-tanker er at den oppnådde indeksen synker når skader på vingtankene blir avgjørende for overlevelsessevnen til skipene.

Den oppnådde indeksen for to arrangement, med og uten U-tanker, ble sammenlignet. Det ble funnet at effekten av å designe U-tanker øker den oppnådde indeksen men minimum 5%, når de langsgående vingtankskottene er plassert på B/20. Virkningen av å designe U-tanker øker etter hvert som avstanden mellom skroget og de langsgående vingtankskottene øker.

Er det mulig å maksimere den oppnådde indeksen ved å evaluere plassering av det langsgående vingtankskottet? Effekten av å endre posisjon på vingtankskottet er forskjellig for forskjellige arrangement konfigurasjoner. Siden ulike skipstyper har ulike arrangement konfigurasjoner, er det vanskelig å forutsi effekten av å flytte på vingtankskottet. Flyttdiagrammet nedenfor kan brukes av designere som et verktøy for å hjelpe dem å maksimere den oppnådde indeksen når de plasserer de langsgående vingtankskottene.

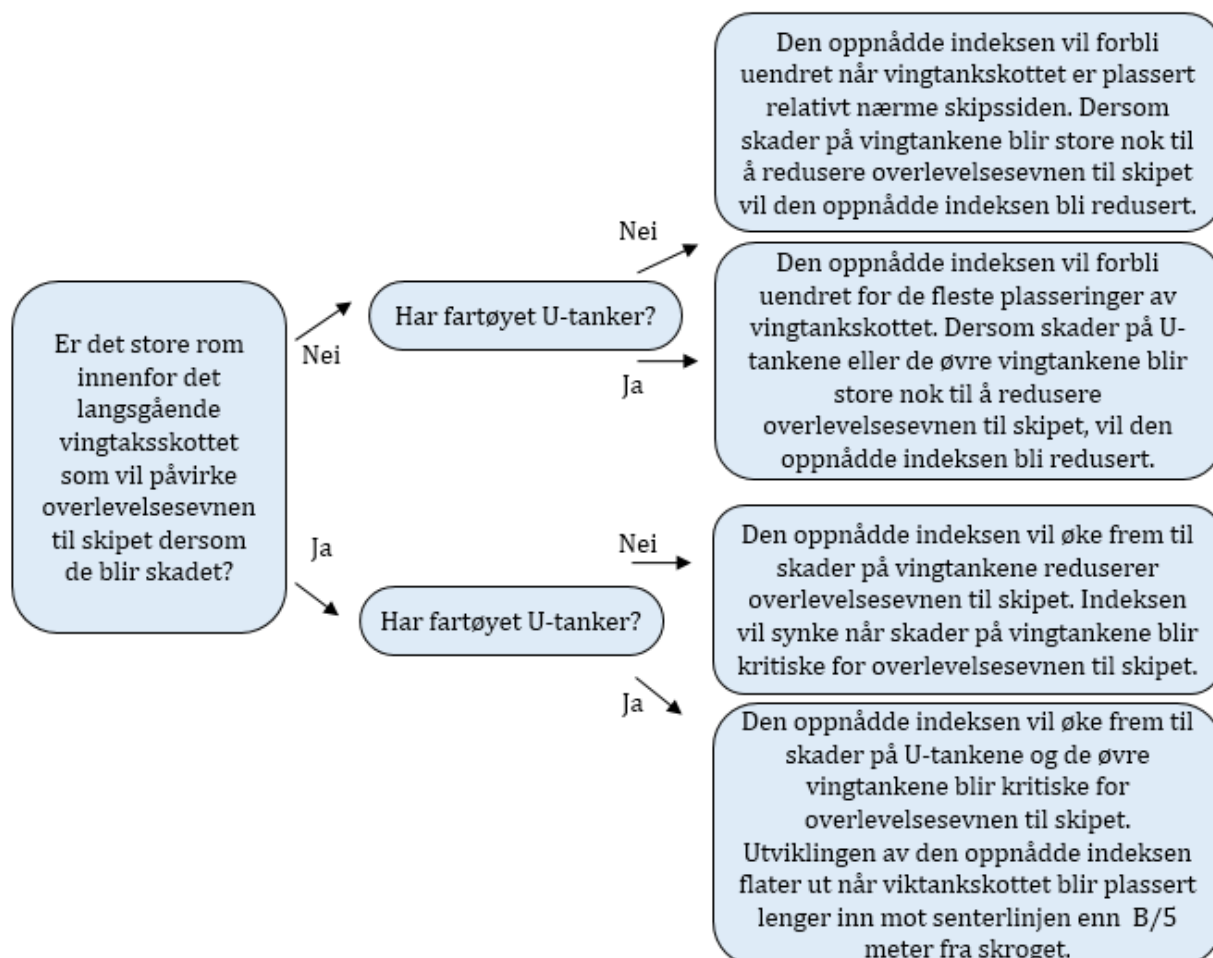


Table of Contents

Preface	i
Abstract	ii
1 Introduction	1
1.1 Background and motivation	1
1.2 Previous work	2
1.3 Objective	4
1.4 Chapter overview	5
2 Theory of damage stability	6
2.1 Deterministic Damage Stability	6
2.1.1 The Deterministic damage stability method - DDS	6
2.2 Probabilistic damage stability - PDS	9
2.2.1 Required index R - Regulation 6	9
2.2.2 Attained index A – Regulation 7	11
2.2.3 P_i - factor – Regulation 7.1	12
2.2.4 S_i -factor – Regulation 7.2	19
2.2.5 V_i -factor – Regulation 7.2	22
3 Method	24
3.1 Designing the vessels	24
3.1.1 Hull shape	26
3.1.2 Stability	28
3.1.3 Superstructure	29
3.1.4 Arrangement	29
3.2 NAPA stability software	34
3.2.1 Using Probabilistic manager to calculate PDS	34
3.2.2 Ways to analyze the results in NAPA	36
3.2.3 Measures to minimize runtime in NAPA	40
4 Results	41
4.1 Total attained index for the different vessels	41
4.1.1 Vessel I	42
4.1.2 Vessel II	44

4.1.3 Vessel III	46
4.1.4 Vessel IV.....	48
5 Discussion.....	50
5.1 The attained index for the different vessels.....	50
5.1.1 The development of the attained index	50
5.1.2 Comparing A_{Total} for arrangements with and without U-tanks.....	65
5.1.3 Comparing A_{Total} for vessels with the same GM values	67
5.2 The attained index for different loading conditions	69
6 Conclusion.....	75
6.1 Limitations.....	75
6.1.1 Stability	76
6.1.2 Arrangement.....	76
6.2 Contributions.....	79
6.3 Further work.....	82
6.3.1 Limit uncertainties of results for vessels in the study.....	82
6.3.2 New aspects that could be analyzed on the existing vessels	83
6.3.3 Studying one vessel type	84
7 Bibliography.....	85
Appendix A.....	I
General arrangement Vessel I.....	I
General arrangement Vessel II	V
General arrangement Vessel III.....	X
General arrangement Vessel IV.....	XV
Appendix B.....	XX
S-factor diagrams	XX
Appendix C.....	XXXV
Electronic files.....	XXXV

Table of Figures

Figure 1-1: Cross section of arrangement with U-tanks4

Figure 1-2: Cross section of arrangement with longitudinal bulkhead in double bottom.....4

Figure 2-1: Ship length as stated in Load line convention, 19667

Figure 2-2: Deterministic requirements8

Figure 2-3: Subdivision length for probabilistic damage stability 10

Figure 2-4: Damage length vs Ship length..... 13

Figure 2-5: Non-dimensional damage length 13

Figure 2-6: 1. Damage condition, seen from above 15

Figure 2-7: 2. Damage condition, seen from above 16

Figure 2-8: 3. Damage condition, seen from above 16

Figure 2-9: Distribution of non-dimensional penetration damages..... 17

Figure 2-10: Density distribution line for non-dimensional penetration damages..... 17

Figure 2-11: Example of GZ-curve 20

Figure 2-12: GZ-curve for submerged opening..... 20

Figure 2-13: Explanation of H_m measures for zone 3 22

Figure 2-14: Vertical damage distribution..... 23

Figure 3-1: Profile view of Vessel I..... 25

Figure 3-2: Plan view of 2nd deck, Vessel I 25

Figure 3-3: Double bottom Vessel I, arrangement B 25

Figure 3-4: Double bottom Vessel I, arrangement C..... 25

Figure 3-5: Hull shapes, Vessel I and II..... 26

Figure 3-6: Hull shapes, Vessel III and IV 27

Figure 3-7: Comparison of hull for Vessel IV and reference vessel..... 27

Figure 3-8: Typical mid-ship arrangement of PSV's (WSD's portfolio) 30

Figure 3-9: Typical mid-ship arrangement of OCV's (WSD's portfolio)..... 30

Figure 3-10: Placement of collision bulkhead 31

Figure 3-11: Profile view of tank top in the stern of Vessel I..... 32

Figure 3-12: Cross section view of knuckled tank top (not used for any vessels in the study) 32

Figure 3-13: Probabilistic manager 35

Figure 3-14: S-factor diagram..... 36

Figure 3-15: One zone damage case from Figure 3-14..... 37

Figure 3-16: P1S diagram for Vessel II, arrangement C 38

Figure 3-17: 2-zone damage potential diagram, Vessel II, arr. C, LBH3 at 0.05*B m from hull..... 39

Figure 4-1: Vessel I, arrangement B..... 42

Figure 4-2: Vessel I, arrangement C 43

Figure 4-3: Vessel II, arrangement B 44

Figure 4-4: Vessel II, arrangement C 45

Figure 4-5: Longitudinal machinery room division, Vessel III 46

Figure 4-6: Vessel III, arrangement B..... 47

Figure 4-7: Vessel III, arrangement C..... 47

Figure 4-8: Vessel IV, arrangement B..... 48

Figure 4-9: Vessel IV, arrangement C 49

Figure 5-1: Vessels with U-tank configuration, arrangement B	51
Figure 5-2: S-fac diagram for Vessel I, arrangement B, D_p , LBH3 at $0.06*B$ meters from the hull	52
Figure 5-3: S-fac diagram for Vessel I, arrangement B, D_p , LBH3 at $0.2*B$ meters from the hull...	53
Figure 5-4: Closer view of damage case when LBH3 is at $0.06*B$ from the hull.....	53
Figure 5-5: Closer view of damage case when LBH3 is at $0.2*B$ from the hull	53
Figure 5-6: Illustration of B_k for damage cases when LBH3 remains intact	54
Figure 5-7: Illustration of B_k and B_{k-1} for damage cases when LBH3 is penetrated.....	54
Figure 5-8: P_i -factor for different damages with different placements of LBH3.....	55
Figure 5-9: S-fac diagram, Vessel IV, arrangement B, D_p , with LBH3 at $0.06*B$ m from the hull ...	56
Figure 5-10: S-fac diagram, Vessel IV, arrangement B, D_p , with LBH3 at $0.14*B$ m from the hull	57
Figure 5-11: Comparison of vessels with arrangement C	58
Figure 5-12: S-factor diagram for Vessel II, D_p , ArrC, LBH3 at $0.05*B$ m from the hull	59
Figure 5-13: S-factor diagram for Vessel II, D_p , ArrC, LBH3 at $0.1*B$ m from the hull	59
Figure 5-14: S-factor diagram for Vessel II, D_p , ArrC, LBH3 at $0.225*B$ m from the centerline.....	59
Figure 5-15: Damage case where LBH3 is at $0.05*B$ meters from the hull	60
Figure 5-16: Damage case where LBH3 is at $0.1*B$ meters from the hull	60
Figure 5-17: Damage case where LBH3 is at $0.225*B$ meters from the hull.....	60
Figure 5-18: Illustration of B_k and B_{k-1} when LBH3 is penetrated for Vessel II, arrangement C....	61
Figure 5-19: S-factor diagram Vessel III, D_1 , Arrangement C, LBH3 at $0.03*B$ m from hull.....	62
Figure 5-20: S-factor diagram Vessel III, D_1 , Arrangement C, LBH3 at $0.07*B$ m from hull.....	63
Figure 5-21: S-factor diagram Vessel III, D_1 , Arrangement C, LBH3 at $0.11*B$ m from hull.....	63
Figure 5-22: S-factor diagram Vessel III, D_1 , Arrangement C, LBH3 at $0.2*B$ from hull.....	63
Figure 5-23: Two zone damages, LBH3 at $0.03*B$ meters from hull	64
Figure 5-24: Two zone damages, LBH3 at $0.07*B$ meters from hull	64
Figure 5-25: Comparing the two arrangement configurations.....	65
Figure 5-26: Percent change between arrangement B and C	66
Figure 5-27: Vessel III with longitudinally divided machinery room.....	67
Figure 5-28: Vessel IV with transversally divided machinery room.....	67
Figure 5-29: S-fac diagram Vessel III, arrangement B, LBH3 at $0.14*B$ m from the centerline.....	68
Figure 5-30: S-fac diagram Vessel IV, arrangement B, LBH3 at $0.14*B$ m from the centeline.....	68
Figure 5-31: S-factor diagram for D_1 condition, Vessel III, arrangement C	69
Figure 5-32: S-factor diagram for D_p condition, Vessel III, arrangement C	70
Figure 5-33: S-factor diagram for D_s condition, Vessel III, arrangement C.....	70
Figure 5-34: S_i -factor for D_s	71
Figure 5-35: S_i -factor for D_1	71
Figure 5-36: S_i -factor for D_p	71
Figure 5-37: GZ-curve for D_s after damage	72
Figure 5-38: GZ-curve for D_1 after damage.....	72
Figure 5-39: GZ-curve for D_p after damage.....	72
Figure 5-40: D_s floating condition.....	73
Figure 5-41: D_p floating condition	73
Figure 5-42: D_1 floating condition	73
Figure 5-43: Floating position for D_1 , D_p and D_s	73
Figure 5-44: Cross section of bow illustrating the flare angle	74

Figure 6-1: U-tank configuration, arrangement B 77
 Figure 6-2: Longitudinally divided double bottom with no U-tanks, arrangement C..... 77
 Figure 6-3: Flowchart to maximizing the attained index for offshore vessels..... 81

Table of Tables

Table 2-1: Typical requirements for Type A, Ship carrying liquid cargo in bulk..... 8
 Table 2-2: Non-dimensional damage lengths 14
 Table 3-1: Main dimensions 24
 Table 3-2: Vessel draughts..... 28
 Table 3-3: GM values for the vessels 29
 Table 3-4: Distance between transversal bulkheads 33
 Table 3-5: Color chart for S-factor diagram 37
 Table 4-1: General information, Vessel I 42
 Table 4-2: General information, Vessel II..... 44
 Table 4-3: General information, Vessel III 46
 Table 4-4: General information, Vessel IV..... 48
 Table 5-1: Results for damage cases in figures above 53
 Table 5-2: Results for damage cases with the red circle in Figure 5-9 and Figure 5-10... 56
 Table 5-3: Results for damage case 15.2.2-1..... 71
 Table 6-1: Comparison of vessels with and without passengers..... 76

Table of Equations

Eq. 1	7
Eq. 2	7
Eq. 3	9
Eq. 4	9
Eq. 5	9
Eq. 6	10
Eq. 7	11
Eq. 8	11
Eq. 9	12
Eq. 10.....	13
Eq. 11.....	13
Eq. 12.....	15
Eq. 13.....	16
Eq. 14.....	16
Eq. 15.....	17
Eq. 16.....	19
Eq. 17	19
Eq. 18.....	20
Eq. 19.....	20
Eq. 20.....	22
Eq. 21.....	33
Eq. 22.....	72

Table of symbols

<i>A</i>	<i>Projected wind area</i>
<i>A</i>	<i>Attained Index</i>
<i>b</i>	<i>Mean transverse distance from shell to longitudinal barrier</i>
<i>B</i>	<i>Ship beam</i>
<i>D</i>	<i>Depth moulded</i>
<i>D_l</i>	<i>Lightest service draught</i>
<i>D_p</i>	<i>Partial subdivision draught</i>
<i>D_s</i>	<i>Deepest subdivision draught</i>
<i>J</i>	<i>Non dimensional damage length</i>
<i>Jk</i>	<i>knuckle point on the red curve</i>
<i>k</i>	<i>Number of particular longitudinal bulkhead as barrier for transverse penetration</i>
<i>Kg</i>	<i>Kilo gram</i>
<i>l</i>	<i>Non dimensioning damage location</i>
<i>MS</i>	<i>Residual stability</i>
<i>M</i>	<i>Momentum</i>
<i>m</i>	<i>Meter</i>
<i>mm</i>	<i>Millimeter</i>
<i>N1</i>	<i>Number of persons whom lifeboats are provided</i>
<i>N2</i>	<i>Number of persons the ship is permitted in excess of N1</i>
<i>P_i</i>	<i>Probability of damage</i>
<i>θ_e</i>	<i>Equilibrium heeling angle after damage</i>
<i>θ_{max}</i>	<i>Maximum heeling angle</i>
<i>θ_{min}</i>	<i>Minimum heeling angle</i>
<i>R</i>	<i>Required index</i>
<i>r</i>	<i>Factor to account for the transversal extent of the damage</i>
<i>R_o</i>	<i>Value of R calculated for cargo vessels larger than 100 meters</i>
<i>S_i</i>	<i>Survivability</i>
<i>T</i>	<i>Ship draught</i>
<i>V_i</i>	<i>Probability for the compartments above the horizontal divisions to stay intact</i>
<i>x</i>	<i>non-dimensional damage length</i>
<i>x1</i>	<i>Distance from aft end of ship to the aft end of zone</i>
<i>x2</i>	<i>Distance from aft end of ship to the forward end of zone</i>
<i>Z</i>	<i>Distance from center of projected wind area to T/2</i>

Table of acronyms

<i>AHTS</i>	<i>Anchor handler Tug supply</i>
<i>Arr.</i>	<i>Arrangement</i>
<i>Ch.</i>	<i>Chapter</i>
<i>CL</i>	<i>centerline</i>
<i>Dk.</i>	<i>Deck</i>
<i>Eq.</i>	<i>Equation</i>
<i>GA</i>	<i>General arrangement</i>
<i>HARDER</i>	<i>Harmonization of rules and design rationale</i>
<i>IMO</i>	<i>International maritime organization</i>
<i>LBH</i>	<i>Longitudinal bulkhead</i>
<i>LBH3</i>	<i>Longitudinal bulkhead number 3, used to address the specific bulkhead used in the study</i>
<i>Loa</i>	<i>Length over all</i>
<i>Lpp</i>	<i>Length between perpendiculars</i>
<i>Ls</i>	<i>Ship length for deterministic regulations</i>
<i>Ls</i>	<i>Subdivision length for probabilistic damage stability requirements</i>
<i>LWTB</i>	<i>Longitudinal wing tank bulkhead</i>
<i>MSC</i>	<i>Maritime safety committee</i>
<i>OCV</i>	<i>Offshore construction vessel</i>
<i>pdf</i>	<i>Probability density function</i>
<i>PDS</i>	<i>Probabilistic damage stability</i>
<i>PhD</i>	<i>Doctor of philosophy</i>
<i>PSV</i>	<i>Platform supply vessel</i>
<i>Reg.</i>	<i>Regulation</i>
<i>SOLAS</i>	<i>Safety of Life at Sea</i>
<i>SPS</i>	<i>Special purpose ship</i>
<i>Ttop</i>	<i>Tank top</i>
<i>WSD</i>	<i>Wärtsilä Ship Design</i>

This page is intentionally left blank

1 Introduction

Naval Architects are in most cases prone to time pressure when designing a vessel. Design companies are working with the so called “no cure, no pay” agreements, which forces them to run many projects simultaneously. Designing a vessel is complicated and it is difficult to predict the results for stability calculations beforehand. Stability regulations are one of the factors that determines how the vessels are designed, and the calculations are time demanding. Naval Architects wants to do few iterations in the design process to save time. In order to cut down on the iterations, ship designers has to rely on previous experience in the early stages of the design process. To minimize the amount of iterations in the design process, designers needs to know how the damage stability properties of a ship varies according to the internal watertight arrangement.

1.1 Background and motivation

Passenger vessels have had to fulfill the probabilistic damage stability requirements since the early 70's, after IMO Resolution A.265(VIII) came into effect. The concept was further considered and IMO made the new probabilistic regulations applicable for all dry cargo ships built after 1992. Thereafter a harmonization process, called HARDER, was started in 2003 where the aim was to harmonize the damage stability regulations for all ship types. After some delays due to the applicability of the harmonized regulations for large passenger ships, IMO concluded that all dry cargo and passenger vessels constructed after January 1, 2009 has to comply with the probabilistic damage stability criteria's listed in SOLAS Chapter II-1, Part B-1. (Papanikolaou & Eliopoulou, 2007)

According to SOLAS, Ch. II-1, Part B, Reg. 4, vessel types that complies with other instruments covering damage stability regulations, are excluded from the application of probabilistic damage stability regulations. Resolution MSC.235(82) covers damage stability for platform supply vessels using the deterministic approach. Platform supply vessels are therefore not obligated to follow probabilistic damage stability regulations, unless the ship owner requests the special purpose ship (SPS) notation.

If a ship has the SPS notation, it can carry more than 12 special personnel without having to be treated as a passenger vessel, with regards to safety requirements. Special personnel are persons who are needed for special operations, such as welding pipelines, which is not connected to the normal ship operations. They are expected to have received safety drills and procedures and have a fair knowledge about the layout of the vessel. The damage stability approach for SPS vessels are the same as for passenger vessels, probabilistic damage stability. But the required safety is lower for SPS vessels, depending on the certified number of personnel. (IMO, 2008c)

When designing vessels according to the deterministic damage stability regulations, the damage extents are defining where to place certain bulkheads. Since there are no damage extents in the probabilistic damage stability requirements, it leaves more flexibility for the

designer when placing bulkheads, but how can the designers take advantage of this flexibility?

Probabilistic damage stability calculations requires a detailed general arrangement in order to calculate whether a ship fulfills the requirements. In general, ship designers follow a top-down based design approach, meaning they start off with the main dimensions and the design gets more detailed as bulkheads and equipment are included later in the design process. The damage stability calculations are done at a late stage of the design process and that's when the designer can confirm if the ship has sufficient stability to fulfill the damage stability regulations. Almost every offshore vessel is different and small modifications to the arrangement can impact the attained index. If the designer could know how the placement of certain bulkheads affects the attained index, it would limit the amount of iterations in the design process.

1.2 Previous work

The regulations regarding probabilistic damage stability are very complicated, and it is time demanding to fully understand how the calculations are conducted. The effects of changes in the arrangement are not easy to comprehend, due to the multiple factors that impacts the results. Since the probabilistic damage stability requirements are relatively new for offshore vessels, there are limited research on how changes in the arrangement affects the attained index for these vessel types.

Probabilistic damage stability has not been a major part of the curriculum at NTNU until 2014, and there has only been one master thesis written about the topic at NTNU since 2002. Most available research on how changes in the arrangement affects the damage stability capabilities of a vessel are related to Ro-Ro or passenger ships. These approaches are utilizing computer software to find the best subdivision to maximize the attained index. This could be connected to the fact that these vessel types have been subject to probabilistic damage stability requirements for many years.

Multiple papers have been published on optimization of subdivision to maximize the attained index. In July 2004, a paper was published by Boulougouris, Papanikolaou and Zaraphonitis about optimizing the arrangement of Ro-Ro Passengers ships using genetic algorithms. This study uses genetic algorithms, where the attained subdivision index, lane meters and steel weight is the object functions. The drawback of using this procedure is the computational time and that the calculations are required to converge to an optimal solution. The input variables in the arrangement was ship depth, minimum double bottom margin and number of bulkheads in front of the machinery room. By using genetic algorithms, the computer programs optimizes the internal arrangement of the vessel and finds an optimal subdivision. The case studies performed, showed that the optimization method could be used for realistic design problems. (Evangelos K., Apostolos D., & Zaraphonitis, 2004)

In 2003 Erik Sonne Ravn wrote a PhD thesis regarding optimization of the subdivision of Ro-Ro vessels. The objective was to maximize the attained index and deck area and minimize the light ship weight, which is known as a multi-objective optimization problem. Mr. Ravn used genetic algorithms to optimize the subdivision. Since the computations are time demanding, he looked into several ways of simplifying the calculations for the attained index. He found that it is possible to optimize the subdivision based on simplified subdivision models to calculate the attained index. He concluded that the most important parameters in the calculation of the attained index was the position of KG, position of Ro-Ro decks, existence of side casings and number of transversal bulkheads. He also found that the position of the double bottom was fairly insignificant for the attained index. (Ravn, 2003)

An article about reducing the uncertainty in subdivision optimization was published in the Journal of Shipping and Ocean Engineering 2 in 2012. The paper studied the dependency between the bulkhead placement and the attained subdivision index. This was conducted to find the best optimization strategies to reduce the optimization time. The study tried to analyze the topology of the attained index, in order to use this in the optimization. It was found that the topology of the attained index is generally non-convex, multimodal and are highly irregular. The irregularity was found to be reducing as the attained index increased, meaning that it was easier to improve the attained index if the initial index was high. The study concluded that using genetic algorithms and other heuristics should be used for optimizing the subdivision. (Puisa, Tsakalakis, & Vassalos, 2012)

The previous work presented in this subchapter mainly focuses on optimization techniques and how they can best be utilized to achieve realistic results. As passenger and Ro-Ro vessels are very different compared to offshore vessels, when it comes to the internal subdivision, the existing available research is of limited use when designing offshore vessels. As there is limited information available for Naval Architects it would be interesting to find out how changes in the arrangement would impact the damage stability properties for offshore vessels.

1.3 Objective

The longitudinal wing tank bulkhead (LWTB) in the mid-ship section of a vessel is a bulkhead that applies for all offshore vessels. Placing this bulkhead at the correct distance from the hull side, in regards to maximizing the attained index, has been a subject of discussion in Wärtsilä Ship Design. Is it possible to maximize the attained index by moving the LWTB? How will the attained index change when the longitudinal bulkhead is moved and will the attained index change equally for different ship sizes? Introducing U-tanks is common practice to maximize the attained index, but how much will it influence the final attained index?

Scope

The thesis is going to analyze how the attained index changes when the transverse position of the LWTB is changed, using a deterministic approach. The thesis will not use any kind of optimization software, as these tools are expensive and requires the user to be familiar with computer programming. In order to find out if the attained index changes proportionally for different ship sizes, the study will determine if there is a correlation between the placement of the longitudinal bulkhead and the attained index for four different vessel sizes. To reveal how the attained index develops for different arrangement configurations, the four vessels will have two different arrangements. One arrangement will have U-tanks and the other will have longitudinal bulkheads in the double bottom with normal wing tanks, as seen in Figure 1-1 and Figure 1-2. Since it is common practice to include U-tanks to maximize the attained index, the report will also find out how much the attained index increases when U-tanks are introduced.

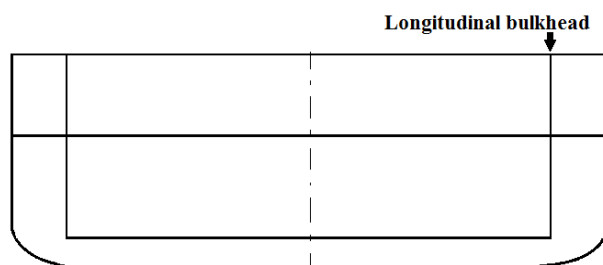


Figure 1-1: Cross section of arrangement with U-tanks

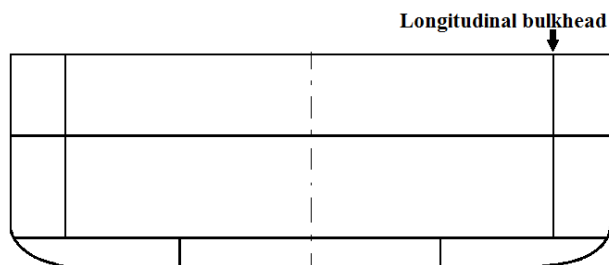


Figure 1-2: Cross section of arrangement with longitudinal bulkhead in double bottom

1.4 Chapter overview

Chapter 2: Theory of damage stability

The second chapter will explain how the regulations regarding probabilistic damage stability should be interpreted. The written material in this chapter is from my project thesis written in fall 2014 as part of another course.

Chapter 3: Method

This chapter describes how the study was conducted. It will explain the dimensions of the different vessels, as well as the reasons for why these vessels were chosen. The chapter also explains how NAPA was used to conduct the calculations.

Chapter 4: Results

Chapter four displays the results for the development of the attained index for the different arrangement configurations. The results are presented for each vessel individually and are briefly discussed.

Chapter 5: Discussion

This chapter discusses the results and compares the results for the different vessels. The development of the attained index for the different placements of the longitudinal bulkhead is analyzed and discussed for the four vessels in the study. The two different arrangement configurations are compared as well as the results for vessels with the same GM values. The development of the attained index for different loading conditions will also be discussed.

Chapter 6: Conclusion

The conclusion will discuss the uncertainties and limitations of the study. The chapter will also include contributions of the study as well as suggestions to further works.

2 Theory of damage stability¹

This chapter will give an introduction to how probabilistic damage stability is calculated. A subchapter regarding deterministic damage stability has been included to show what probabilistic damage stability evolved from. It should be noted that the written material in Chapter 2, is from the project thesis written in, fall 2014.

2.1 Deterministic Damage Stability

In order to understand probabilistic damage stability (PDS) it is important to know what the method evolved from. This chapter will explain the methods of deterministic damage stability (DDS) calculations that used to be the dominating method for damage stability calculations. In general, ship stability is the ability for a ship to return to its initial upright position after an internal or external force has been applied. To know whether a ship will capsize or not, there are two key factors, the moment acting to capsize the vessel and the righting moment. The righting moment is defined by the hull shape and superstructure geometry; whereas the capsizing moment can be wind, sea conditions or water intrusion that acts to tip the ship over. (Amdahl, et al., 2011)

When calculating damage stability it is the intrusion of water that is the dominating factor that affects the stability of the vessel. The principles for calculating damage stability are based on the acting gravity force and change of buoyancy forces. All the compartments under the waterline contribute to the buoyancy of the vessel. When a compartment is bilged, water will fill the volume causing the ship to sink down due to the lost buoyancy. As the underwater volume increases, due to sinking, the buoyancy force will increase accordingly until it equalizes the gravity force. If the damage is on either side of the vessel the ship will heel over due to the unsymmetrical buoyancy, and if the damage is too large compared to the remaining buoyancy of the vessel, the vessel will eventually sink. Regulations regarding damage stability were developed in order to limit the risk of sinking, to ensure the safety of the people on board. (Patterson & Ridley, 2014, ss. 222-270)

2.1.1 The Deterministic damage stability method - DDS

Deterministic damage stability calculation is a method to control if a ship is “safe enough”. The method implies that a ship should survive certain damage scenarios depending on the beam of the vessel as well as the ship length. Calculations are conducted for many different damage conditions and the vessel should fulfill certain criteria's, given by SOLAS, in order to be certified by the classification societies. The requirements are dependent on vessel type, number of passengers, cargo type, etc. The same parameters are used for different ship types, but the magnitude of the parameters will change according to the vessel type, ship length, number of passengers etc. (Patterson & Ridley, 2014, ss. 222-270). At the end of this

¹ Theory chapter was written in project thesis, fall 2014

chapter there are listed some typical parameters that are used when deterministic damage stability calculations are conducted.

Damage extent

When considering different damage scenarios the extent of the damage has to be calculated. Damage extents were constituted in SOLAS Ch. II-1, 1981 Amendments, Reg. 1 to 54, and are still the applied lengths used when calculating deterministic damage stability. The longitudinal damage extent is based on the length of the ship and is calculated in the following way:

$$\text{Damage extent} = 3\text{m} + 3\% * L_s, \text{ or } 11\text{m whichever is the lesser} \quad \text{Eq. 1}$$

L_s =Ship length

The ship length, often referred to as the rule length, is neither L_{pp} nor L_{oa} , but a length that was stated in the International Convention on Load Lines, 1966. The length is given as: “96 per cent of the total length on a waterline at 85 per cent of the least moulded depth measured from the top of the keel, or as the length from the fore side of the stem to the axis of the rudder stock on that waterline, if that be greater.” Figure 2-1 illustrates how the ship length is estimated. L_s is the ship length used in all calculations regarding SOLAS requirements. (IMO, 1966)

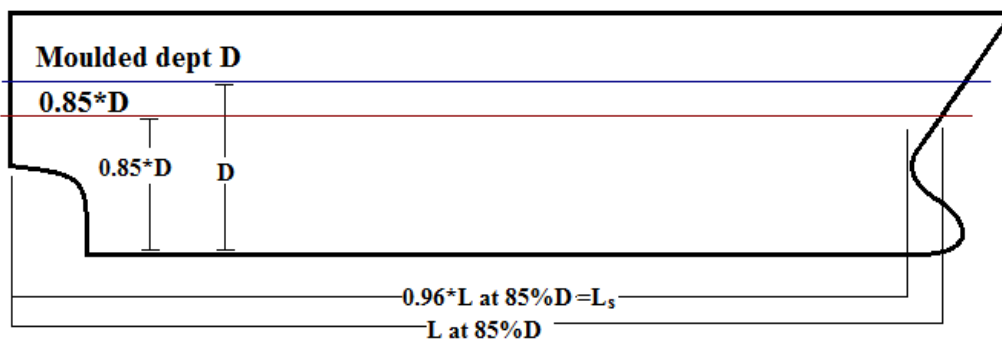


Figure 2-1: Ship length as stated in Load line convention, 1966

The transverse damage extent was constituted in the same amendment as damage extent and is measured from the side of the ship ninety degrees on to the center line from the deepest subdivision load line. (Olufsen & Hjort, 2013)

$$\text{Transverse extent} = \frac{B}{5} \text{ or } 11.5\text{m, whichever is lesser} \quad \text{Eq. 2}$$

B =Ship beam

The vertical extent of the damage is measured from the base line upwards and has no limitations. The damage extents are the first and most critical measures for the designer to take into account when designing a ship that needs to comply with the deterministic damage stability regulations. (Patterson & Ridley, 2014, ss. 265-266)

Calculations

After the damage extents are found these values are used when the damage scenarios are created. The ship is damaged in all possible ways, within the limits of the calculated damage extents, in order to obtain the results from the most critical damage scenario. The ship has to comply with all the regulations given for the ship in all damage scenarios, to be certified by the flag state or one of the classification societies.

Regulations to be fulfilled

There is a large difference, according to the ship type and function, regarding which regulations the ship has to fulfill in order to comply with the international rules. Since it is not the scope of this report to discuss regulations regarding DDS we will not go into details about how the regulations changes according to ship type. Some typical requirements for a Type A vessel can be seen in the table below, to get an overview of the parameters.

Table 2-1: Typical requirements for Type A, Ship carrying liquid cargo in bulk

<i>Requirement parameters</i>	<i>Values for requirements</i>
<i>Minimum GM:</i>	<i>The minimum GM must be at least 0.05meters.</i>
<i>Range of stability:</i>	<i>The range of positive GZ must be at least 20°</i>
<i>Maximum GZ:</i>	<i>The maximum GZ must be at least 0.1 m</i>
<i>Max heel:</i>	<i>Total list must not exceed 15°, but may be 17° if the deck edge is not submerged</i>
<i>Area under GZ</i>	<i>The total area under positive GZ must be at least 0.0175 m Rad</i>

(Patterson & Ridley, 2014, ss. 265-266)

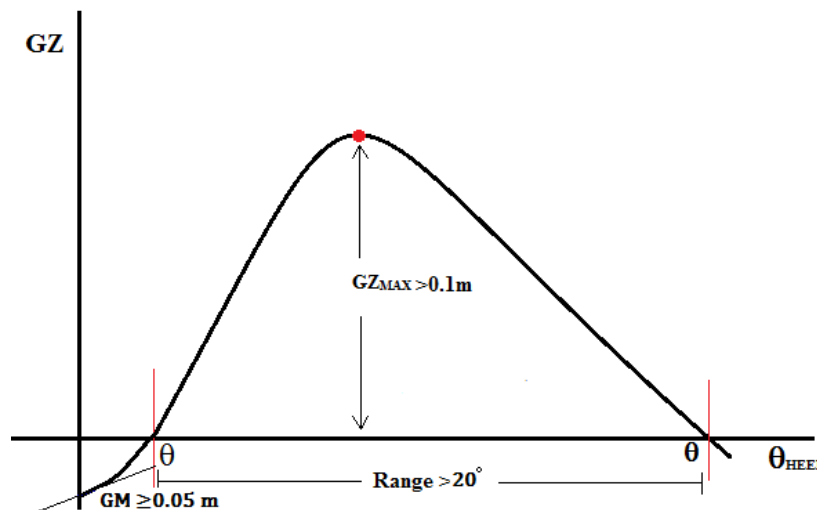


Figure 2-2: Deterministic requirements

2.2 Probabilistic damage stability - PDS

In this chapter we will explain how the PDS method is conducted using the formulas given in the regulations. In the next chapter we will exemplify the method by showing each step of the process when calculating stability on an example ship with simple geometry. As mentioned earlier, PDS bases its calculations on probability of damages and the survivability of the damages. This method of damage stability calculations leaves more freedom for the designer because he is not bound to follow the damage extents known from DDS. In order to comply with the regulations regarding PDS, a calculated attained index, A, needs to be larger than a calculated required index R. We will start by explaining how the required index R is calculated. (Olufsen & Hjort, 2013)

$$A \geq R \quad \text{Eq. 3}$$

2.2.1 Required index R - Regulation 6

The required index R for passenger vessels was established through the work of the HARDER project. Calculations on sample ships were conducted and a formula for the required index was proposed based on the results from the sample ship observations. (Olufsen & Hjort, 2013, s. 28) The formula for R varies according to three categories, passenger ships, cargo ships larger than 100m and cargo ships between 80 and 100m. The deterministic method is applied for cargo ships with a length below 80 meters. For passenger ships, the index varies according to the subdivision length and how many persons the ship is certified for. It should be noted that L_s is different for probabilistic damage stability and deterministic damage stability. The definition of the L_s for probabilistic damage stability can be found later in this subchapter. (IMO, 2006a)

$$R = 1 - \frac{5000}{L_s + 2.5N + 15225} \quad \text{Eq. 4}$$

$$N = N_1 + 2N_2$$

N_1 = Number of persons for whom lifeboats are provided

N_2 = Number of persons the ship is permitted in excess of N_1

L_s = Subdivision length

Cargo ships only includes the ship length when calculating the required index. The required index R for cargo ships larger than 100 meters is calculated using Eq. 5. (IMO, 2006a)

$$R = 1 - \frac{128}{L_s + 152} \quad \text{Eq. 5}$$

L_s = Subdivision length

When calculating R for cargo ships less than 100 meters but greater than 80 m in length, the calculations must be conducted according to Eq. 6. (IMO, 2006a)

$$R = 1 - \left[1 / \left(1 + \frac{L_s}{100} \times \frac{R_0}{1 - R_0} \right) \right] \quad \text{Eq. 6}$$

R_0 = Value for R calculated using Eq. 5

The subdivision length is based on the buoyant hull and the reserve buoyancy of the hull. Figure 2-3 shows how the subdivision length is found for different ship variations.

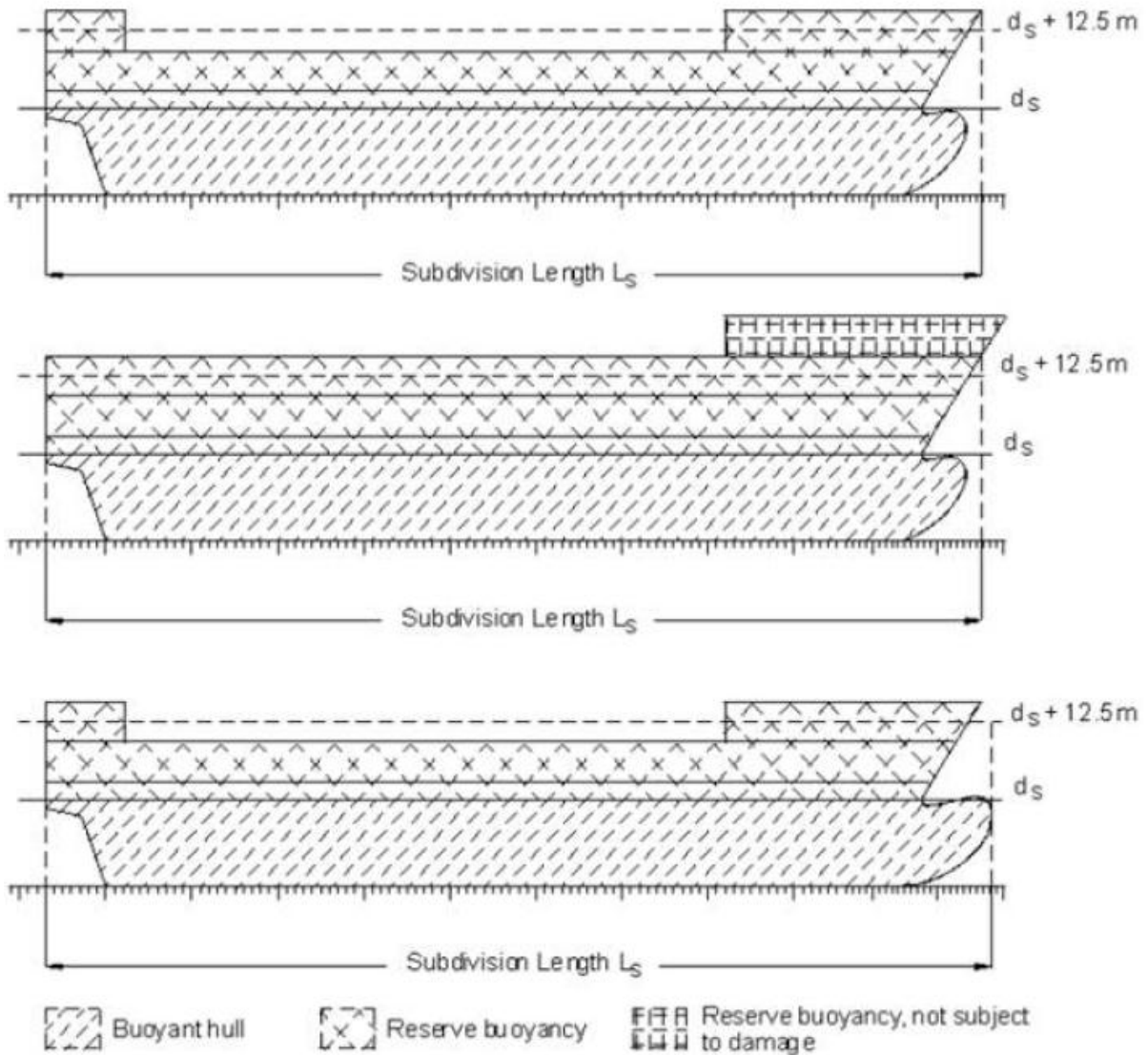


Figure 2-3: Subdivision length for probabilistic damage stability

(IMO, 2008a)

2.2.2 Attained index A – Regulation 7

The attained index A is calculated for multiple damages, depending on the geometric complexity of the vessel. Calculating the attained index is the basis of PDS, and requires knowledge about the ship notations and which formulas to apply for the different ship types. As seen in Eq. 7, A equals the sum of the survivability for the damage, multiplied with the probability for the damage, times the probability that the space above the horizontal subdivisions will remain intact. (IMO, 2006a)

$$A_c = \sum_{i=1}^{i=t} P_i S_i V_i \quad \text{Eq. 7}$$

A_c = Attained index for particular loading condition

i = Damage or damage zone under consideration

t = Number of damages that has to be investigated

P = Probability for damage

S = Survivability

V = Probability for the compartments above the horizontal divisions to stay intact

Briefly, the *P_i*-factor only depends on the geometry of the watertight arrangement of the ship, and is a factor for the probability of experiencing a specific damage. The *S_i*-factor is dependent on the survivability of the vessel after the damage has occurred for a specific damage scenario. Since *P_i* only takes the longitudinal and transverse damage extent into account a *V_i*-factor is implemented to include vertical extent of damage on the vessel. The calculations behind these factors will be covered in the following subchapters. (IMO, 2006a)

The attained index is calculated for all damage scenarios with three different loading conditions.

D_s - Deepest subdivision draught

D_p - Partial subdivision draught

D_l - Lightest service draught

When the attained index has been calculated for all damage scenarios with the three different loading conditions it is weighted differently and added up to the final attained index. (IMO, 2006a)

$$A_{final} = 0,4A_{D_s} + 0,4A_{D_p} + 0,2A_{D_l} \quad \text{Eq. 8}$$

Since the operation time in the three loading conditions is different, the attained index is multiplied with a factor. The factor accounts for the different operation times, implying that the vessel operates 40% of its time in with the deepest load line, 40% in the partial condition and 20% in the lightest service draught. (Baltersen & Erichsen, 2007)

2.2.3 P_i- factor – Regulation 7.1

As mentioned earlier the P_i-factor is only dependent on the geometry of the watertight arrangement and the zone division. Since P_i is the probability of a specific damage on the ship, $\sum P_i$ for the whole ship length has to equal 1. The formula to calculate P_i is as follows: (IMO, 2006a)

$$P_i = p(x_{1j}, x_{2j}) \cdot [r(x_{1j}, x_{2j}, b_k) - r(x_{1j}, x_{2j}, b_{k-1})] \quad \text{Eq. 9}$$

j = Aft damage zone number, starting at 1 in the stern

k = Number of particular longitudinal bulkhead as barrier for transverse penetration

*x*₁ = Distance from aft end of ship to the aft end of zone

*x*₂ = Distance from aft end of ship to the forward end of zone

b = Mean transverse distance from shell to longitudinal barrier

r = Factor to account for the transversal extent of the damage

The formula for P_i, shown in Eq. 9, only applies for one zone damages. The expression of P_i for multi-zone damages can be found in “Explanatory notes to SOLAS chapter II-1”. Due to the complexity of the formula for multi-zone damages it is not explained in this report. $p(x_{1j}, x_{2j})$ is an expression for the probability of damage length in the longitudinal direction. “*r*” used in the equation for P_i is a factor that includes the probability of the damage to breach longitudinal watertight bulkheads. The probability of breaching watertight integrity vertically is not included in the P_i-factor, but is taken into consideration when calculating the V_i-factor. (IMO, 2006a)

Calculating $p(x_1, x_2)$

Figure 2-4 shows the data collected from the HARDER project. The figure shows how long the damage lengths are in relation to ship length. The information collected in the HARDER project was compared to the results for deterministic damage extent calculated using Eq. 1. This showed that the calculation of damage length using Eq. 1, did not give satisfactory results. The damage lengths, calculated with the deterministic formula, did not represent the actual damages ships encountered in collisions and groundings. In order to calculate damage extents that would be more accurate the formula for calculating the extents for PDS were derived from statistics in the HARDER project. Figure 2-5 shows the non-dimensional distribution of the damage extents shown in Figure 2-4. (Lützen, 2001)

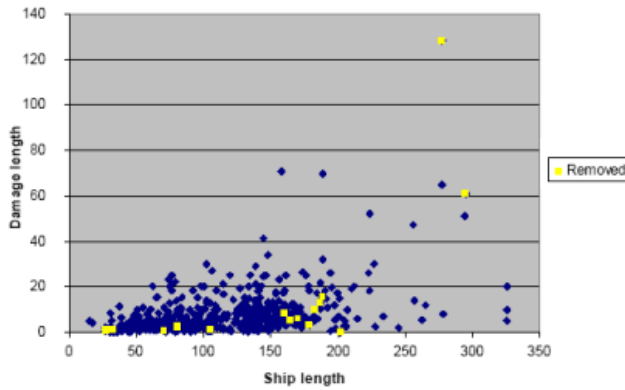


Figure 2-4: Damage length vs Ship length (Olufsen & Hjort, 2013, s. 15)

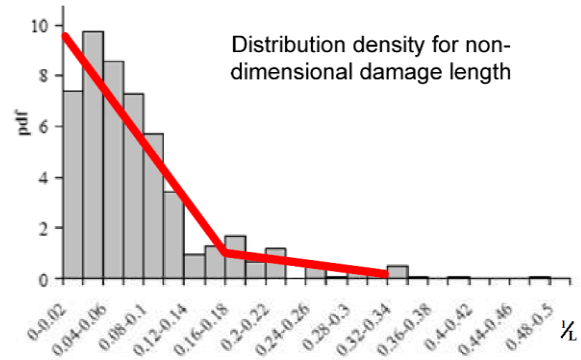


Figure 2-5: Non-dimensional damage length (Olufsen & Hjort, 2013, s. 15)

The red line in Figure 2-5 is the distribution as applied in the probabilistic damage stability regulations. Pdf is the probability density function and the numbers on the X-axis is the non-dimensional damage length, J_k . In order to describe the non-dimensional damage length, many different functions has been used. Marie Lützen’s PhD thesis from 2001 concluded that a Bi-linear function, where the parameters are described as fractions, should be used, because this would easily be implemented in the regulations. The Bi-linear function is used, as proposed by Lützen, when the regulations in SOLAS were revised at a later point. The bi-linear function describes the non-dimensional damage length in the following way: (Lützen, 2001, ss. 134-144)

$$b(x) = \begin{cases} b_{11} \cdot x + b_{12} & \text{for } x \leq J_k \\ b_{21} \cdot x + b_{22} & \text{for } x > J_k \end{cases} \quad \text{Eq. 10}$$

J_k = knuckle point on the red curve
 x =non-dimensional damage length

The damage statistics used for the initial SOLAS requirements, resolution A.265(VIII), showed that there was a significant higher chance for damage in the bow compared to the aft part. Therefore the calculations included the following function for the non-dimensional damage location: (Lützen, 2001, ss. 134-144)

$$a(l) = \begin{cases} 1.6 \cdot l + 0.4 & \text{for } l \leq 0.5 \\ 1.2 & \text{for } l > 0.5 \end{cases} \quad \text{Eq. 11}$$

l =non-dimensional damage location

The HARDER project collected information about earlier damage cases and checked to see if they found a correlation between damage length, ship length and position of damage. The research found that the damage location distribution was not significant and in order to simplify the calculations the non-dimensional damage location function was set to 1, meaning an equal probability of damage along the whole ship length. (Lützen, 2001, ss. 135-136)

The information shown in Table 2-2 are values representing the red curve in Figure 2-5. The overall normalized max damage length, J_{max} is the point where the red line crosses the x-axis and is the non-dimensional maximum damage length a ship can encounter. The knuckle point on the curve is represented as J_{kn} , and P_k is the cumulative probability at this point. (IMO, 2006a)

Table 2-2: Non-dimensional damage lengths

<i>Overall normalized max damage length:</i>	$J_{max}=10/33$
<i>Knuckle point in the distribution:</i>	$J_{kn}=5/33$
<i>Cumulative probability at J_{kn}:</i>	$P_k=11/12$
<i>Maximum absolute damage length:</i>	$l_{max}=60\text{ m}$
<i>Length normalized distribution ends:</i>	$L^*=260\text{ m}$

The following coefficients are derived from the statistics on non-dimensional damage length and implemented according to Eq. 10. (IMO, 2006a)

$$b_{11} = 4 \frac{1 - p_k}{(J_m - J_k)J_k} - 2 \frac{p_k}{J_k^2} \qquad b_{12} = \text{Dependent on ship length}$$

$$b_{21} = -2 \frac{1 - p_k}{(J_m - J_k)^2} \qquad b_{22} = -b_{21}J_m$$

The J_m factor is the maximum non-dimensional damage length for the particular ship in question, and J_k is the knuckle point in the distribution. Since the damage statistics varies according to ship length, J_m , J_k and b_{12} varies accordingly. (IMO, 2006a)

When $L_s \leq L^*$:

$$J_m = \min \left(J_{max}, \frac{l_{max}}{L_s} \right)$$

$$b_{12} = b_0 = 2 \left(\frac{p_k}{J_{kn}} - \frac{1 - p_k}{J_{max} - J_{kn}} \right)$$

$$J_k = \frac{J_m}{2} + \frac{1 - \sqrt{1 + (1 - 2p_k)b_0J_m + \frac{1}{4}b_0^2J_m^2}}{b_0}$$

The conditions for finding the maximum damage length, J_m , shows that if L_s is below 198 meters, J_{max} will be the least value and subsequently used for J_m . Consequently J_k will remain constant for all vessels with a length less than 198 meters.

When $L_s > 260$ meters, J_m^* and J_k^* factors are introduced. This is because the gathered number of damages for vessels above 260m, as seen in Figure 2-4, is very low compared to the total amount of damages. Therefore the distribution function was cut at 260m, consequently splitting up the functions for calculating J_m and J_k . Since the statistics used for

ships larger than 260 meters are different from the damage statistics for vessels smaller than 260 meters J_m and J_k has to be adjusted accordingly. This is solved by introducing J_m^* and J_k^* and converting them to J_m and J_k as seen in the following calculations: (Hjort, 2014)

When $L_s > L^*$:

$$J_m^* = \min\left(J_{max}, \frac{l_{max}}{L^*}\right) \implies J_m^* = \frac{l_{max}}{L^*} \implies J_m = \frac{J_m^* \cdot L^*}{L_s}$$

$$J_k^* = \frac{J_m^*}{2} + \frac{1 - \sqrt{1 + (1 - 2p_k)b_0 J_m^* + \frac{1}{4}b_0^2 J_m^{*2}}}{b_0} \implies J_k = \frac{J_k^* \cdot L^*}{L_s}$$

$$b_{12} = 2\left(\frac{p_k}{J_k} - \frac{1 - p_k}{J_m - J_k}\right)$$

$$J_m^* = \min\left(J_{max}, \frac{l_{max}}{L^*}\right) \text{ for ships larger than 260 meters.}$$

The formula for b_{12} , when the ship under consideration is above 260 meters, is almost the same as when $L_s < L^*$. The only difference is that when $L_s > L^*$, J_k is used instead of J_{kn} and J_m replaces J_{max} .

When J_m , J_k and b_{12} are calculated, the normalized damage length, J_n , can be found. J_n is needed for the calculations of $p(x_1, x_2)$ in Eq. 12 and Eq. 13. (IMO, 2006a)

$$J = \frac{(x_2 - x_1)}{L_s} \qquad J_n = \min\{J, J_m\}$$

J = the non-dimensional length of the considered compartment

J_n = a measure on the non-dimensional damage length

Calculating $p(x_1, x_2)$ for three different conditions:

1. Where neither limits of the compartment or group of compartments under consideration coincides with the aft or forward terminal

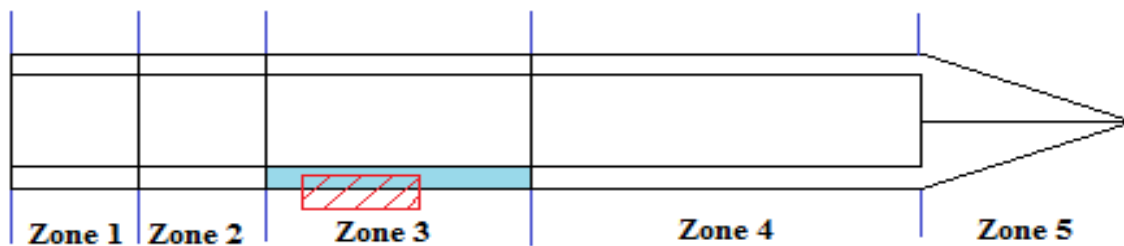


Figure 2-6: 1. Damage condition, seen from above

For $J \leq J_k$:

Eq. 12

$$p(x_1, x_2) = p_1 = \frac{1}{6} J^2 (b_{11} J + 3b_{12})$$

For $J > J_k$:

$$\begin{aligned}
 p(x_1, x_2) &= p_2 \\
 &= -\frac{1}{3}b_{11}J_k^3 + \frac{1}{2}(b_{11}J - b_{12})J_k^2 + Jb_{12}J_k - \frac{1}{3}b_{21}(J_n^3 - J_k^3) \\
 &\quad + \frac{1}{2}(b_{21}J - b_{22})(J_n^2 - J_k^2) + b_{22}J(J_n - J_k)
 \end{aligned}$$

2. When one of the sides, forward or aft, of the compartment or group of compartments coincides with the forward or aft terminal.

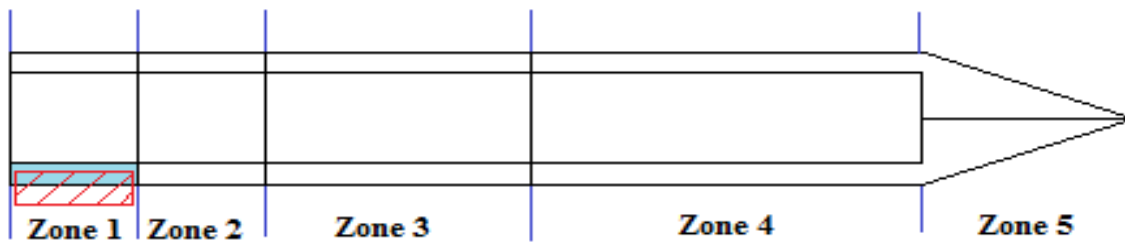


Figure 2-7: 2. Damage condition, seen from above

For $J \leq J_k$: $p(x_1, x_2)$	For $J > J_k$: $p(x_1, x_2)$	Eq. 13
----------------------------------	-------------------------------	--------

$p(x_1, x_2) = \frac{1}{2}(p_1 + J)$	$p(x_1, x_2) = \frac{1}{2}(p_2 + J)$
--------------------------------------	--------------------------------------

As seen the p_1 and p_2 values calculated for the first damage scenario is used in the second damage scenario to calculate $p(x_1, x_2)$.

3. When the compartment or group of compartments extends over the whole ship length:

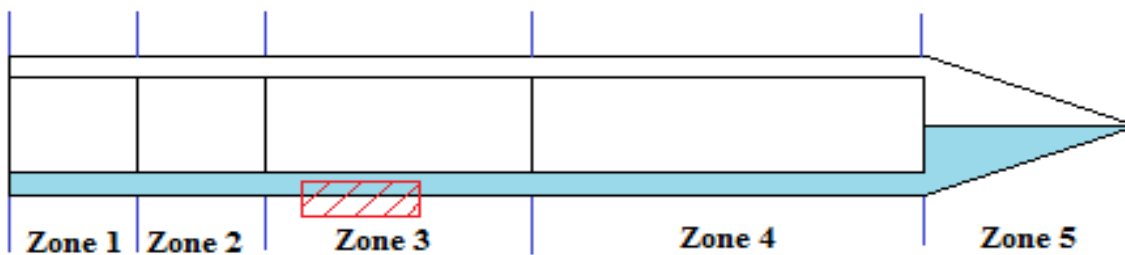


Figure 2-8: 3. Damage condition, seen from above

$p(x_1, x_2) = 1$	Eq. 14
-------------------	--------

The derivation of the $p(x_1, x_2)$ formulas can be found in Marie Lützen's PhD thesis, "Ship Collision Damage", (ss. 138-144).

Calculating $r(x_1, x_2, b_k)$

In order to calculate P_i as seen from Eq. 9, "r" has to be calculated; where "r" is the probability that a penetration is less than a given transverse breadth, b. $r(x_1, x_2, b)$ is calculated based on damage statistics in the same manner as $p(x_1, x_2)$. The formulas for calculating $r(x_1, x_2,$

b) are derived from the statistics displayed in Figure 2-10. The statistics were gathered from more than 400 damage cases. (Lützen, 2001, ss. 134-149)

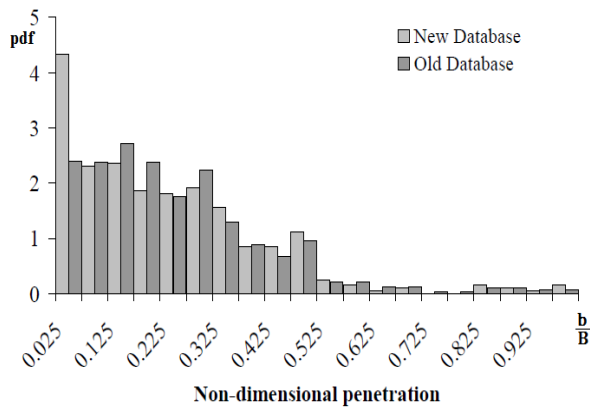


Figure 2-9: Distribution of non-dimensional penetration damages
(Lützen, 2001, s. 148)

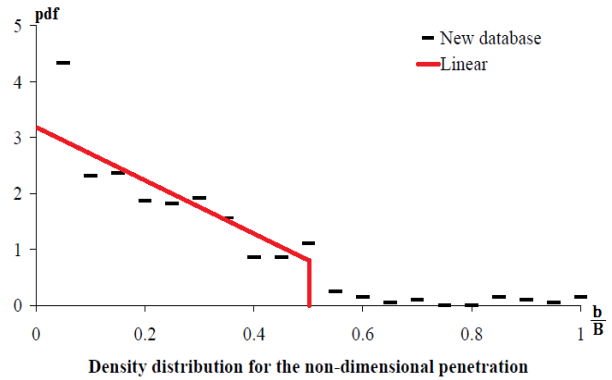


Figure 2-10: Density distribution line for non-dimensional penetration damages
(Lützen, 2001, s. 149)

The penetration depth b , used in Eq. 15, is measured from the deepest draught as a transverse distance from ship side normal to the centerline, to a longitudinal barrier. Whenever the longitudinal barrier is not parallel to the ship hull, b should be determined by an assumed line. We will not go into details on how b is calculated for such cases in this report, but if it is of any interest to the reader, explanations on this can be found in “Explanatory notes to SOLAS Chapter II-1 Part B”. (IMO, 2008a)

The formula to calculate $r(x_1, x_2, b)$ from Eq. 9 is as follows:

$$r(x_1, x_2, b) = 1 - (1 - C) \cdot \left[1 - \frac{G}{p(x_1, x_2)} \right] \tag{Eq. 15}$$

Where:

$$C = 12 \cdot J_b \cdot (-45 \cdot J_b + 4)$$

$$J_b = \frac{b}{15B}$$

b =penetration depth

B =Maximum ship beam at deepest draught

The same conditions as in $p(x_{1j}, x_{2j})$ are used when calculating G in $r(x_{1j}, x_{2j}, b_k)$:

1. *When neither of the longitudinal sides of the compartment or group of compartments coincides with the forward or aft terminals, then:*

$$G = G_2 = -\frac{1}{3}b_{11}J_0^3 + \frac{1}{2}(b_{11}J - b_{12})J_0^2 + Jb_{12}J_0$$

Where: $J_0 = \min(J, J_b)$

2. *When one of the sides, forward or aft, of the compartment or group of compartments coincides with any of the terminals, then:*

$$G = \frac{1}{2}(G_2 + G_1J)$$

3. *When the compartment or group of compartments extends over the whole ship length (L_s):*

$$G = G_1 = \frac{1}{2}b_{11}J_b^2 + b_{12}J_b$$

(IMO, 2006a)

The derivation of $r(x_1, x_2, b)$ can be found in Marie Lützen's PhD thesis, "Ship Collision Damage", (ss. 144-147). The formula for $r(x_1, x_2, b)$ represents the red line seen in Figure 2-10 (IMO, 2006a).

2.2.4 S_i-factor – Regulation 7.2

As mentioned earlier the S_i-factor is dependent of the survivability of the vessel after a specific damage scenario. The survivability factor S, calculated for scenario *i*, is found from the minimum of S_{intermediate,i} or (S_{final,i} · S_{mom,i}). The survivability factor is calculated in the following way: (IMO, 2006a)

$$S_i = \text{minimum}[S_{\text{intermediate},i} \text{ or } (S_{\text{final},i} \cdot S_{\text{mom},i})] \quad \text{Eq. 16}$$

There are no requirements for intermediate stage stability for cargo ships so S_{intermediate,i} is set to 1, but for passenger ships the parameters has to be calculated. S_{final,i} is the probability of survival in the final stage of the flooding. The value is based on the obtained heeling angle, GZ_{max}, range of positive GZ and the equilibrium heeling angle. GZ_{max} must never be taken as more than 0.12 and range must not be taken as more than 16 degrees when calculating S_{final}. (IMO, 2006a)

$$S_{\text{final}} = K \cdot \left[\frac{GZ_{\text{max}}}{0.12} \cdot \frac{\text{Range}}{16} \right]^{\frac{1}{4}} \quad \text{Eq. 17}$$

$$K = \sqrt{\frac{\theta_{\text{max}} - \theta_e}{\theta_{\text{max}} - \theta_{\text{min}}}}$$

K=1 if $\theta_e \leq \theta_{\text{min}}$, K=0 if $\theta_e \geq \theta_{\text{max}}$

θ_e =Equilibrium heeling angle after damage

θ_{min} =Minimum heeling angle

θ_{max} =Maximum heeling angle

θ_{min} =7 degrees and θ_{max} =15 degrees - For passenger ships

θ_{min} =25 degrees and θ_{max} =30 degrees - For cargo ships

Range=The range with positive righting arm, not to be taken as more than 16

GZ_{max}= Maximum value of GZ, never t be taken as more than 0.12

(IMO, 2006a)

K is based on the obtained heeling angle. This value is implemented to give acceptable heeling angles for the different vessel types. As seen from Eq. 17, S_i will be 0 if the ship heels more than 15 degrees for passenger ships and 30 degrees for cargo vessels. The designer has to be careful when arranging the watertight integrity to avoid ending up with larger heeling angles than θ_{max} . This is because the damage conditions for such cases would not contribute to the attained index. (IMO, 2006a) As seen from the requirements for deterministic damage stability there are many similarities. GZ_{max} and Range is used for both calculations but in a different way. In order to avoid excessive heeling it is common for Naval Architects to exclude longitudinal bulkheads in the double bottom in order to get symmetrical damages (Fykse, 2014).

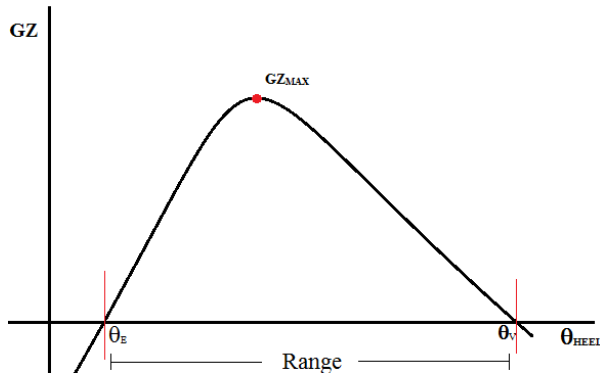


Figure 2-11: Example of GZ-curve

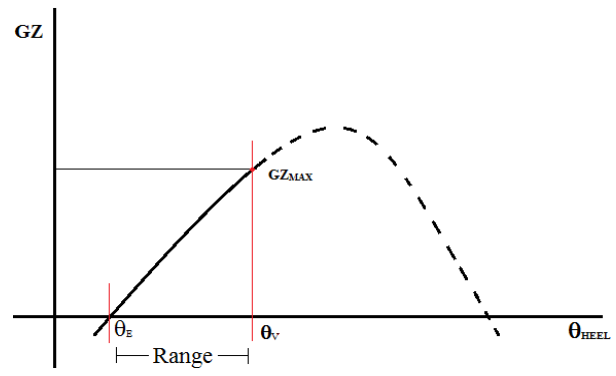


Figure 2-12: GZ-curve for submerged opening

GZ_{max} is the maximum positive righting levers found from the GZ-curve. It is measured in meters and should be the maximum GZ-value between θ_e and θ_v . θ_v is the angle where GZ becomes negative or the angle when an opening, that is not considered to be watertight, is submerged. The *Range* is measured in degrees and is found by looking at the GZ-curve as well. The *Range* is the positive measure between θ_e and θ_v as illustrated in figures above. Figure 2-12 shows an example where the GZ_{max} will be lower than the actual GZ_{max} for the vessel. The reason for this is that an opening is submerged when the heeling reaches θ_v and the GZ curve is cut at this point. (IMO, 2008a) In order to avoid this, designers place all openings a certain distance above bulkhead deck thus eliminating the problem of cutting the GZ curve before the GZ reaches its maximum value (Fykse, 2014).

The $S_{intermediate,i}$ is only calculated for passenger vessels and the calculation is similar to the S_{final} calculations.

$$S_{intermediate} = \left[\frac{GZ_{max}}{0.05} \cdot \frac{Range}{7} \right]^{\frac{1}{4}} \quad \text{Eq. 18}$$

GZ_{max} : not to be taken as more than 0.05m

Range: not to be taken as more than 7°

If the heeling angle exceeds 15°, $S_{intermediate}=0$

$S_{mom,i}$ is given as the probability to withstand the maximum heeling moments from either wind, passengers movement or survival crafts being lowered. $S_{mom,i}$ is not calculated for cargo vessels, so $S_{mom,i}=1$ when calculating S_i for cargo vessels. $S_{mom,i}$ is calculated based on ship displacement, GZ_{max} and M_{heel} . It is important to note that $S_{mom,i}$ cannot have a value larger than 1. (IMO, 2006a)

$$S_{mom,i} = \frac{(GZ_{max} - 0.04) \cdot Displacement}{M_{heel}} \quad \text{Eq. 19}$$

$$M_{heel} = \max\{M_{passenger}, M_{wind}, M_{Survivalcraft}\}$$

$S_{mom} \leq 1$, the S_i factor can never be above 1

$M_{passenger}$ is the moment caused by the movement of passengers to either side of the vessel and is calculated according to the formula below. The weight of the passengers is assumed

to be 75kg and the center of gravity for the passengers is moved with a distance of $0.45 \cdot B$ transversally. (IMO, 2006a)

$$M_{\text{passengers}} = (0.075 \cdot N_p) \cdot (0.45 \cdot B)$$

N_p = Maximum number of passengers permitted

B = Ship beam

The moment from the wind effect is calculated as follows:

$$M_{\text{wind}} = (P \cdot A \cdot Z) / 9.806$$

$P = 120 \text{ N/m}^2$

A = Projected wind area

Z = Distance from center of projected wind area to $T/2$

T = Ship draught

$M_{\text{survivalcraft}}$ is the maximum assumed heeling moment from lowering the survival crafts fully loaded. When these three moments are calculated the maximum moment can be found and used as M_{heel} to calculate $S_{\text{mom},i}$. (IMO, 2006a)

After the calculations for $S_{\text{mom},i}$, S_{final} and $S_{\text{intermediate},i}$ are conducted the designer will get the S_i -factor, for one particular damage, depending on the magnitude of $S_{\text{intermediate},i}$ and $(S_{\text{final},i} \cdot S_{\text{mom},i})$.

2.2.5 V_i -factor – Regulation 7.2

In order to account for contributions from horizontal divisions S_i and P_i is multiplied by a factor V_i . The V_i -factor represents the probability that a deck above the waterline will remain intact after the ships has been rammed by an arbitrary ship. V_i is included because the assumed buoyancy above the waterline will influence the residual ship stability. So if a compartment above the waterline is submerged, it will contribute to the buoyancy thus affecting the GZ-curve. V_i is based on the probability that a specific damage will not exceed a given height above the water line and is calculated in the following way:

$$V_i = v(H_{m,d}) - v(H_{(m-1),d}) \tag{Eq. 20}$$

H_m =Least height to first horizontal boundary above waterline, measured from the baseline. The horizontal boundary must limit extent of flooding vertically and be within the longitudinal range of the damage.

$H_{(m-1)}$ =Least height to (m-1)th horizontal boundary above waterline, measured from the baseline. The horizontal boundary must limit extent of flooding vertically and be within the longitudinal range of the damage.

m =Horizontal boundary upwards from waterline.

d =Draught.

V_i should in no cases be taken as less than zero or more than one.

(IMO, 2006a)

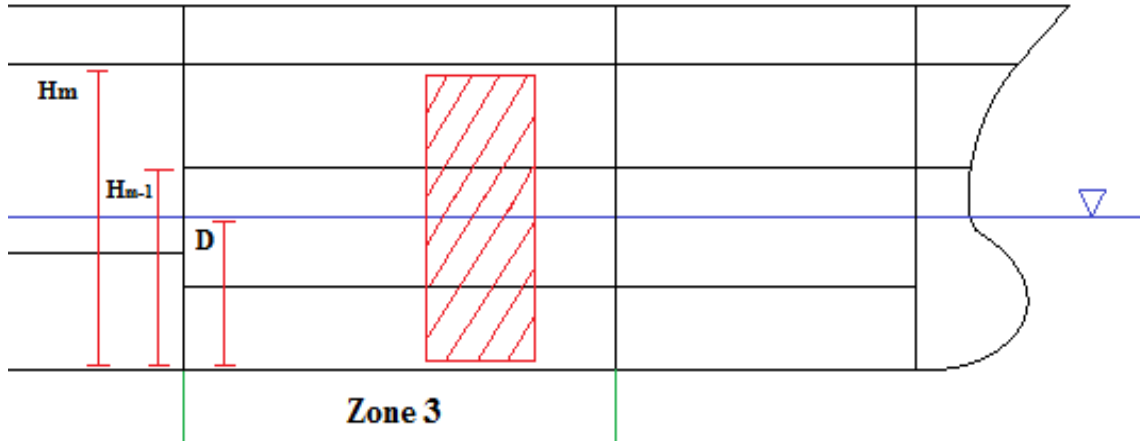


Figure 2-13: Explanation of H_m measures for zone 3

$V(H_m, d)$ and $v(H_{(m-1)}, d)$ are calculated using the following formulas:

If $(H-d) \leq 7.8$:

$$v(H, d) = 0.8 \frac{(H - d)}{7.8}$$

If $(H-d) > 7.8$:

$$v(H, d) = 0.8 + 0.2 \frac{(H - d) - 7.8}{4.7}$$

$v(H_{m,d}) = 1$ if H_m coincides with the uppermost watertight boundary of the ship within the longitudinal range of the damage.

$v(H_{0,d}) = 0$

(IMO, 2006a)

Eq. 20 represents the statistics from the HARDER project found in Figure 2-14. The upper limit of the damage is set to 12.5 meters above the waterline. The formula to calculate V_i represents the red line seen in Figure 2-14. (H-d) is the distance from the initial waterline, for the loading condition, to the horizontal limit above the damage in question.. (IMO, 2006a)

The old requirements were based on the fact that ships would be rammed by other ships with approximately the same length. Since there were no statistics available the vertical extent of damage was based on the length dependent bow-height requirements. When HARDER collected statistics regarding vertical extent of damage the old calculations proved to give a liberal estimation of the V_i -factor. Therefore the regulations were changed according to the gathered information from HARDER. (Olufsen & Hjort, 2013, ss. 23-24)

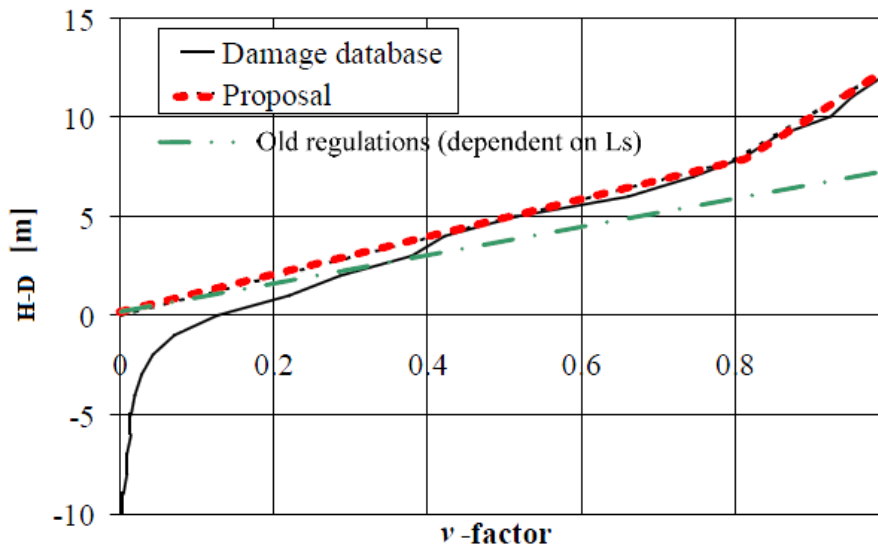


Figure 2-14: Vertical damage distribution

(Olufsen & Hjort, 2013, s. 24)

3 Method

Scope and main activities

This dissertation is a study to maximize the attained index for offshore vessels by analyzing the effects of changes in the arrangement. The placement of the LWTB in the mid-ship section will be studied to increase the survivability of damaged ships. There are two focus areas that have been analyzed in the thesis, the placement of the LWTB in the mid-ship section and the effect of U-shaped double bottom tanks.

Four vessels will be designed with two arrangement configurations. One arrangement with U-tanks in the mid-ship section, and one with longitudinal bulkheads in the double bottom, as seen in Figure 3-3 and Figure 3-4 . Probabilistic damage stability calculations will be conducted for the two different arrangement configurations with different placements of the LWTB. The results will be compared to find out how the attained index develops for different ship sizes and arrangements with varying placements of the longitudinal bulkhead.

3.1 Designing the vessels

The four ships were all designed specifically for this study. The hulls for all vessels were created in the stability software NAPA. The general arrangements of the four vessels designed for the study can be found in Appendix A and the figures on the next page shows the layout for Vessel I. Table 3-1 displays the different dimensions for the four vessels.

Table 3-1: Main dimensions

	<i>Lpp [m]</i>	<i>Beam [m]</i>	<i>Draught moulded [m]</i>	<i>Max. draught [m]</i>
<i>Vessel I – PSV</i>	<i>80.1</i>	<i>22</i>	<i>9</i>	<i>7.2</i>
<i>Vessel II – PSV</i>	<i>95</i>	<i>24</i>	<i>9.6</i>	<i>7.4</i>
<i>Vessel III – OCV</i>	<i>118</i>	<i>28</i>	<i>12</i>	<i>8.5</i>
<i>Vessel IV – OCV</i>	<i>130</i>	<i>30</i>	<i>12.5</i>	<i>8.6</i>

The sizes of the four ships were chosen based on Wärtsilä Ship Design’s specifications. As seen from Table 3-1, the different vessels corresponds with certain ship types. Vessel I and II are typical platform supply vessels (PSV) or anchor handler tug supply vessels (AHTS). Vessel III and IV are typical sizes of offshore construction vessels (OCV). These vessel types are designs where Wärtsilä conducts probabilistic damage calculations, which is why these vessel sizes have been chosen. (Fykse, 2015)

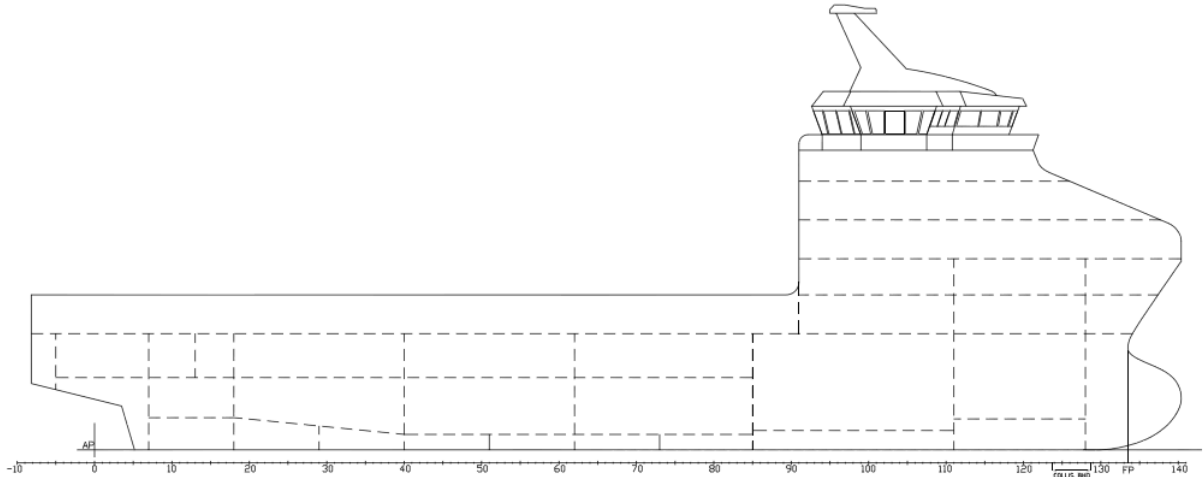


Figure 3-1: Profile view of Vessel I

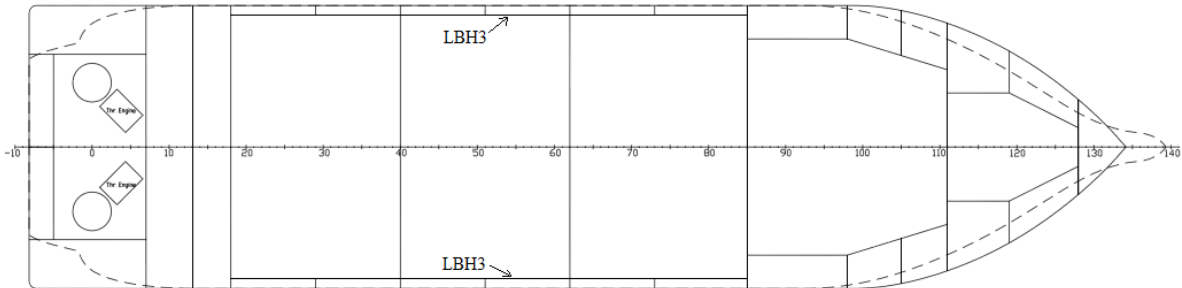


Figure 3-2: Plan view of 2nd deck, Vessel I

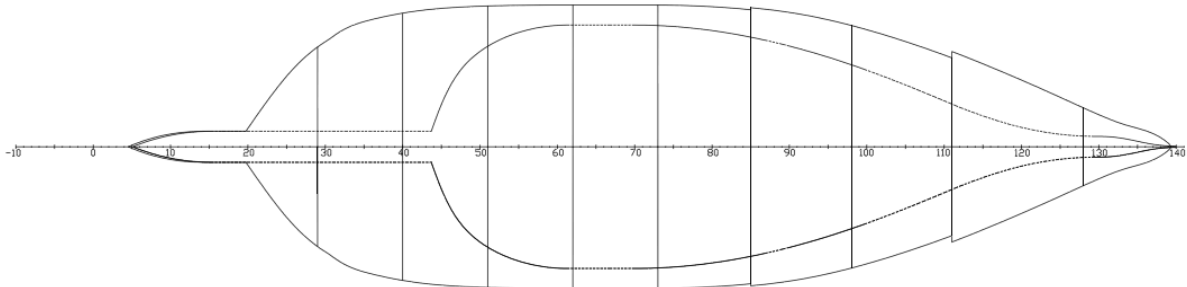


Figure 3-3: Double bottom Vessel I, arrangement B

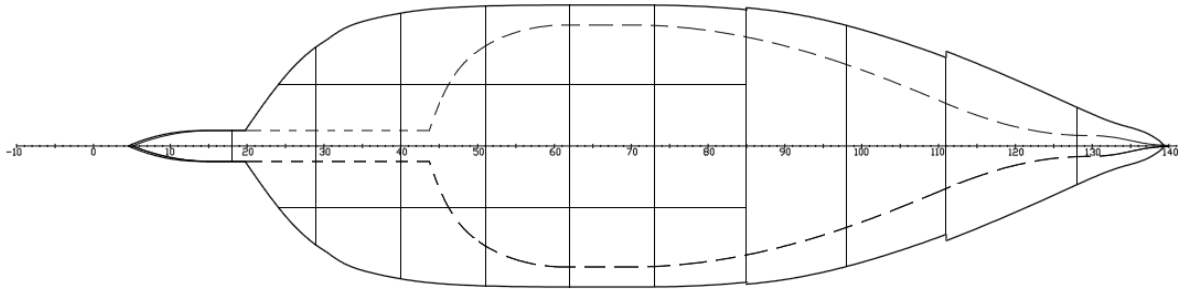


Figure 3-4: Double bottom Vessel I, arrangement C

3.1.1 Hull shape

The stern of the vessels are shaped with regards to two azimuth thrusters. As seen from the general arrangement (GA) in Appendix A, tunnel thrusters and retractable thrusters are not included. The decision of not including recesses in the hull for thrusters and moonpools will be discussed in the following subchapters.

In order to save considerable amount of time, the hull lines for the different ships were not designed from scratch for this study. The hull lines for Vessel I were taken from an existing PSV vessel. By using an authentic hull shape the results from the calculations should be genuine. To keep the hydrostatics amongst the ships as similar as possible, the same hull shape were used for all four vessels. Significant variance in the size of the vessels lead to problems concerning the scaling of the hull. The magnitude of the depths moulded (D) and draughts (T) are not proportional to the length of a vessel. D and T where therefore chosen based on reference vessels. In order to simplify the hull modeling process, the lengths and beams were scaled to the desired magnitude for the different vessels. Figure 3-5 and Figure 3-6 displays the cross sections for the hulls used in this study.

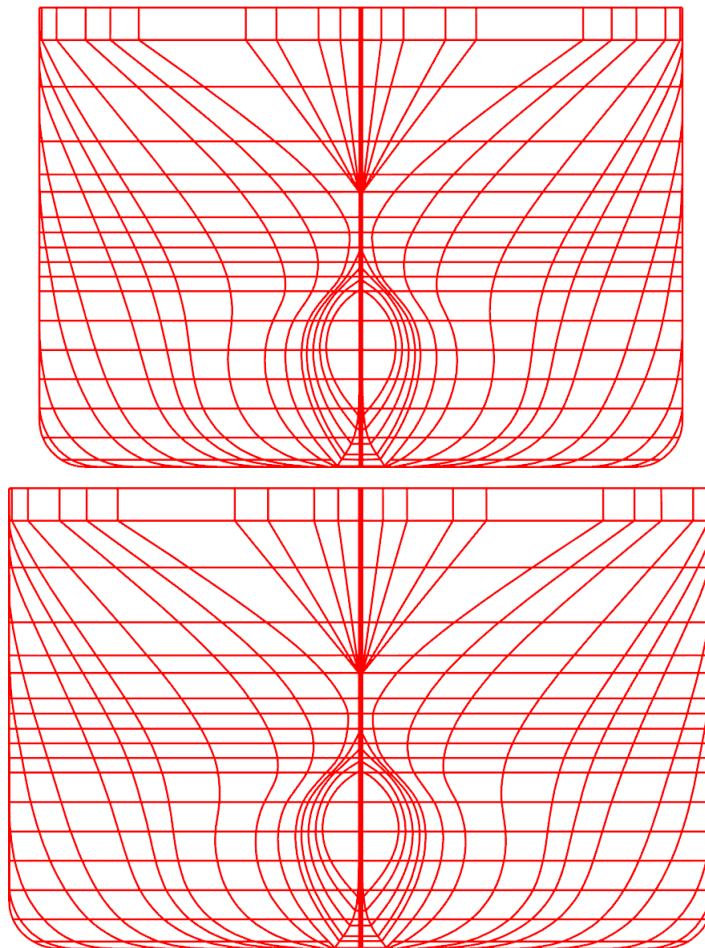


Figure 3-5: Hull shapes, Vessel I and II

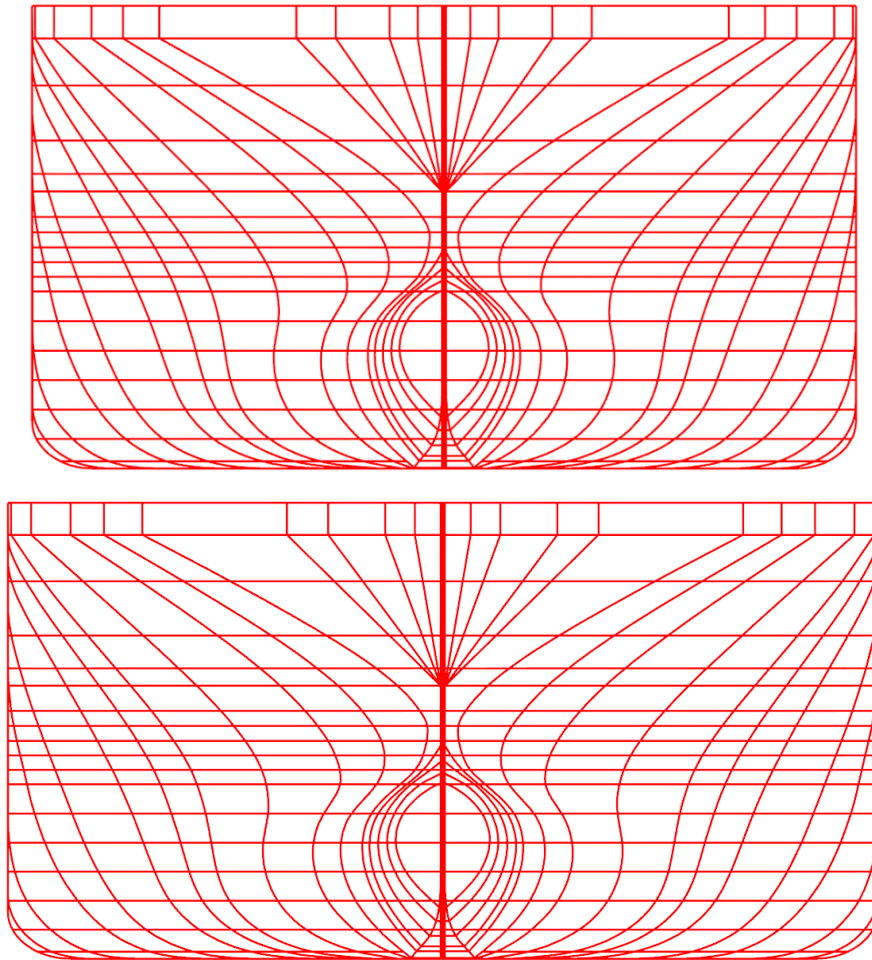


Figure 3-6: Hull shapes, Vessel III and IV

As seen from Figure 3-7 the hull shape for Vessel IV is not identical to the hull shape of its reference vessel. The bulb is not optimized for the new draughts and the flare angle for the larger vessels are too large. After a discussion with Senior Naval Architects Ulf Ottesen and Ketil Fykse at Wärtsilä Ship Design (WSD), it was concluded that the differences in bulb form and the general bow shape would play an insignificant role for the results. This conclusion was most likely incorrect, and will be furthered discussed in chapter 5.

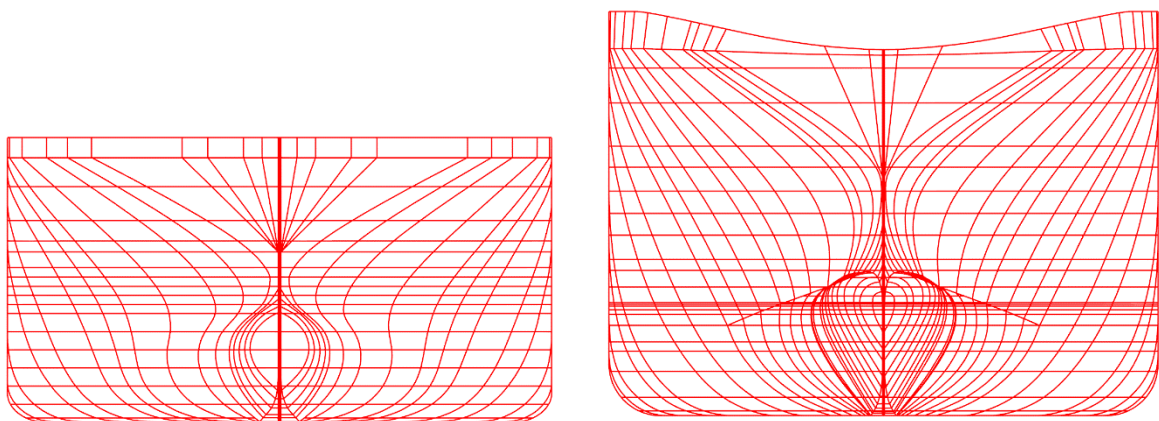


Figure 3-7: Comparison of hull for Vessel IV and reference vessel

3.1.2 Stability

The intact stability of a vessel will influence the results of the damage stability calculations. The center of gravity and draught for the different loading conditions are one of the few inputs needed for the damage stability calculations. As estimating a lightship and acquire different intact loading conditions to calculate the intact stability is not within the scope of this thesis, reference vessels were used when estimating the draughts and GM values.

Draughts

The draughts for the different loading conditions for the four vessels are shown in Table 3-2. The lightest anticipated loading condition is D_l , and D_s is the deepest anticipated subdivision draught, which corresponds to the summer load line draught (IMO, 2008b). *“The partial subdivision draught (D_p) is the light service draught plus 60% of the difference between the light service draught and the deepest subdivision draught”* (IMO, 2008b).

Table 3-2: Vessel draughts

	<i>Vessel I</i>	<i>Vessel II</i>	<i>Vessel III</i>	<i>Vessel IV</i>
<i>Lightest service draught, D_l</i>	<i>4.8 m</i>	<i>5 m</i>	<i>6.6 m</i>	<i>6.7 m</i>
<i>Partial subdivision draught, D_p</i>	<i>6.28 m</i>	<i>6.44 m</i>	<i>7.74 m</i>	<i>7.84 m</i>
<i>Deepest subdivision draught, D_s</i>	<i>7.2 m</i>	<i>7.4 m</i>	<i>8.5 m</i>	<i>8.6 m</i>

The draughts chosen for Vessel I and II were based on reference vessels, as Wärtsilä’s portfolio contained several vessels with the same dimensions. Selecting the draughts for Vessel III and IV were more challenging than for the PSV’s, as there were no reference vessels with corresponding dimensions in Wärtsilä’s portfolio. PSV’s are vessels that execute similar tasks and the draughts are therefore similar. OCV’s have different specifications and intended work operation, and the draughts varies correspondingly. The draughts and depths moulded for several reference vessels were used to calculate a mean value, which was used for Vessel III and IV.

GM values

The GM values for all vessels in the different loading conditions can be seen in Table 3-3 on the following page. The values were chosen in the same manner as the draughts. Reference vessels in WSD’s portfolio were used, to acquire the GM values needed. Similar vessels that could be used as reference vessels were examined in collaboration with Dino Ivkovic, Naval Architect at the stability department of WSD. As there were not many reference vessels matching the main dimensions of the OCV’s in the study, the magnitudes of the GM values were discussed. We found that the GM values varied extensively according to the specific vessels operational requirements. As the results of the damage stability calculations are highly dependent on the stiffness of the vessels, we decided to use equal GM values for some of the vessels. This would allow us to compare the total attained index for the vessels with the same GM values. The values were selected using the same approach as when selecting the draughts for Vessel III and IV.

Table 3-3: GM values for the vessels

	<i>Vessel I</i>	<i>Vessel II</i>	<i>Vessel III</i>	<i>Vessel IV</i>
<i>Lightest service draught, D_l</i>	<i>1.6 m</i>	<i>1.6 m</i>	<i>1.8 m</i>	<i>1.8 m</i>
<i>Partial subdivision draught, D_p</i>	<i>1.6 m</i>	<i>1.6 m</i>	<i>1.8 m</i>	<i>1.8 m</i>
<i>Deepest subdivision draught, D_s</i>	<i>2.3 m</i>	<i>2.3 m</i>	<i>2.5 m</i>	<i>2.5 m</i>

3.1.3 Superstructure

The superstructure of the vessels were scaled according to their reference vessels. All vessels were designed with the superstructure in the forward part, as this is most common for offshore vessels. The projected area of the superstructure influences the wind moment acting on the vessel, and the wind moment affects the survivability of a vessel in a damage condition. As the wind area and the center of the projected area influences the survivability, the superstructures were designed according to the reference vessels.

3.1.4 Arrangement

The study aims to provide results that are as generic as possible. All vessels were designed according to reference vessels and the general arrangement of all vessels can be found in Appendix A. As each vessel corresponds to a ship type, it is important to find out how the typical internal subdivisions are for these ship types. For example, a PSV does not have the same watertight subdivision as an OCV. Most PSV's have a similar subdivision as seen in Figure 3-8. A PSV arrangement normally contains liquid mud/brine along the side and dry bulk tanks in the center. To get results that are applicable for most vessels, the arrangements in the study were designed as generic as possible.

As seen in Figure 3-9, an OCV arrangement is very different from a PSV. The compartments are larger for OCV's and the arrangements are not as symmetric as for PSV's. There are similarities between different arrangements and in order to get as generic results as possible the bulkheads that are found for most vessel types were used. The transversal bulkheads are a feature that reoccurs for most vessel types, as well as the wing tank bulkheads. The longitudinal bulkheads closest to the centerline, containing the mud/brine, are typical for PSVs, but are not common for OCVs nor AHTSs. These bulkheads were therefore not included in the arrangements of any of the vessels in the study. It should be noted that all vessels in the study have a frame spacing of 600 mm and all bulkheads are placed on frames.

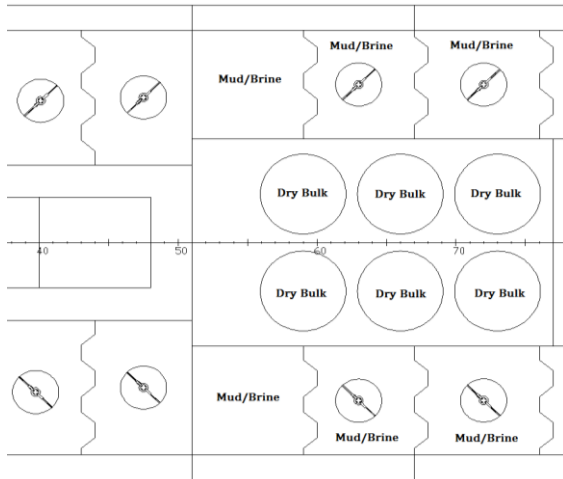


Figure 3-8: Typical mid-ship arrangement of PSV's (WSD's portfolio)

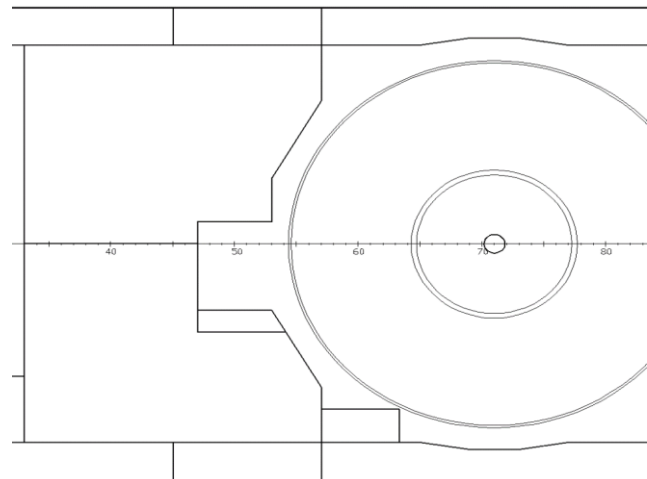


Figure 3-9: Typical mid-ship arrangement of OCV's (WSD's portfolio)

Size of machinery room and thruster rooms

The internal arrangement of the ships were designed so that the arrangements would be as authentic as possible. The machinery rooms were designed according to reference vessels, with the same length and breadth, to ensure that the size would be realistic. To verify that the engine-/thruster room sizes were proportional with the vessels length, "length factors" were calculated for all arrangements.

$$A = \frac{L_s}{\text{Length of thruster room}} \qquad B = \frac{L_s}{\text{Length of machinery room}}$$

$L_s = \text{Ship length}$

The factor would not necessarily be equal for all the vessels, because the engine size is not proportional with ship length. But as long as the factors, A and B, were approximately the same for the reference vessels as for the designs used in this study, the uncertainty of the results would be minimized.

Collision bulkhead

The placement of the collision bulkheads were calculated according to SOLAS Chapter II-1, B-2, Regulation 12 - Peak and machinery space bulkheads, shaft tunnels, etc.:

“A collision bulkhead shall be fitted which shall be watertight up to the bulkhead deck. This bulkhead shall be located at a distance from the forward perpendicular of not less than $0.05L$ or 10 m , whichever is the less, and, except as may be permitted by the Administration, not more than $0.08L$ or $0.05L + 3\text{ m}$, whichever is the greater.

Where any part of the ship below the waterline extends forward of the forward perpendicular, e.g., a bulbous bow, the distances stipulated in paragraph 1 shall be measured from a point either:

- 1 at the mid-length of such extension;*
- 2 at a distance $0.015L$ forward of the forward perpendicular; or*
- 3 at a distance 3 m forward of the forward perpendicular, whichever gives the smallest measurement.”*

After calculating the two distances it's up to the designer to place the collision bulkhead between the limits. Figure 3-10 shows how the placement of the bulkhead was done for Vessel IV. The bulkhead has to be placed within the limits shown with the red arrows. It is common practice to place the bulkhead close to the furthest limit, to utilize the space behind the collision bulkhead for equipment and payload. The placement of the collision bulkhead influences how the rest of the machinery room bulkheads are placed. If the collision bulkhead has to be moved later in the design process, other parts of the arrangement has to be modified. During the design phase it is common that the length of the vessel is changed, and new limits for the collision bulkhead has to be calculated. To avoid having to move the collision bulkhead, if the ship length is changed, it is common to leave a margin between the bulkhead and the limits. (Vickovic, 2015)

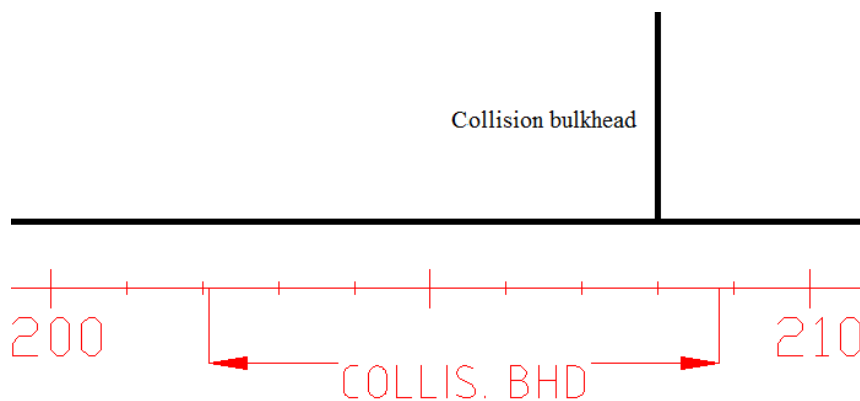


Figure 3-10: Placement of collision bulkhead

Figure 3-10 illustrates how the collision bulkhead is placed within the limits from the calculations. The figure is a profile drawing of the front of Vessel IV, where the frames are shown with the red lines. Since it is common to place the collision bulkhead close to the furthest limit, this was conducted for all vessels in the study.

Shape of tank top

The height of the tank top is governed by SOLAS Ch. II-I, Part B-2, regulation 9, and should not be less than $B/20$. This is not required by some of the certification societies, but it is common practice to use $B/20$ as a measure for the minimum size of the double bottom (Fykse, 2015). Due to the curvature in the aft body of the vessels, the tank tops were raised in order to exceed the $B/20$ measure, as seen in Figure 3-11.

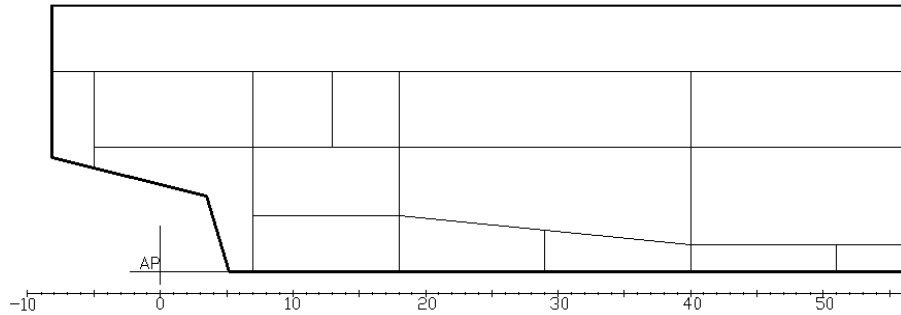


Figure 3-11: Profile view of tank top in the stern of Vessel I

It is common to have a knuckled tank top as seen in Figure 3-12. Since the placement of the knuckle point is influenced by where the LWTBs are placed, this would cause problems when modeling the different arrangements in NAPA. Since the longitudinal bulkhead is moved for every new run for all the vessels, a knuckled tank top would increase the workload considerable. This is because the definition of the tank top would have had to be changed for every movement of the longitudinal bulkhead. It was decided that the amount of work required to implement these changes for every run were not necessary, since the results would not be significantly changed. It should be noted that some of the arrangements does not meet the required height of $B/20$, for the double bottom stated in SOLAS, Ch. II-1, Part B, Reg. 9. The heights of the different tank tops were based on the reference vessels in Wärtsilä's portfolio, and the shapes of the different tank tops can be seen in the GA's in Appendix A.



Figure 3-12: Cross section view of knuckled tank top (not used for any vessels in the study)

Distance between transversal bulkheads

When the deterministic approach is used to examine a vessels survivability after damage, a damage extent is calculated using Eq. 1, found in SOLAS Ch. II-1, 1981 Amendments, Reg. 1 to 54. The probabilistic approach does not limit the damage extent, and all damage lengths are taken into consideration.

The probabilistic regulation, found in SOLAS Ch. II-1, Part B-1 Reg. 6 and 7, does not consider damages due to grounding. Damage scenarios under the waterline is considered using the deterministic approach found in Reg. 9. The distance between the transversal bulkheads were therefore governed by the damage extent found in regulation 9.

$$\text{Damage extent} = \frac{1}{3} \cdot L^{\frac{2}{3}}, \text{ or } 14.5 \text{ m, whichever is less} \quad \text{Eq. 21}$$

L = Rule length

After the damage extents were calculated, the transversal bulkheads were placed so that a bottom damage would not include two transverse bulkheads. If the distance is smaller than the maximum damage extent, one damage case will cover three zones. As this is not favorable, the smallest distance above the maximum damage extents were chosen. The calculated damage extents and distances between the transversal bulkheads can be seen in Table 3-4. This study does not look into bottom damages regulated by regulation 9. But in order to have as realistic arrangements as possible, regulation 9 was used to decide the distance between the transversal bulkheads.

Table 3-4: Distance between transversal bulkheads

<i>Ship</i>	<i>L_{pp} [m]</i>	<i>Rule Length [m]</i>	<i>Max. damage extents according to Reg. 9 [m]</i>	<i>Distance between transversal bulkheads [m]</i>
<i>Vessel I</i>	<i>80.1</i>	<i>81.6</i>	<i>6.271</i>	<i>6.600</i>
<i>Vessel II</i>	<i>95</i>	<i>96.8</i>	<i>7.027</i>	<i>7.200</i>
<i>Vessel III</i>	<i>118</i>	<i>103.5</i>	<i>7.348</i>	<i>7.800</i>
<i>Vessel IV</i>	<i>130</i>	<i>134.6</i>	<i>8.754</i>	<i>9.000</i>

3.2 NAPA stability software

NAPA was the stability software used for the study. It is the leading stability software used by almost 400 organizations (NAPA, 2015). All tanks and compartments are modeled, using text files, and used in the damage stability calculations. Four vessels were modeled with two different arrangements for each vessel in the study. Two separate text files were made for modeling the two arrangements to be able to go back and do reruns if needed.

3.2.1 Using Probabilistic manager to calculate PDS

The Probabilistic manager is a manager used when calculating probabilistic damage stability in NAPA. The manager was used to calculate the attained index for all damage cases. It consists of numerous macros which utilizes the information written in the input text files, but there are also information that have to be inputted in the manager itself.

Main input in Probabilistic manager

For vessels where probabilistic damage stability calculations are conducted the Probabilistic manager is used. The manager requires the user to input certain information in order to perform the calculations. Figure 3-13 displays how the probabilistic manager looks like. For the vessels used in this study, “passenger vessel” were chosen for the vessel type. The vessels in the study are cargo ships, but they need to comply with the probabilistic regulations due to their SPS notation. It is stated in the regulations that all vessels with SPS notation, should follow the passenger vessel requirements (IMO, 2006a). That is why the ships are classified as passenger vessels in regards to probabilistic damage stability calculations. The passenger numbers were set to 0 for all the vessels. After discussions with Naval Architects, Dino Ivkovic and Ketil Fykse, the conclusion was that the influence from passengers would be insignificant.² Since all arrangements used in the study is symmetrical around the centerline, it does not matter which side of the vessel that is studied, but port side was investigated for the four vessels in the study.

Subdivision tables had to be filled out manually for every new vessel arrangement. The subdivision tables are used to tell NAPA how the ship should be subdivided in regards to damage extents and zones. Since the arrangements were changed for every run, the subdivision tables would have had to be changed for every run manually. In order to avoid this, a longitudinal surface was made. The surface defined the placement of the longitudinal bulkhead limiting the wing tanks in the mid-section of the ship, as well as the placement of the subdivisions. This surface was called LBH3 and was the only definition that had to be changed in the subdivision table when running calculations for a new placement of the longitudinal bulkhead. Figure 3-2 illustrates the longitudinal extent of LBH3.

² *The effect of passengers will be discussed in chapter 6*

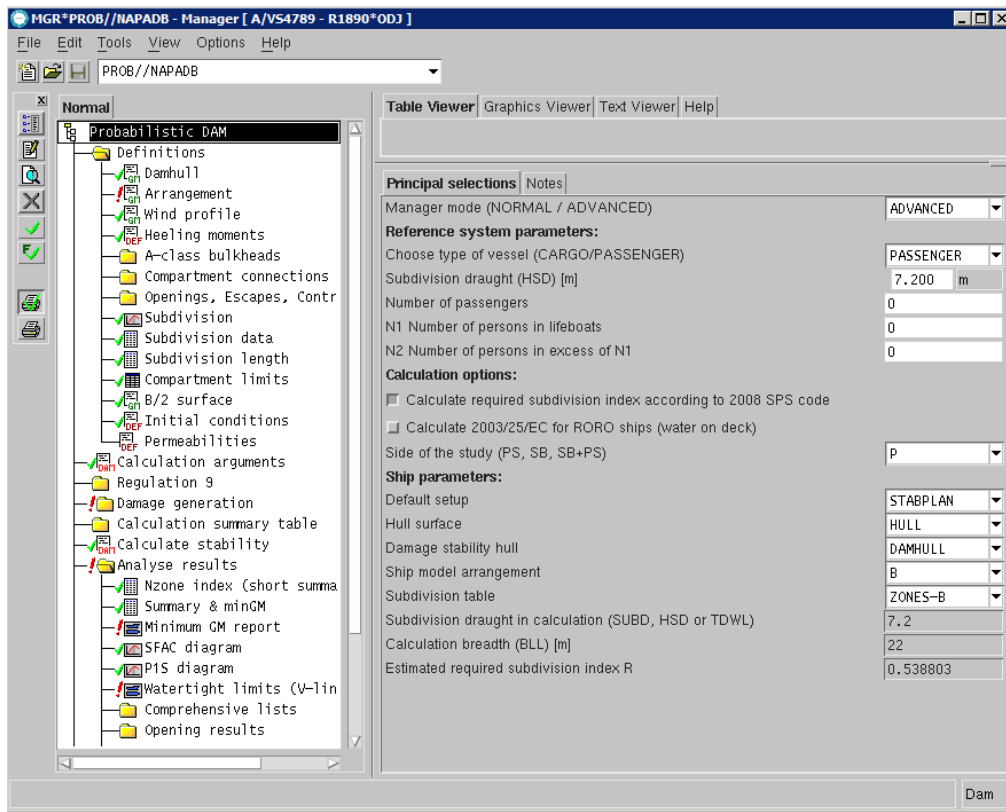


Figure 3-13: Probabilistic manager

3.2.2 Ways to analyze the results in NAPA

There are several in tools in the Probabilistic manager to help the designer with analyzing the results of the calculations. The calculations required to calculate the attained index are complicated, and the results are not easy to understand by only looking at the final attained index. Every tool gives a deeper insight to the results, by displaying relevant information visually. The different tools have been used simultaneously to understand the underlying results. This subchapter will only explain the analyzing tools used for this study, but there are multiple tools available in NAPA that were not used in this study. All the tools mentioned in this subchapter have contributed to a better understanding of the results for the vessels in the study.

S-factor diagrams

S-factor diagrams are very helpful when analyzing the S_i -factor for different damage cases. It gives an overall view of the vessel where the color of the different squares tells the designer which areas of the ship that is vulnerable to damages. As seen in Figure 3-14, the vessel is divided into many triangles. The first horizontal row of triangles represents one zone damages, the 2nd row represents two zone damages, and so on.

When looking at the plan view of the vessel in Figure 3-14, the zone subdivision can cause confusion. NAPA includes all zone subdivisions in all decks. As seen on the vessel below, there are more red lines than bulkheads in the plan view. The double bottom have more transversal bulkheads than 2nd deck, and the subdivisions from the double bottom are also shown in the plan view of the 2nd deck. This can be confusing, but all red lines with no black lines in the background shows where there is subdivisions somewhere else on the vessel.

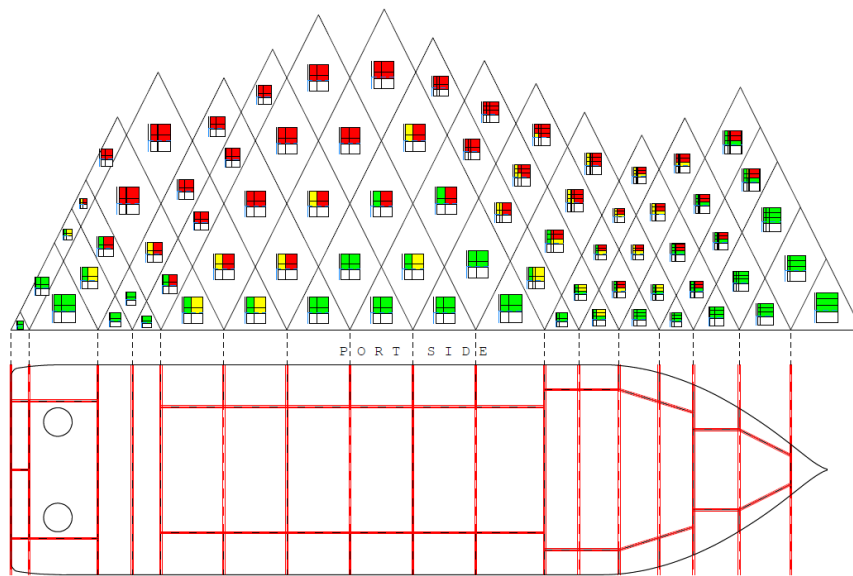


Figure 3-14: S-factor diagram

To analyze individual damage cases, it is possible to take a closer look in each individual triangle. The colors of the squares represents the S_i -factor value for particular damage cases, and the table below displays the meaning of the different colors.

Table 3-5: Color chart for S-factor diagram

<i>Color</i>	<i>S_i-factor value</i>
<i>Green</i>	<i>When $S \geq 0.99$</i>
<i>Yellow</i>	<i>When $0.05 \leq S \leq 0.99$</i>
<i>Red</i>	<i>When $S \leq 0.05$</i>
<i>White</i>	<i>When $p * r * v < 0.00001$</i>

(Puustinen, 2012)

Figure 3-15 shows how each damage case can be found. The horizontal lines represent horizontal watertight boundaries above the lightest service draught. This is because grounding damages are not included in the probabilistic damage calculations. As seen in Figure 3-15, the waterline is above the 2nd deck, so damages to the tanks below 2nd deck gets a V_i -factor of 0. The uppermost line represents the maximum vertical damage extent. This is stated by the rules to be the subdivision draught + 12.5 meters (IMO, 2008a). The vertical lines represents longitudinal watertight bulkheads (LBH). The left line always represents the hull side and the right line is always the center line (CL) of the vessel. (Puustinen, 2012)

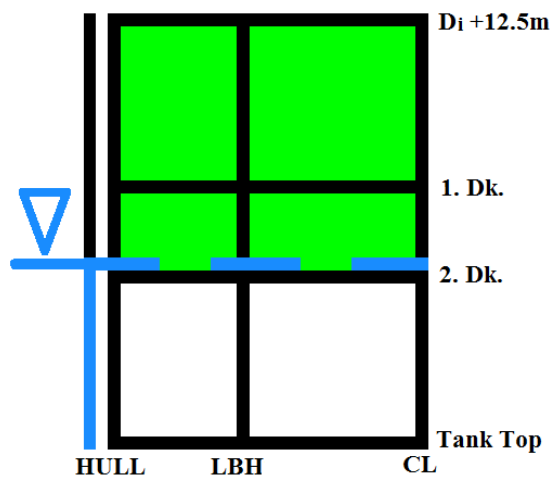


Figure 3-15: One zone damage case from Figure 3-14

P1S Diagrams

A P1S diagram is a way to display the results to help the designer when investigating the results for a vessel. As seen from Figure 3-16, the P1S diagram makes the calculated results more transparent by identifying problematic cases. The product of $P_i \cdot (1-S_i)$ is calculated for each case and displayed in the diagram. Each case is presented with different symbols according to the damage extent and placed at the longitudinal location on the vessel. (Puustinen, 2012)

The P1S diagrams were mainly used to identify problematic damage cases and compare the results together with the S-factor diagram. The P1S diagram includes the probability of the damage, which is not included in the S-factor diagram. When problematic cases are found it is possible to look at the S-factor diagram and find out which cases that are most critical.

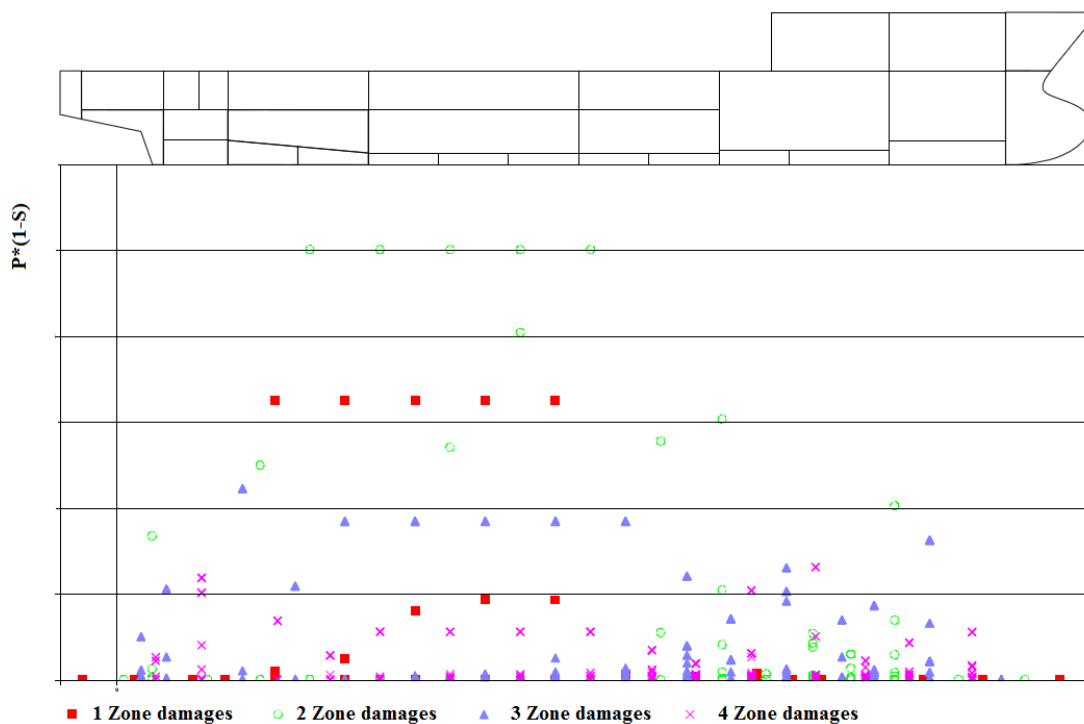


Figure 3-16: P1S diagram for Vessel II, arrangement C

Zone potential diagram

The zone potential diagram can help the designer with finding out which damage zones that have the largest potential for the attained index. There are several diagrams that can be displayed to visualize the results in various ways. It is possible to choose how many zones that are damaged, to display the diagram according to the user needs. The diagram compares the maximum attained index for the selected number of zones to the actual attained index for the zones. (NAPA, 2011)

Figure 3-17 shows a zone potential diagram for two zone damages. The blue columns are the maximum potential attained index, which is the attained index if $S_i=1$ for all damage cases for the zones in question (Puustinen, 2012). The red columns are the actual attained indexes for the deepest loading condition, the orange columns are for the partial loading condition and the yellow are for the lightest loading condition (Puustinen, 2012). Comparing the results from the zone potential diagram with the results from P1S and the S-factor diagrams, are helpful when analyzing damage scenarios. The zone potential diagrams were helpful when comparing the development of the attained index for the different loading conditions.

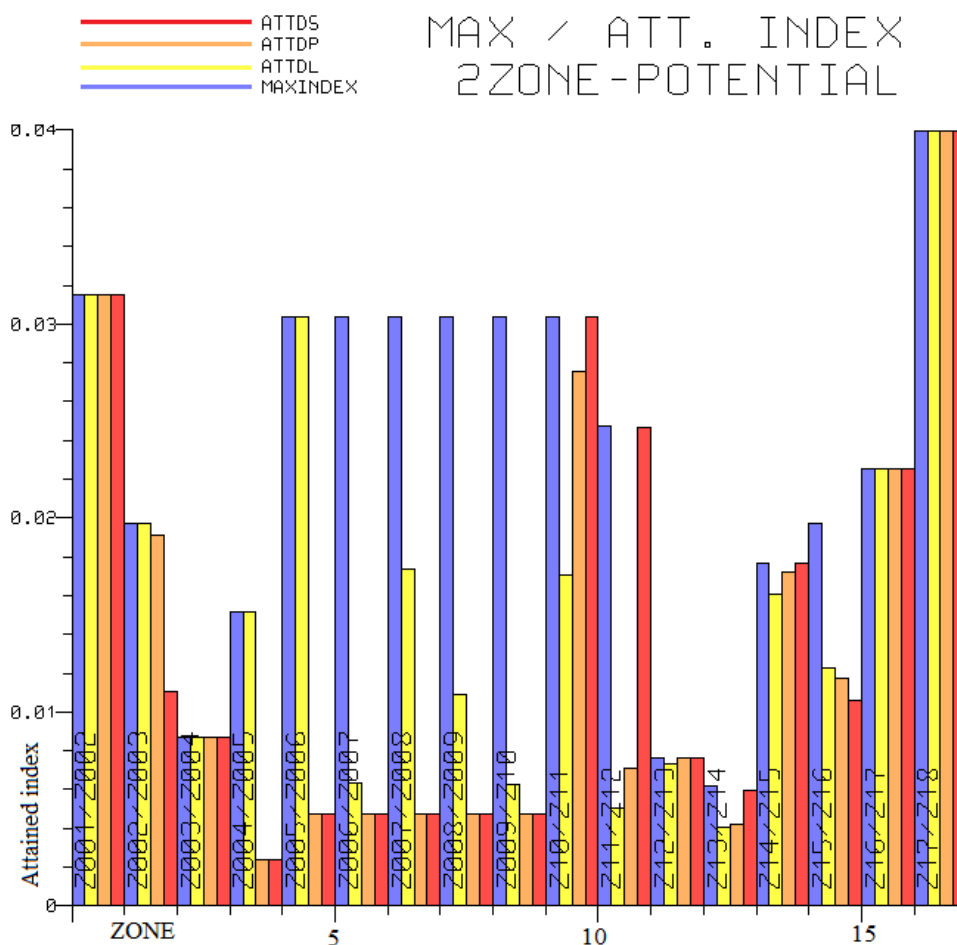


Figure 3-17: 2-zone damage potential diagram, Vessel II, arr. C, LBH3 at 0.05*B m from hull (NAPA, 2015)

3.2.3 Measures to minimize runtime in NAPA

Calculations in NAPA requires computational power and are very time consuming. Probabilistic damage stability calculations for an authentic vessel with multiple subdivisions, openings and advanced geometry requires hours of computational time. There are thousands of calculations conducted for every run and this study would take too long to conduct if every detail would have been included in the calculations. Several measures were therefore taken to minimize the runtime in NAPA.

Arrangement

In order to minimize calculations for the P_i -factor, several measures were taken to simplify the arrangement. If there are curvatures in the model, the software has to calculate the B_k factor using the principles found in SOLAS MSC.281(85): "Explanatory notes to the SOLAS Chapter II-1 Subdivision and damage stability regulations". Circular surfaces such as dry bulk tanks, tunnel thrusters and curved decks were therefore kept at a minimum. Many offshore construction vessels has moon pools fitted to be able to perform operations in higher sea levels. In order to make the model as simple as possible, moon pools were not included in any of the vessels.

As seen in the tank plans in Appendix C, there are lots of simplifications when modeling the tanks. In the machine room area there are normally many smaller tanks for fuel settling, overflow tanks, sludge tanks, bilge tanks, gray water tanks, sewage tanks, etc. In order to have as few damage cases as possible, all such tanks were combined in larger compartments.

All these simplifications to the arrangement reduces the calculation time in NAPA significantly. To be able to run as many arrangement configurations as possible, it is crucial to minimize the calculation time without influencing the results significantly.

Editing the Probabilistic manager

Since the Probabilistic manager in NAPA is used by designers when calculating damage stability in general, the manager includes calculations that are not needed for this study. Initially the user has to click on every macro that has to be rerun when changes are made to the arrangement. By editing the manager, the user can neglect certain macros if wanted. All unnecessary macros were removed from the manager to eliminate the time spent on selecting individual macros. For example the macros conducting the time consuming analyzing tools were removed from the manager. The backside of removing certain macros was discovered when analyzing the results. Since some of the needed macros were removed from the edited manager, the arrangement configurations that were furthered analyzed had to be rerun in order to include the S_i -factor diagrams, P1S- diagram and the zone-potential diagrams for the specific arrangement. The most important information regarding the attained index however, can be found for every arrangement configuration in Appendix C.

4 Results

The attained index A , is calculated for the four vessels with varying placement of the LWTB in the mid-ship section. Furthermore, the vessels have two distinct arrangement configurations. Arrangement B has U-tanks that goes up to the 2nd deck in the mid-ship section, and arrangement C has no U-tanks.

Arrangement A was almost identical to arrangement B. The transversal bulkheads for arrangement A went all the way up to 1st deck in the mid-ship section to split up the center cargo tanks. Probabilistic damage stability calculations were not conducted for arrangement A for all vessels, as arrangement A was not considered to be a realistic arrangement configuration. Arrangement A will therefore not be furthered discussed in the report.

This chapter presents the results for the damage stability calculations. It is not common to place the LWTB as close to the centerline as conducted for some of the vessels in this study. The wing tanks are usually as small as possible to utilize the internal volume of the vessel for payload instead of water ballast (Vickovic, 2015). Calculations were conducted for placements of LBH3 from $0.02*B$ up to $0.32*B$ meters from the hull. This was done to get the full picture of the development of the attained index.

4.1 Total attained index for the different vessels

This subchapter presents the results for all damage stability calculations conducted in the study. The only variation within each graph is the placement of LBH3. The two longitudinal bulkhead in the double bottom in arrangement C, remains at the same place regardless of the placement of LBH3. The aim of this subchapter is to present how the total attained index is a combination of the attained index for each loading condition.

The results gathered in the study, for the vessels with the two arrangement configurations, are shown in separate graphs for the different vessels and arrangements. The measure for the placement of LBH3 has been converted to a dimensionless value (b/B), which can be multiplied with the breadth of the vessel to get the distance from LBH3 to the hull. The graphs offer an insight in how the attained index for each loading condition contributes to the final attained index. It is important to keep in mind that A_{D1} is only 20% of the total attained index, whereas A_{Dp} and A_{Ds} is 80% of the total attained index (SOLAS, Chapter II-1, Part B-1, Regulation 7.1). The results will only be briefly discussed in this chapter, as discussions regarding the results will follow in chapter 5.

4.1.1 Vessel I

General

Table 4-1: General information, Vessel I

L_{pp} [m]	Breadth [m]	Depth moulded [m]	D_s		D_p		D_l	
			T [m]	GM [m]	T [m]	GM [m]	T [m]	GM [m]
80	22	9	7.2	2.3	6.28	1.6	4.8	1.6

Vessel I is the smallest vessel in this study with a length of 80 meters and a breadth of 22 meters. The hull on this vessel is an authentic PSV hull, which is not scaled in any directions. Since the hull is authentic, the reliability of the results are higher for this vessel compared to the larger vessels.

Arrangement B, U-tank configuration

The attained index for arrangement B increased as LBH3 was moved towards the centerline. The development of A_{Total} for the different loading conditions were approximately the same. A_{Dl} results in the highest value for A_{Total} , followed by A_{Dp} and A_{Ds} . As seen from the graph in Figure 4-1, the attained index increased until LBH3 reached $B/5$ meters from the hull. Further elaboration of the development of the attained index can be found in subchapter 5.1.1.

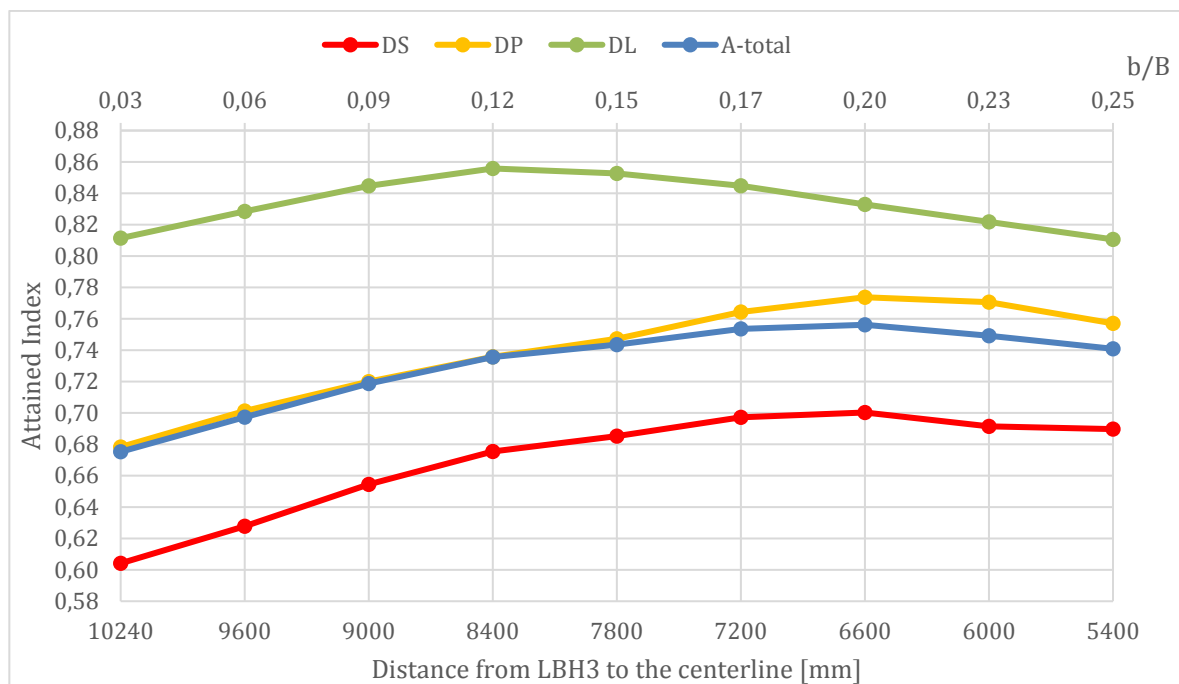


Figure 4-1: Vessel I, arrangement B

Arrangement C, without U-tanks

The attained index for this arrangement remained relatively unaffected when LBH3 was moved towards the centerline. A_{Total} declined when LBH3 passed approximately $0.15 \cdot B$ meters from the hull. The development of A_{Total} was not consistent for the different loading conditions. As seen from the graph, A_{Ds} increased whereas A_{Dl} decreased. A_{Dl} still results in the highest attained index, followed by A_{Dp} and A_{Ds} , which was the same as for arrangement B.

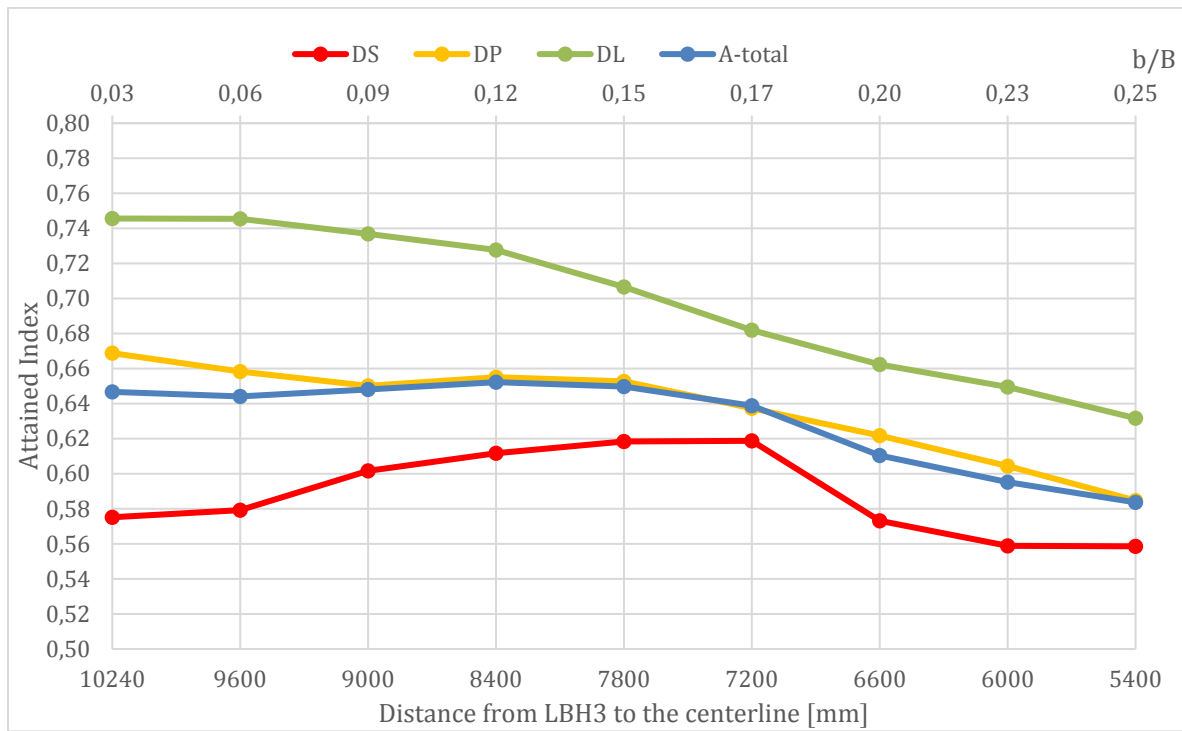


Figure 4-2: Vessel I, arrangement C

4.1.2 Vessel II

General

Table 4-2: General information, Vessel II

L_{pp} [m]	$Breadth$ [m]	$Depth\ moulded$ [m]	D_s		D_p		D_l	
			T [m]	GM [m]	T [m]	GM [m]	T [m]	GM [m]
95	24	9.6	7.4	2.3	6.44	1.6	4.5	1.6

The hull for Vessel II was a scaled version of Vessel I and was comparable to a large PSV. The arrangement configuration was the same as for Vessel I in regards to the placement of machinery room, thruster room, roll-reduction tanks, etc.

Arrangement B, U-tank configuration

When LBH3 was moved towards the centerline, the attained index increased. The progress of A_i , when LBH3 was moved, were approximately the same for the different loading conditions. A_{Dl} increased faster when the bulkhead was relatively close to the hull, but declined when LBH3 was further than $0.13 \cdot B$ from the hull. A_{Dp} and A_{Ds} had a steady slope, increasing for most movements of LBH3 towards the centerline. The total attained index increased until the bulkhead reached $0.23 \cdot B$ meters from the hull.

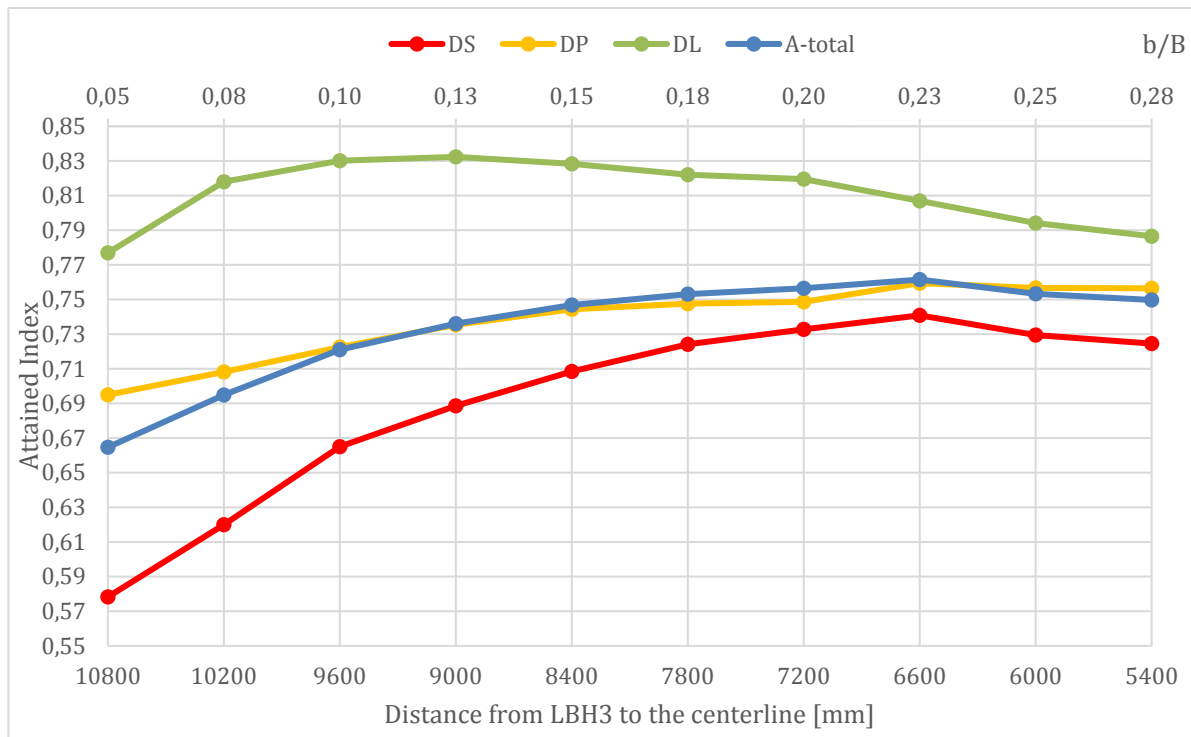


Figure 4-3: Vessel II, arrangement B

Arrangement C, without U-tanks

The attained index for this arrangement remained relatively unaffected when LBH3 was moved towards the centerline. A_{Total} declined slightly when LBH3 passed $0.15 \cdot B$ meters from the hull. The development of A_i was not consistent for the different loading conditions. As seen from Figure 4-4, A_{Ds} developed very different compared to A_{Dl} and A_{Dp} . A_{Ds} increased for some movements, whereas A_{Dl} and A_{Dp} decreased. This was almost the same situation as seen for arrangement C for Vessel I. A_{Total} increased as LBH3 was moved from $0.05 \cdot B$ to $0.08 \cdot B$ m, but it leveled out and declined as the bulkhead was moved closer to the centerline.

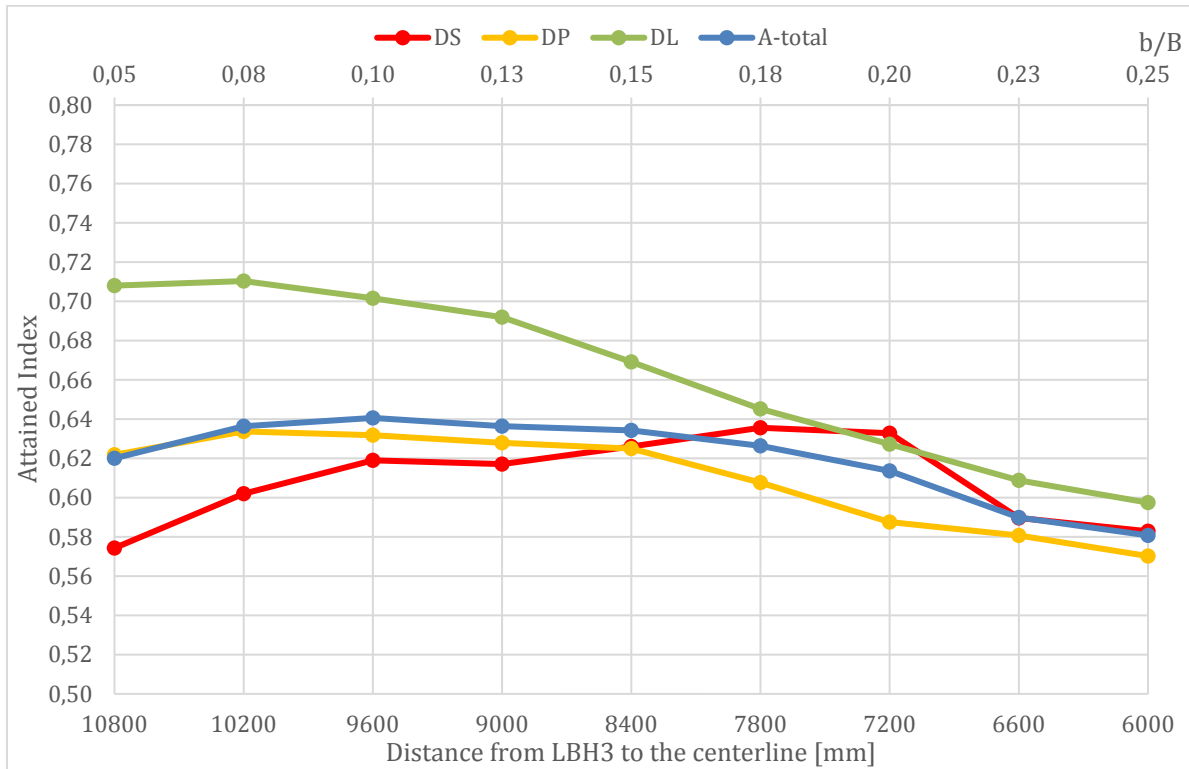


Figure 4-4: Vessel II, arrangement C

4.1.3 Vessel III

General

Table 4-3: General information, Vessel III

L_{pp} [m]	Breadth [m]	Depth moulded [m]	D_s		D_p		D_l	
			T [m]	GM [m]	T [m]	GM [m]	T [m]	GM [m]
118	28	12	8.5	2.5	7.74	1.8	6.6	1.8

Vessel III, a vessel with a length of 118 meters and breadth of 28 meters, was comparable with a small offshore construction vessel. The arrangement was the same as Vessel I and II regarding thruster room placement, cargo tanks in the mid-ship section and superstructure, but the machinery room was different. Vessel III had two machinery rooms and the machinery rooms were longitudinally divided. This will cause large unsymmetrical damages, and are therefore usually avoided for vessels where probabilistic damage calculations are conducted. In order to see how much the division of the machinery room affected the attained index, Vessel IV had a transversal subdivision of the machinery room. The effect of longitudinally divided vs transversely divided machinery room will be discussed in the next chapter.

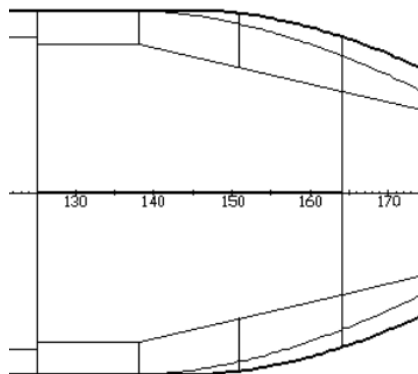


Figure 4-5: Longitudinal machinery room division, Vessel III

Arrangement B, U-tank configuration

The step between Vessel II and III changed the relation between A_{Dl} , A_{Dp} , and A_{Ds} . As seen in Figure 4-6, the attained index for D_s was higher than D_p and D_l for most placements of LBH3. This will be furthered discussed in chapter 5. The total attained index constantly increased as LBH3 was moved towards the centerline for the first movements. The development of A_{Dl} when LBH3 was relocated did not match the development of A_{Ds} and A_{Dp} . This can most likely be explained by using the same argumentation as described in subchapter 5.2.

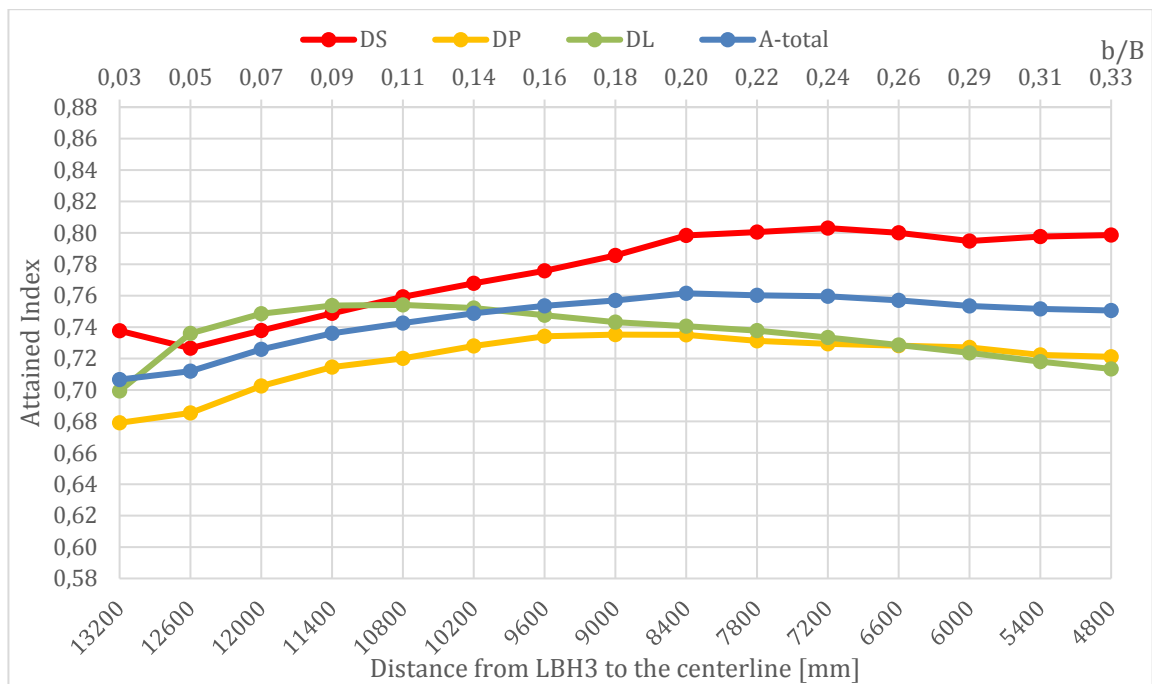


Figure 4-6: Vessel III, arrangement B

Arrangement C, without U-tanks

The attained index for this arrangement decreased as LBH3 was moved towards the centerline. A_{Total} declined slowly when the wing tank breadth passed $0,07 \cdot B$ meters from the hull side. A_i developed relatively consistently for all loading conditions. A_{Dl} decreased faster than A_{Dp} when LBH3 reaches $0,11 \cdot B$ meters from the hull, but other than that the developments of the different loading conditions were similar.

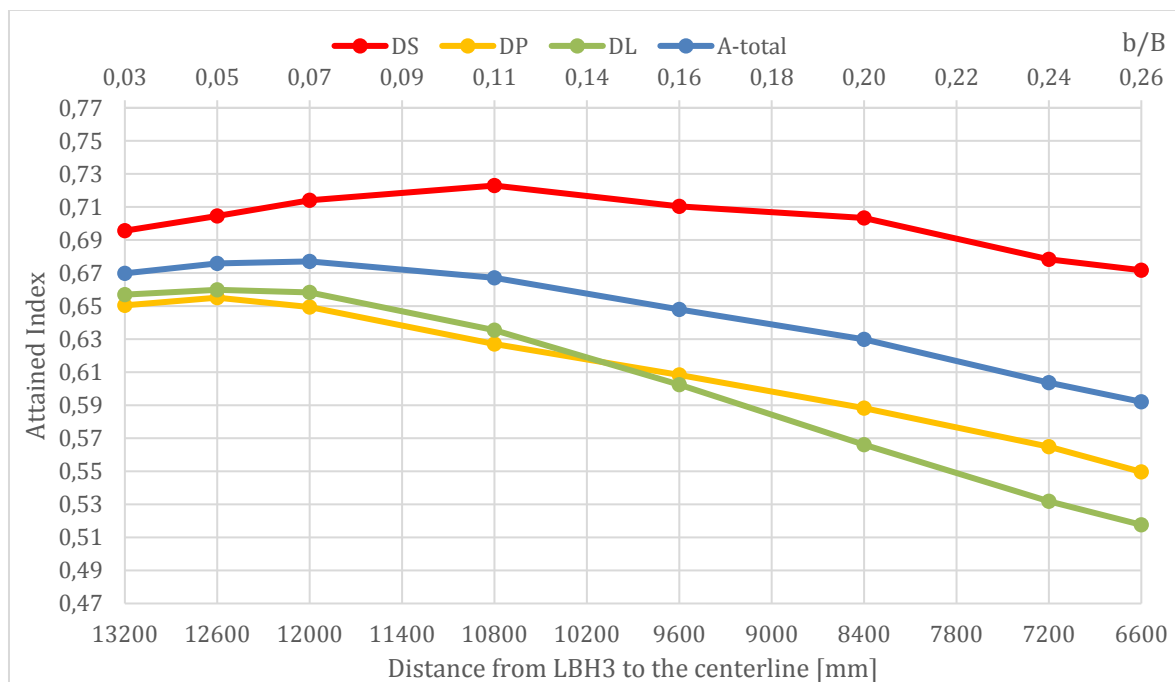


Figure 4-7: Vessel III, arrangement C

4.1.4 Vessel IV

General

Table 4-4: General information, Vessel IV

L_{pp} [m]	Breadth [m]	Depth moulded [m]	D_s		D_p		D_l	
			T [m]	GM [m]	T [m]	GM [m]	T [m]	GM [m]
130	30	12.5	8.6	2.5	7.84	1.8	6.7	1.8

Vessel IV had typical dimensions of an offshore construction vessel. This ship was the largest vessel in the study with a length of 130 meters between the perpendiculars. The arrangement configuration was the same for this vessel as for the others in the study, except for the machinery room. As mentioned for Vessel III, the two largest vessels had two machinery rooms. Vessel IV had a transversal bulkhead to divide the two machinery rooms. A comparison of the results for the two machinery room configurations can be found in chapter 5.1.3.

Arrangement B, U-tank configuration

The same relation between A_{D_s} , A_{D_p} , and A_{D_l} , as seen for Vessel III, applied for Vessel IV. The attained index for D_s was higher than D_p and D_l for all placements of LBH3. When LBH3 was moved further from the hull, the total attained index increased constantly, corresponding with the other vessels with the same arrangement configuration.

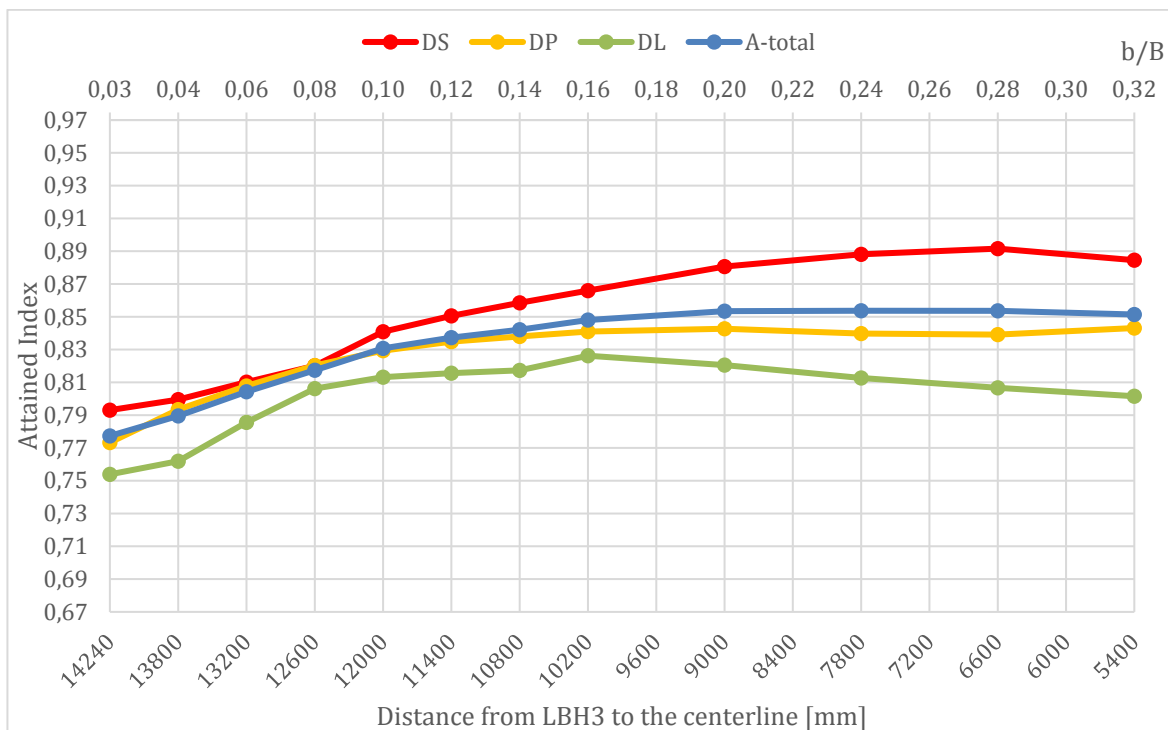


Figure 4-8: Vessel IV, arrangement B

Arrangement C, without U-tanks

When there were no U-tanks in the arrangement, the total attained index declined as LBH3 was moved towards the centerline and the volumes of the wing tanks increased. A_{Total} increased until the wing tank breadth was larger than $0.06 \cdot B$ m. When the wing tanks were too large the attained index declined as LBH3 was moved towards the centerline. A_i developed consistently for all loading conditions. A_{DS} is not as consistent as the rest, but the overall progress was the same.

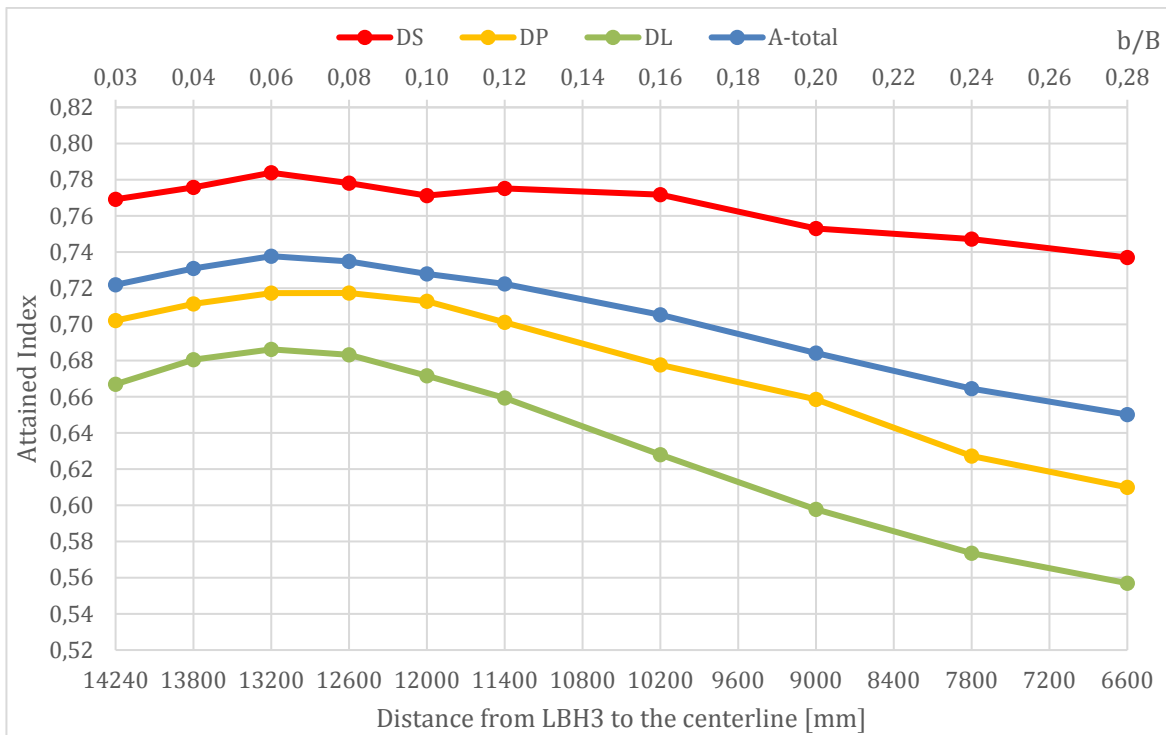


Figure 4-9: Vessel IV, arrangement C

5 Discussion

Introduction

The previous chapter presented the results from the probabilistic damage stability calculations. This chapter will compare the results from the four vessels with the different arrangement configurations. The main objective of this chapter is to analyze the development of the total attained index for the four vessels. The parameters affecting the results of the attained index will be analyzed to conclude why A_{Total} changed as the placement of the LWTB changed. As U-tanks are common to introduce to increase the attained index, the results for arrangement B and C will be compared to see how much the subdivision in the double bottom affects the total attained index. The developments were analyzed to find out if there is a correlation between the developments of the attained indexes for different ship sizes with different arrangement configurations. As seen from the results presented in Chapter 4, the attained indexes for Vessel III and IV, were higher for the deeper loading conditions compared to the lighter conditions. To find out why this was different from Vessel I and II, the attained index for the different loading conditions for Vessel III and IV will be discussed.

5.1 The attained index for the different vessels

The following subchapters aims to compare the calculated attained indexes for the vessels in the study. The approach is to compare the vessels with the same arrangement configuration and thereafter compare the development of A_{Total} for arrangement B and C. Since the GM values are different for some of the vessels, it is of limited interest to compare the exact values, because the magnitude of GM influences A_{Total} significantly. But the specific values for the total attained indexes are to some extent comparable for vessels with the same GM values.

S-factor diagrams were used when analyzing the S_i -factor for different damage cases. Enlarged versions of the S-factor diagrams presented in this chapter can be found in Appendix B or Appendix C.

5.1.1 The development of the attained index

This subchapter's goal is to describe the development of the attained index for the four vessels in the study. The results for all vessels are combined in the same graphs to see if there are correlations in the development of the attained index for the different vessels as LBH3 is moved.

The results gathered in the study, for the vessels with the two arrangement configurations, are shown in Figure 5-1 and Figure 5-11. LBH3 was first placed as close to the hull as permitted by the rules and relocated frame by frame towards the centerline. The moved

distance compared to ship breadth was not equal for all vessels, as LBH3 was moved in steps of 600 mm. The points on the graphs are therefore situated at different x-values.

In order to compare the results with the deterministic damage requirements, B/5 are included in the graph. The minimum required height of the double bottom, B/20, has also been included, as this is a common placement of the LWTB (IMO, 2006a).

The development of A_{Total} for arrangement B

The development of the attained index for arrangement B corresponds to Wärtsilä's expectations. From experience they have discovered that it is generally beneficial to move the LWTB closer to the center line in order to improve the attained index. As seen from Figure 5-1, the attained index levels out when LBH3 reaches approximately B/5. The development is similar for the different vessels even though the specific value for the attained index is different.

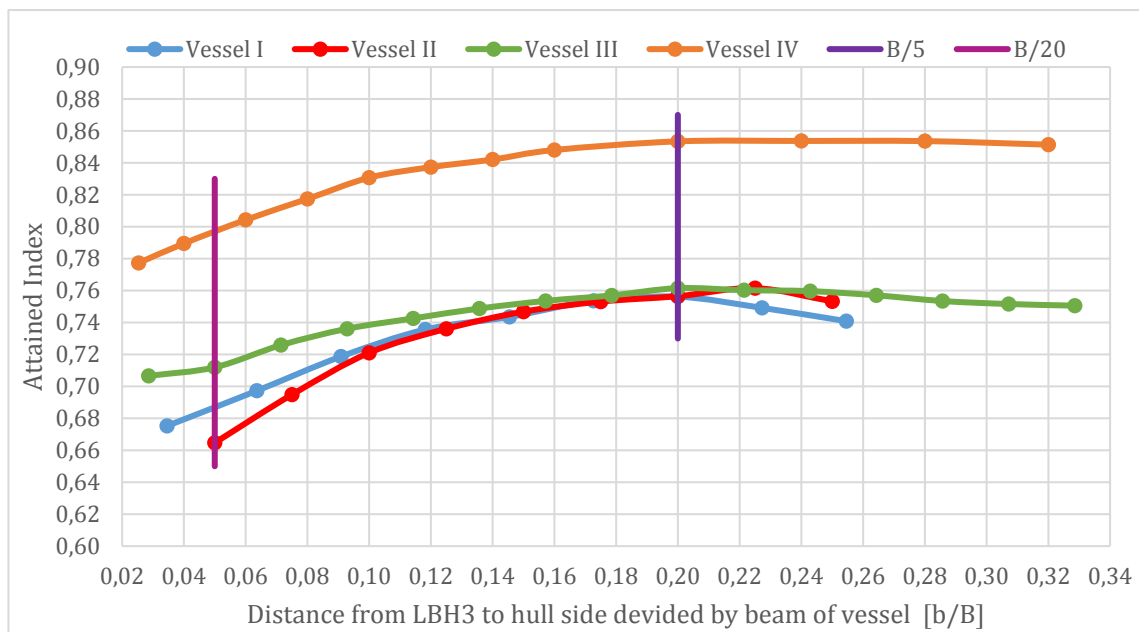


Figure 5-1: Vessels with U-tank configuration, arrangement B

When trying to find out why the attained index increases when moving LBH3 towards the centerline, we need to look at which factors that will play a part in the calculations. We know from Eq. 7 that $A = \sum_1^{i=t} V_i P_i S_i$. Each factor will be analyzed individually when discussing the development of A_{Total} . It is also important to look at how the different factors affects each other to find out why the attained index is changing. Since the development of the attained index is similar for the four vessels it is expected that the different factors behave in the same manner for all vessels. Two vessels will be analyzed to find out why the attained is increasing as LBH3 is moved towards the centerline. Vessel I and IV will be analyzed as they are the smallest and largest vessels.

Vessel I

V_i-factor

When calculating the V_i-factor, the height from the initial waterline to the horizontal subdivisions will influence the results. Since the waterline and the horizontal subdivisions remains the same when LBH3 is moved, the V_i-factor will not be influenced. As seen from Figure 5-4 and Figure 5-5, damages to compartments below the waterline has a white color. The V_i-factor for U-tank damages will be zero and will therefore not contribute to the attained index. But V_i is the same for all placements of LBH3, and will therefore not influence the attained index.

S_i-factor

The volumes of the internal compartments changes as LBH3 is relocated, which will influence the stability of the vessel after damage. By shifting the placement of the LWTB towards the centerline, the volumes of the upper wing tanks and U-tanks increases and the volumes of the center tanks decreases. When there is a damage to the upper wing tanks, the vessel will heel over. If the vessel heels more than 7 degrees after a damage, the S_i-factor will start to decrease. It can be seen from Eq. 17, that when the equilibrium heeling angle, (θ_e), exceeds 7 degrees the K factor will decrease. If θ_e exceeds 15 degrees the K factor equals 0, and the S_i-factor will consequently be zero. The upper wing tanks are not large enough to heel the vessel over significantly until LBH3 is relatively close to the centerline.

From the S-factor diagrams in Figure 5-2 and Figure 5-3, it seems like damages to the wing tanks starts to get critical, when LBH3 is moved inwards. This is due to the reduced GZ_{max} , *Range* and the increasing heeling moment, resulting in a lower S_i-factor that influences A_{Total} negatively. The circled, two zone damages, has been chosen to explain the development of the S_i-factor, and can be seen in Figure 5-4 and Figure 5-5.

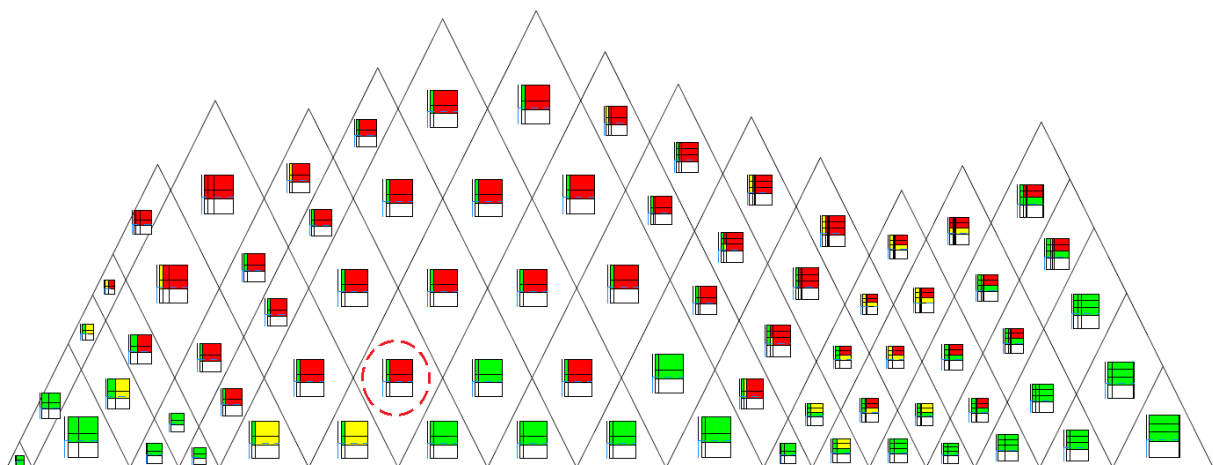


Figure 5-2: S-fac diagram for Vessel I, arrangement B, D_p, LBH3 at 0.06*B meters from the hull

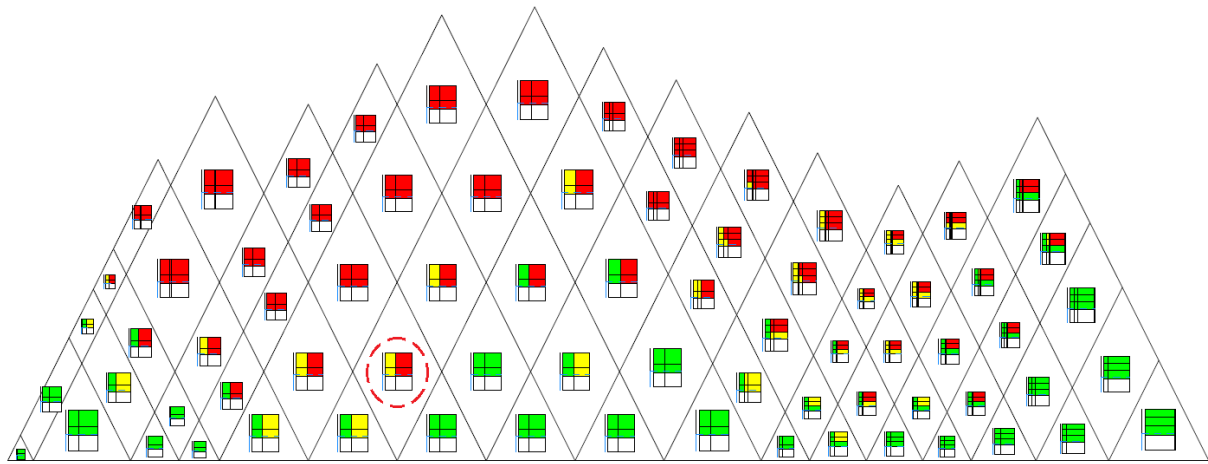


Figure 5-3: S-fac diagram for Vessel I, arrangement B, D_p, LBH3 at 0.2*B meters from the hull

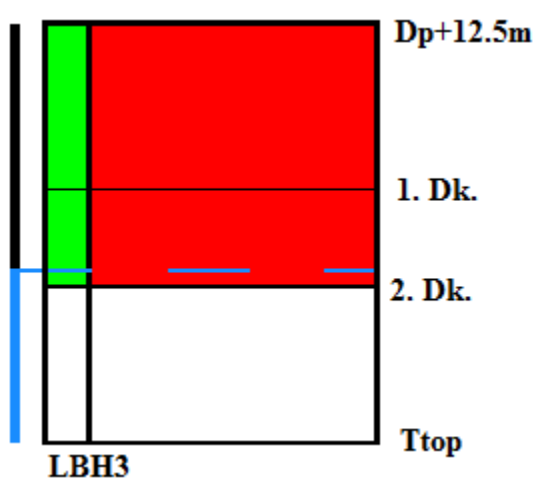


Figure 5-4: Closer view of damage case when LBH3 is at 0.06*B from the hull

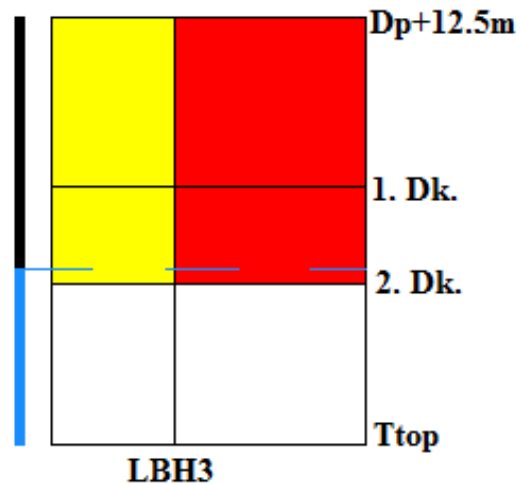


Figure 5-5: Closer view of damage case when LBH3 is at 0.2*B from the hull

Table 5-1: Results for damage cases in figures above

Case	S_i -factor, LBH3 at $0.06*B$	S_i -factor, LBH3 at $0.2*B$
Wing tank damage	1	0.993
Center tank damage	0	0

From Figure 5-4 and Figure 5-5 it seems like the S_i -factor is reduced for wing tank damages as LBH3 is moved towards the centerline. Even though it seems like there is changes to the S-factor diagram as LBH3 is moved, the S_i -factors are not changing significantly. From Table 5-1, we can see how much the S_i -factor changes as LBH3 is moved towards the centerline. The wing tank damage gets a yellow color, but the factor is only reduced by 0.007 as LBH3 is moved from 0.06*B to 0.2*B. When comparing the two S-factor diagrams it can be seen that the overall S_i -factors remains approximately the same for most damage cases, even

though some damages changes color. This indicates that both arrangements will withstand most damages in the same manner. Since the S_i -factors are not changing significantly, it indicates that it is the P_i -factor that will influence the results.

P_i -factor

P_i is dependent on the damage extent longitudinally and transversely as seen from Eq. 9: $P_i = p(x1_j, x2_j) \cdot [r(x1_j, x2_j, b_k) - r(x1_j, x2_j, b_{k-1})]$. $P(x1, x2)$ is the longitudinal contribution to the P_i -factor and is calculated based on statistics for damage extents in the longitudinal direction (Lützen, 2001). $[r(x1_j, x2_j, b_k) - r(x1_j, x2_j, b_{k-1})]$ is the transversal factor that is calculated based on statistics from damage penetration (Lützen, 2001). For damage cases where LBH3 is penetrated, b_k is the distance from the hull to the centerline of the vessel, and b_{k-1} is the distance from LBH3 to the hull. An illustration of b_k and b_{k-1} for the two damage scenarios can be seen in Figure 5-6 and Figure 5-7.

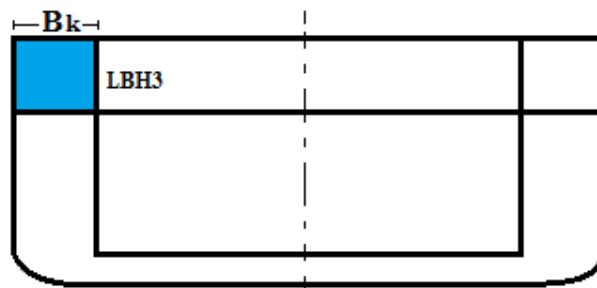


Figure 5-6: Illustration of B_k for damage cases when LBH3 remains intact

The P_i -factor for damage cases where LBH3 remains intact will depend on $r(B_k)$, as illustrated in Figure 5-6. $r(B_{k-1})$ is not included when calculating the P_i -factor for this damage case. From Figure 2-9: *Distribution of non-dimensional penetration damages*, we can see that if b increases, r increases accordingly. As LBH3 is moved towards the centerline, B_k will increase and P_i will increase accordingly. This means that the probability of damage cases to the wing tanks and U-tanks will increase when LBH3 is moved towards the centerline.

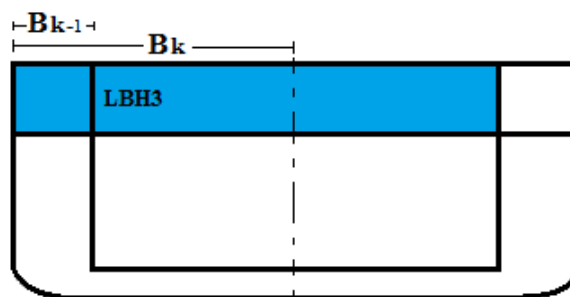


Figure 5-7: Illustration of B_k and B_{k-1} for damage cases when LBH3 is penetrated

$r(b_k)$ is only dependent on the distance from the hull to the centerline which will remain the same regardless of the placement of LBH3. $r(b_{k-1})$ however, will change when LBH3 is moved, because it is dependent on the distance from LBH3 to the hull. As LBH3 is moved towards the centerline, $r(b_{k-1})$ will increase and $r(b_k)$ will remain constant. Since $P(x1, x2)$ is multiplied with $[r(x1_j, x2_j, b_k) - r(x1_j, x2_j, b_{k-1})]$ to get the P_i -factor, a larger B_{k-1} , will result

in a lower P_i -factor. This means that the probability of damage cases that penetrates LBH3 decreases as LBH3 is moved towards the centerline. The graph below illustrates how the P_i -factor changes according to the placement of LBH3.

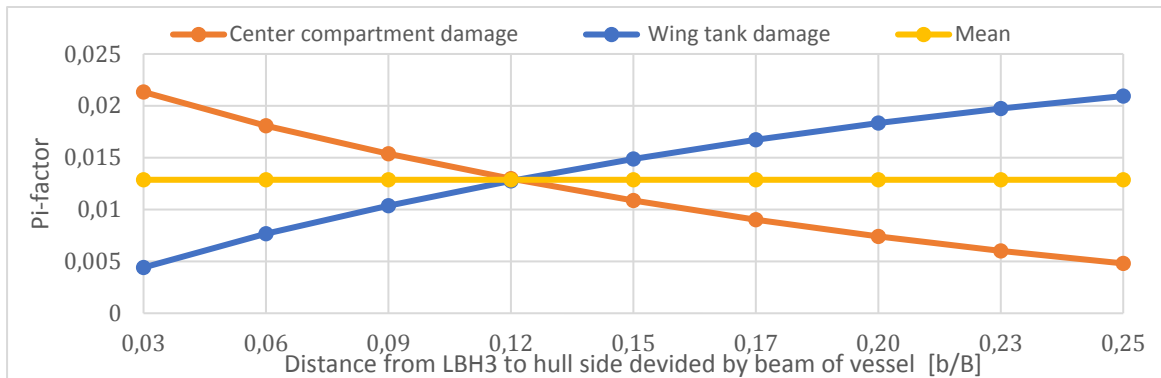


Figure 5-8: P_i -factor for different damages with different placements of LBH3

As seen from the results in Figure 5-8, the P_i -factor for one damage case evens out the other damage case in the same zone. Since the P_i -factor is multiplied with V_i and S_i to form the total attained index, it can influence the results. If the S_i - and V_i -factors remains the same for all damage cases for two different arrangements, the P_i -factor can alter the results. When damages with a favorable S_i - and V_i -factor gets a higher probability, the total attained index will increase.

Total attained index $A = \sum_1^{i=t} V_i P_i S_i$

How are the individual factors influencing the total attained index when they are combined? The volume of the compartments inside LBH3 are large, which influences the S_i -factor negatively when damaged. The effect on the S_i -factor when these compartments are damaged can be seen in Figure 5-2 and Figure 5-3. When LBH3 is moved towards the centerline, the S_i -factor for most wing tank damages remains the same.

The S_i -factor for damages when LBH3 is penetrated, remains approximately the same regardless of the placement of the bulkhead. When LBH3 is moved closer to the centerline, the probability of damages to the center cargo tanks decreases. These damage cases are critical and the S_i -factors for these cases are low. The probability of wing tank and U-tank damages increases as LBH3 is moved towards the centerline. These cases generally has a high S_i -factor.

When LBH3 is moved towards the centerline the probability for damages where the S_i -factor is high increases and the probability of critical cases decreases. This is why the total attained index increases as LBH3 is moved inwards for the first moves. When LBH3 is placed relatively close to the centerline, damages to the wing tanks will start to get critical and the vessel will heel over due to the massive volume of the wing tank. This is why the development of the total attained index levels out as LBH3 is moved close to the centerline.

Vessel IV

V_i-factor

When calculating the V_i-factor, the height from the initial waterline to the horizontal subdivisions will influence the results. Since the waterline and the horizontal subdivisions remains the same when LBH3 is moved, the V_i-factor will not be influenced. As seen from the S-factor diagrams, damages to the U-tanks does not get a V_i-factor of 0, because the waterline is below 2nd deck.

S_i-factor

By analyzing the S-factor diagrams for the two placements of the bulkhead, we can see how the S_i-factor is changing when LBH3 is relocated. As seen from Figure 5-9 and Figure 5-10, S_i remains 1 for all one zone damages for both placements of LBH3. For some two and three zone damages we can see that the S_i-factor is influenced. The color remains the same for many damage cases, but since the S_i-factor can be between 0 and 1 when the color is yellow, these cases has to be further analyzed. By checking the exact S_i-factor values for the damage cases with the red circle in Figure 5-9 and Figure 5-10 we find the following results:

Table 5-2: Results for damage cases with the red circle in Figure 5-9 and Figure 5-10

<i>Case</i>	<i>S_i-factor, LBH3 at 0.06*B</i>	<i>S_i-factor, LBH3 at 0.14*B</i>
<i>Wing tank damage</i>	<i>1</i>	<i>1</i>
<i>Center tank damage</i>	<i>0.74</i>	<i>0.95</i>

This indicates that both arrangements will withstand most damages in the same manner. Both arrangements will withstand damages that does not penetrate LBH3, but will encounter problems for some two and three zone cases when the bulkhead is breached. Even though it seems like the S_i-factor is the same for all cases that are yellow, the S_i-factor is actually increasing. The S_i-factor does not vary significantly, but it will influence the total attained index.

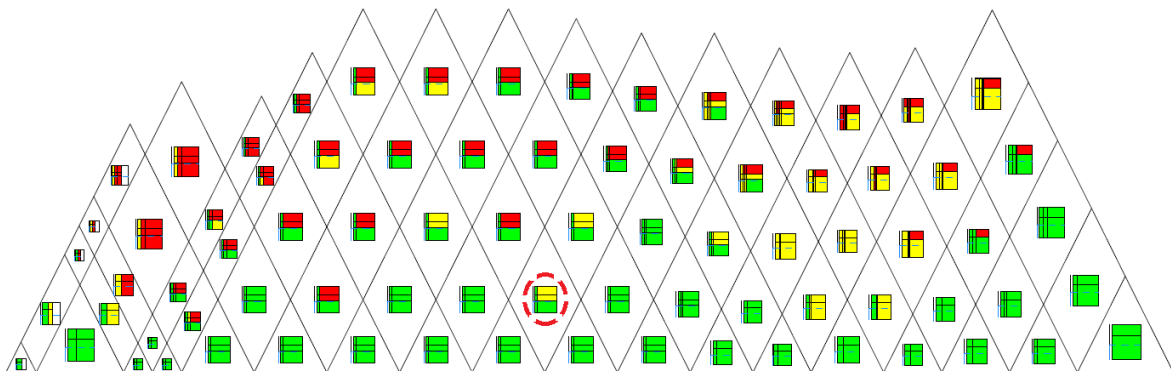


Figure 5-9: S-fac diagram, Vessel IV, arrangement B, D_p, with LBH3 at 0.06*B m from the hull

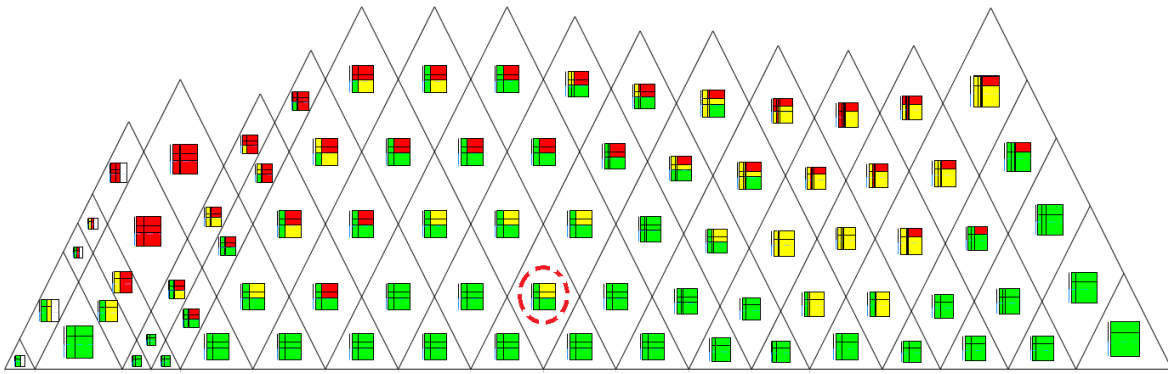


Figure 5-10: S-fac diagram, Vessel IV, arrangement B, D_p , with LBH3 at $0.14 \cdot B$ m from the hull

P_i-factor

As concluded earlier, P_i will decrease for damage cases where LBH3 is penetrated as LBH3 is moved towards the centerline. Consequently P_i will increase for wing tank and U-tank damages, when LBH3 is moved closer to the centerline.

Total attained index for Vessel IV, $A = \sum_{i=1}^t V_i P_i S_i$

How are the individual factors influencing the total attained index when they are multiplied? The volume of the compartments inside LBH3 are large, which influences the S_i -factor negatively for some damage cases. When LBH3 is moved towards the centerline, the S_i -factor for most wing tank damages has an S_i -factor of 1. The S_i -factor for center tank damages will increase slightly when the longitudinal bulkhead is moved inwards, but it is still below 1 for many damage cases.

As LBH3 is moved closer to the centerline, the probability of center tank damages decreases and the probability of wing tank damages increases. Wing tank damages are not critical and the S_i -factor is 1 for most cases. Center tank damages are not very critical, but the S_i -factor is below 1 for many cases.

The probability of damages that has a high S_i -factor increases as LBH3 is moved towards the centerline, and the probability decreases for damages with a lower S_i -factor. This is why the total attained index will increase as LBH3 is moved closer to the centerline.

Conclusion for the development of A_{total} for all vessels with arrangement B

The combination of P_i and S_i is the decisive factor for the development of the attained index for arrangement B. The probability decreases for center compartment damages that results in a low S_i -factor. The probability increases for wing tank and U-tank damages that results in a high S_i -factor. This is why the total attained index increases as LBH3 is moved towards the centerline.

When LBH3 is placed relatively close to the centerline, damages to the wing tanks and U-tanks will start to get critical due to the large volumes. This is why the development of the total attained index levels out as LBH3 is moved close to the centerline.

The development of A_{Total} for arrangement C

The development of the attained index for the different vessels with arrangement C does not correspond as well as for arrangement B. As seen from Figure 5-11, the overall attained index decreases as LBH3 is moved towards the centerline. A_{Total} increases for the first movements of LBH3 for Vessel II, III and IV, but the attained index remains relatively constant for Vessel I.

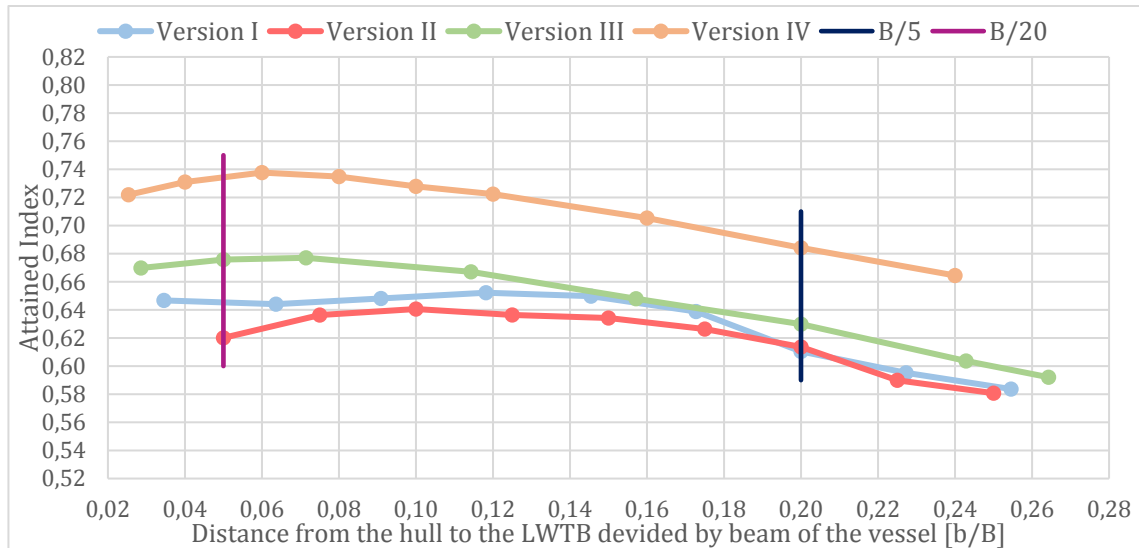


Figure 5-11: Comparison of vessels with arrangement C

When analyzing the development of A_{Total} for arrangement C, we can use the same approach as for arrangement B. We know that $A = \sum_{i=1}^t V_i P_i S_i$, and by analyzing the development of the different factors we can find out which factors that will influence the total attained index for the different vessels. Since the development is not proportional for all vessels, it is necessary to analyze more than one ship. We will start out by looking at Vessel I and II, as the development of the attained index is similar for these vessels.

Vessel I and II

V_i -factor

The V_i -factor is only dependent on the distance between the initial waterline and the horizontal subdivisions. Since the height of the decks as well as the draught remains the same for all movements of LBH3, the V_i -factor will remain the same. It is important to note that all damages to the lower wing tanks and lower cargo compartments gets a V_i -factor of 0 for D_p and D_s because the waterlines are above 2nd deck for these loading conditions.

S_i -factor

As mentioned in the analysis for arrangement B, the S_i -factor is influenced by the stability of the vessel after damage. When LBH3 is moved, the volumes of the internal compartments will change, which will influence the stability of the vessel when damaged. As LBH3 is moved towards the centerline, the volume of the wing tanks will increase and the center tank volumes will decrease. The S-factor diagrams displayed in Figure 5-12, Figure 5-13 and Figure 5-14 can be used when analyzing Vessel II.

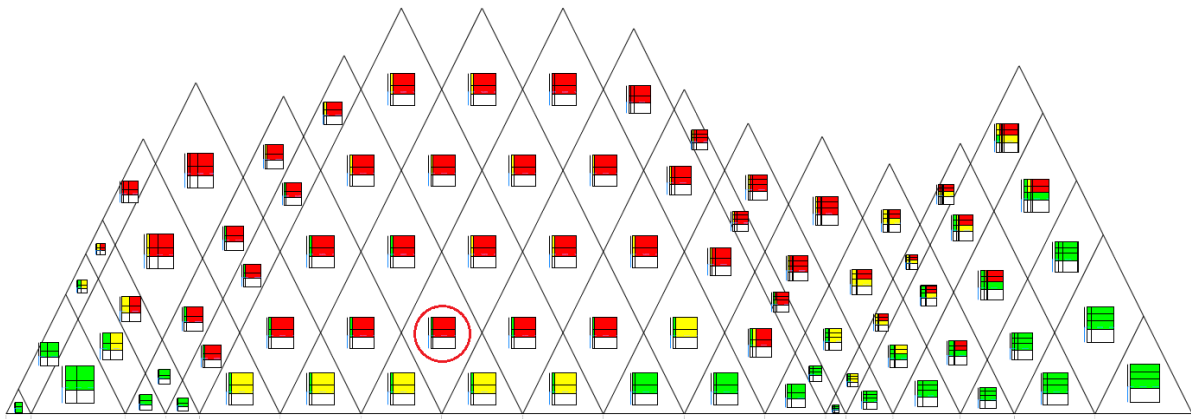


Figure 5-12: S-factor diagram for Vessel II, D_p , ArrC, LBH3 at $0.05*B$ m from the hull

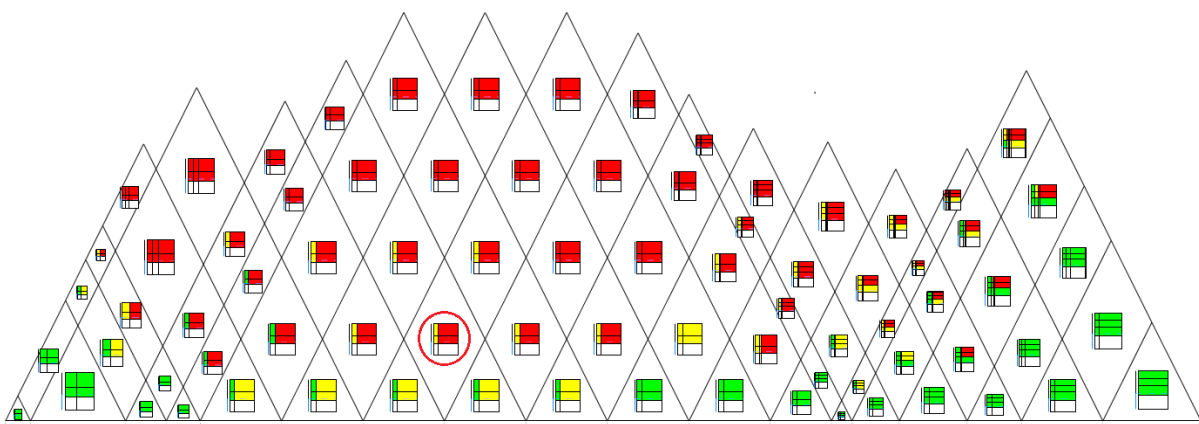


Figure 5-13: S-factor diagram for Vessel II, D_p , ArrC, LBH3 at $0.1*B$ m from the hull

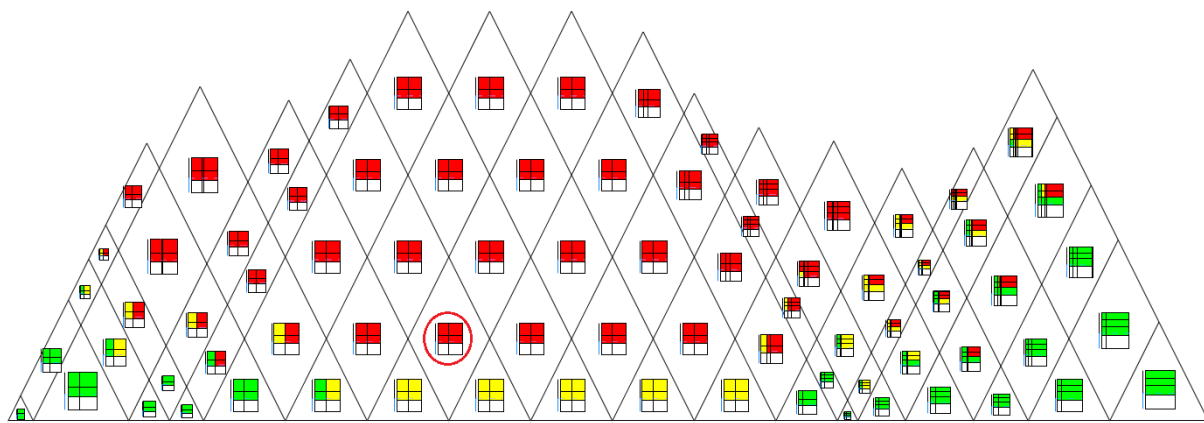


Figure 5-14: S-factor diagram for Vessel II, D_p , ArrC, LBH3 at $0.225*B$ m from the centerline

We can see from the red and yellow colors in the S-factor diagrams, that most damage cases to the center compartments, will result in an S_i -factor of less than one. This is due to the large volumes of the center cargo tanks. As LBH3 is moved further from the hull, the volumes of the cargo tanks are reduced, but the S_i -factor still remains 0 when the center compartments are flooded.

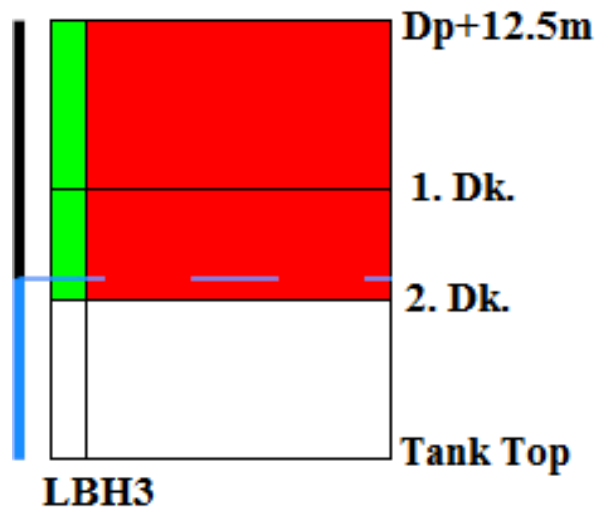


Figure 5-15: Damage case where LBH3 is at $0.05 \cdot B$ meters from the hull

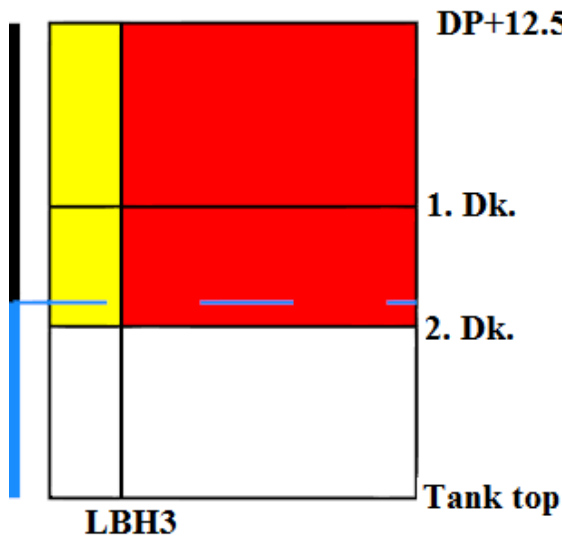


Figure 5-16: Damage case where LBH3 is at $0.1 \cdot B$ meters from the hull

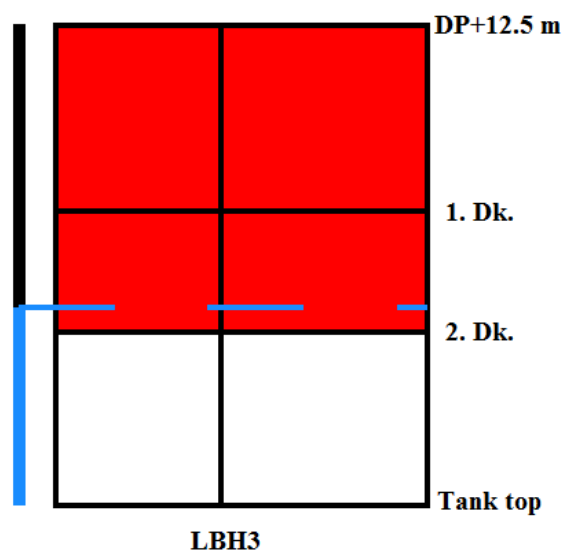


Figure 5-17: Damage case where LBH3 is at $0.225 \cdot B$ meters from the hull

Figure 5-15, Figure 5-16 and Figure 5-17 shows that the wing tank damages changes S_i -factor when LBH3 is moved from $0.05 \cdot B$ meters to $0.225 \cdot B$ meters from the hull. Wing tank damages results in an S_i -factor of 1 when LBH3 is placed at $0.05 \cdot B$. When LBH3 is at $0.1 \cdot B$ meters, the S_i -factor is around 0.85 for wing tanks damages, but when LBH3 is at $0.225 \cdot B$ meters from the hull the S_i -factor is 0.

P_i-factor

As mentioned earlier, the P_i-factor is dependent on damage length and placement of longitudinal bulkheads: $P_i = p(x_{1j}, x_{2j}) \cdot [r(x_{1j}, x_{2j}, b_k) - r(x_{1j}, x_{2j}, b_{k-1})]$. As concluded earlier, P_i will decrease when LBH3 is moved towards the centerline for damages to the center compartments. Consequently P_i will increase for cases when LBH3 remains intact.

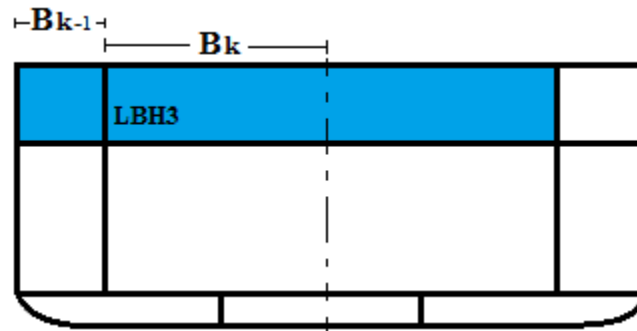


Figure 5-18: Illustration of B_k and B_{k-1} when LBH3 is penetrated for Vessel II, arrangement C

Total attained index for Vessel I and II, arrangement C

As for arrangement B, the volumes of the compartments inside LBH3 are large, having a considerable impact on the S_i-factor when damaged. The S_i-factor is 0 for most cases when LBH3 is penetrated, regardless of the placement of LBH3. When wing tanks are damaged their S_i-factors are nearly 1 for most cases, when LBH3 is close to the hull. But as LBH3 is moved inwards the S_i-factor decreases for wing tank damages.

The probability of wing tank damages increases as LBH3 is moved towards the centerline. For the first moves, these cases have a high S_i-factor. Damages penetrating LBH3 are critical regardless of the placement of the bulkhead. When LBH3 is moved towards the centerline, the probability of center tank damages decreases. When the probability increases for damages that results in a high S_i-factor and the probability decreases for damage cases that results in a low S_i-factor, the total attained index will increase. That is why the total attained index is increasing for the first moves for Vessel II.

As LBH3 is moved further the S_i-factor is decreasing for wing tank damages. When the bulkhead is relatively close to the centerline, both wing tank damages and center tank damages are critical. This is why the total attained index is decreasing as the bulkhead is moved further towards the centerline.

Vessel III and IV

The total attained index increases for the first moves of LBH3. As the bulkhead is moved further from the hull the total attained index decreases. But why is this happening?

V_i- factor

The arguments used for Vessel I and II can be used for Vessel III and IV as well. The V_i-factor is only dependent on the distance between the initial waterline and the horizontal subdivisions. Since the height of the decks as well as the draught remains the same for all movements of LBH3, the V_i-factor will remain unchanged.

P_i-factor

As concluded earlier, P_i will decrease for damages to the center tanks as LBH3 is moved towards the centerline. Consequently P_i will increase for wing tank damages as LBH3 is moved closer to the centerline.

S_i-factor

As mentioned for Vessel I and II, the S_i-factor is influenced by the stability of the vessel after damage. When analyzing Vessel III, we can see from Figure 5-19, Figure 5-20, Figure 5-21 and Figure 5-22 that most two zone damages penetrating LBH3 results in an S_i-factor of less than one for all placements of the bulkhead. This is due to the vast volumes of the center cargo tanks.

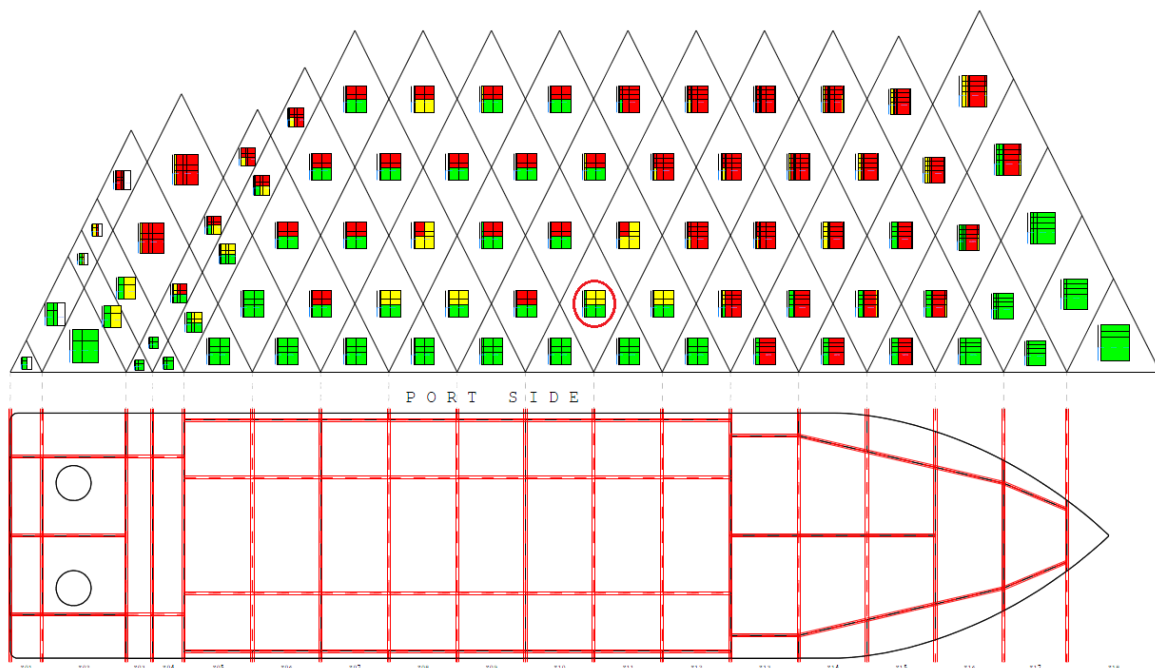


Figure 5-19: S-factor diagram Vessel III, D₁, Arrangement C, LBH3 at 0.03*B m from hull

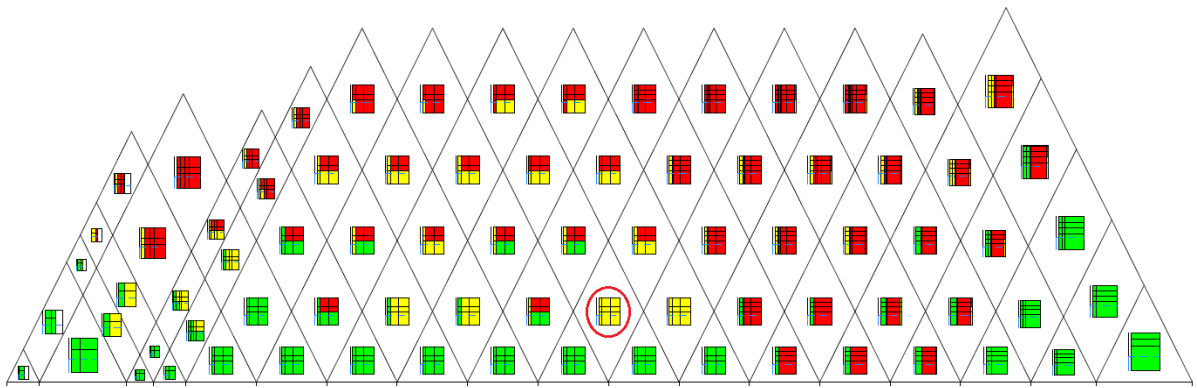


Figure 5-20: S-factor diagram Vessel III, D₁, Arrangement C, LBH3 at 0.07*B m from hull

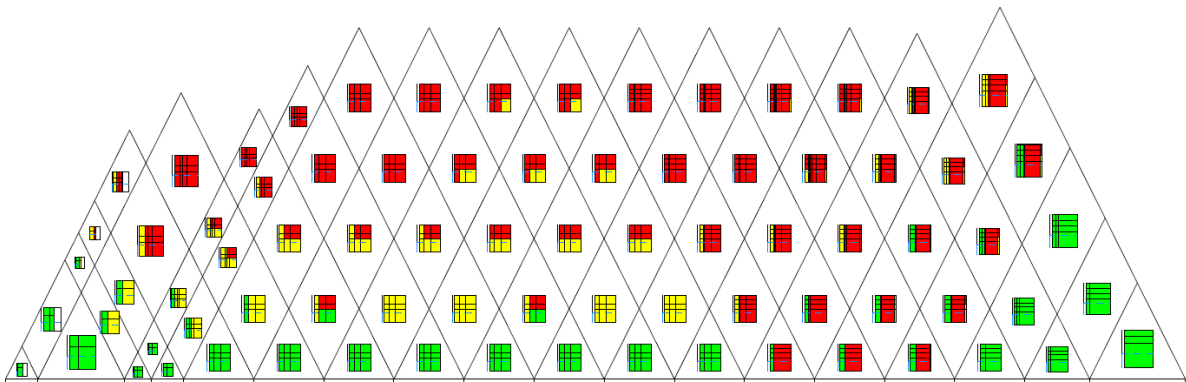


Figure 5-21: S-factor diagram Vessel III, D₁, Arrangement C, LBH3 at 0.11*B m from hull

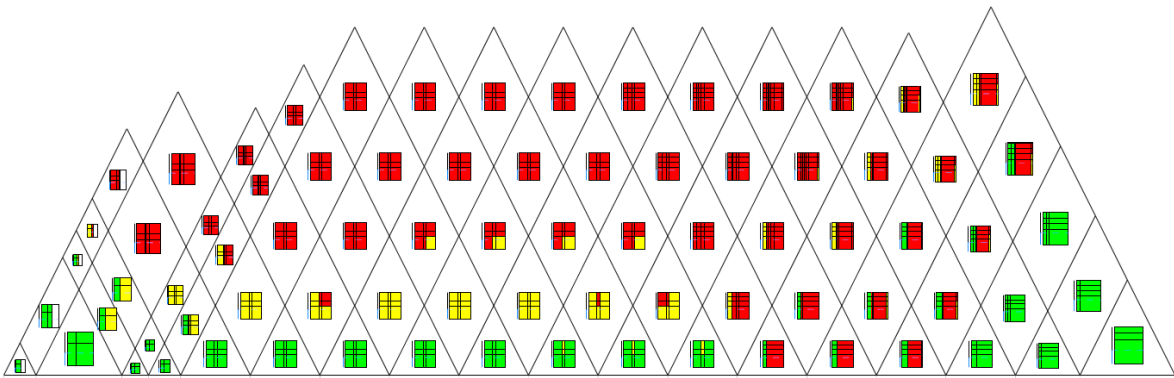


Figure 5-22: S-factor diagram Vessel III, D₁, Arrangement C, LBH3 at 0.2*B from hull

As LBH3 is moved further from the hull, the volumes of the center cargo tanks are reduced. But the S_i -factor still remains zero or less than one for most damages to the center tanks. The S_i -factor is reducing for wing tank damage cases as LBH3 is moved further towards the centerline, due to the large equilibrium heeling angle.

As LBH3 is moved for the first moves, the S_i -factor for wing tank damages are not decreasing significantly. The color for two zone wing tank damages in Figure 5-24 is yellow, but the S_i -factor is 0.97 when LBH3 is at 0.07*B. The S_i -factor is therefore not changing considerably as LBH3 is moved for the first moves.

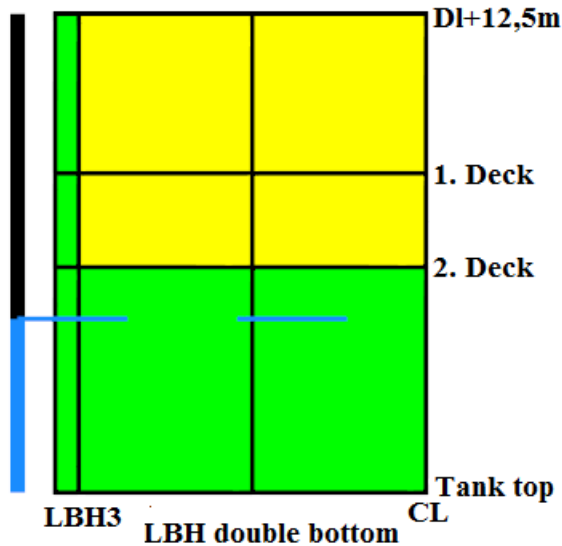


Figure 5-23: Two zone damages, LBH3 at $0.03 \cdot B$ meters from hull

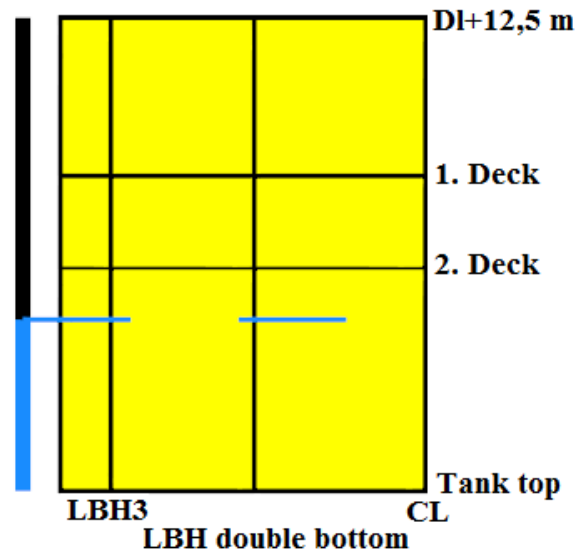


Figure 5-24: Two zone damages, LBH3 at $0.07 \cdot B$ meters from hull

Total attained index for Vessel III and IV, arrangement C

As for Vessel I and II, the volumes of the center compartments are large. The S_i -factor for most center compartment damages are below 1, regardless of the placement of LBH3. For wing tank damages, the S_i -factors are high when LBH3 is close to the hull, but it decreases as LBH3 is moved further towards the centerline. The total attained index increases for the first moves of LBH3 because the S_i -factor for wing tank damages remains high as LBH3 is relocated. Since the probability increases for cases with a high S_i -factor and decreases for cases with a low S_i -factor, the total attained index increases. When LBH3 is moved further towards the centerline the S_i -factors are decreasing for all wing tank damages. This is why the total attained index will decrease as LBH3 is moved further towards the centerline.

Conclusion for the development of A_{total} for all vessels with arrangement C

The combination of P_i and S_i was the decisive factor for the development of the attained index for arrangement C. The attained index is increasing for the first moves for Vessel II, III and IV. This is due to the S_i -factor for wing tank damages when LBH3 is relatively close to the hull. Wing tank damages are not critical until LBH3 is moved further in. The P_i -factor decreases for center compartment damages, which are cases that results in a low S_i -factor, as LBH3 is moved towards the centerline. The P_i -factor for wing tank damages increases and these cases have a high S_i -factor, when the wing tanks are relatively small. This is why the total attained index will increase for the first moves for Vessel II, III and IV.

Arrangement C does not have U-tanks. When U-tanks are damaged, the water flows down in the double bottom and results in symmetrical damages. When the wing tanks are damaged for vessels with arrangement C, the vessel will heel over. The further LBH3 is moved from the hull, the larger the volumes of the wing tanks, leading to a larger heeling moment. This is why the attained index is decreasing as LBH3 is moved further towards the centerline.

5.1.2 Comparing A_{Total} for arrangements with and without U-tanks

This subchapter will compare arrangement B and C to find out how much the attained index is influenced by introducing U-tanks. The combined results can be seen in Figure 5-25, with arrangement B as the dark colors and arrangement C with lighter colors. As seen from the graph, the arrangement with U-tanks, B, achieves a significantly better index compared to arrangement C for all vessels regardless of the placement of LBH3.

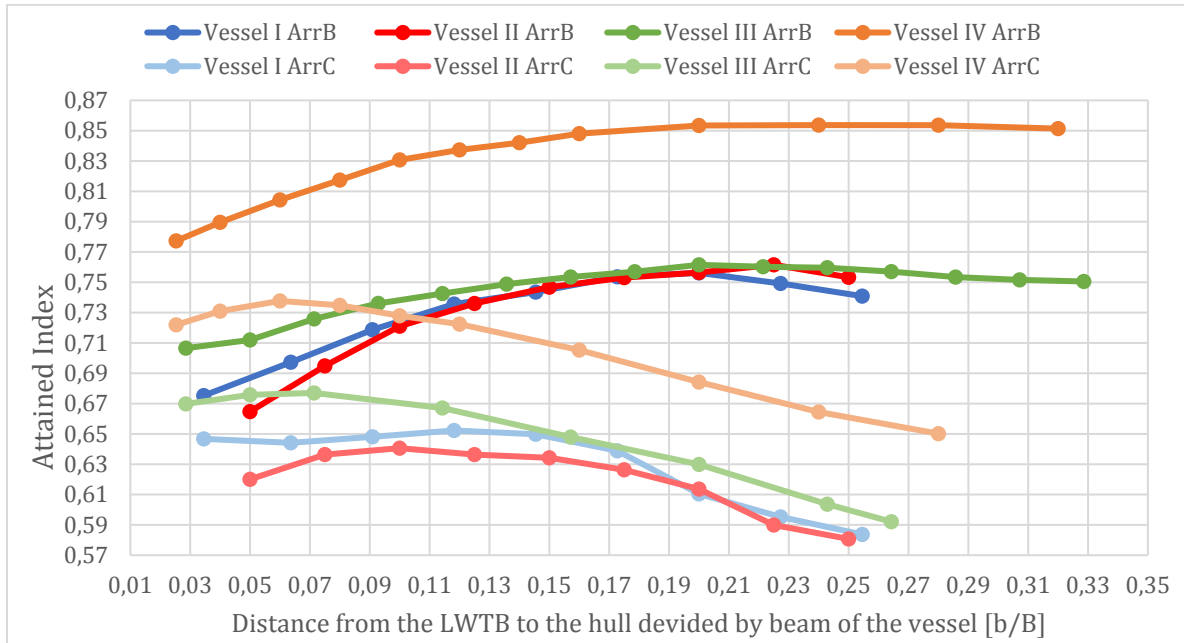


Figure 5-25: Comparing the two arrangement configurations

Figure 5-26 displays the difference between the arrangements for different placements of LBH3. From the results we can see that the closer LBH3 is to the center line, the larger the difference in attained index. But why is the attained index for arrangements with U-tank configurations at least 5% better than arrangements without U-tanks?

Discussion

To analyze why the attained index for arrangement B is significantly better than arrangement C, we can look at chapter 5.1.1 regarding the development of A_{Total} for the two arrangements. When the wing tanks are damaged, the S_i -factor is lower for arrangement C than for arrangement B, because wing tank damages are unsymmetrical for arrangement C. Since the vessels with U-tanks will have less unsymmetrical fillings, they will achieve a better S_i -factor for wing tank damages, leading to a better total attained index. The further the bulkhead is moved towards the centerline, the larger the unsymmetrical damages. That's why the difference between the two arrangement configurations increases as LBH3 is moved inwards.

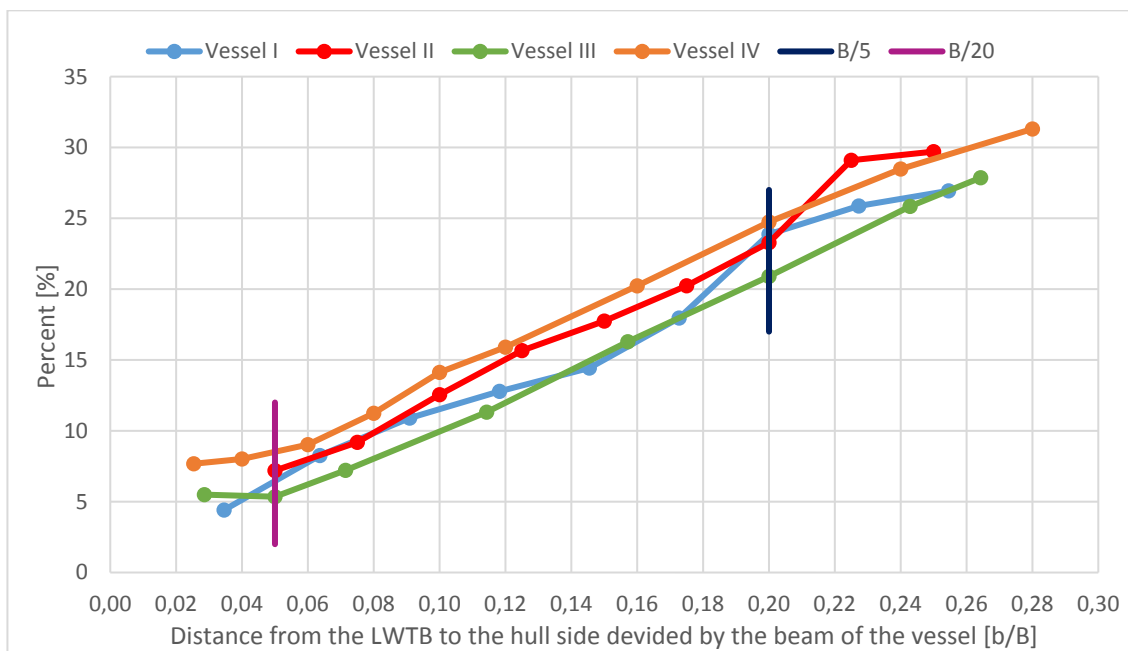


Figure 5-26: Percent change between arrangement B and C

5.1.3 Comparing A_{Total} for vessels with the same GM values

Vessel I and II

Vessel I and II has the same GM values and can therefore to some extent be compared. As seen from Figure 5-25, Vessel I and II, arrangement B, have a similar attained index for most placements of LBH3. When the wing tank bulkhead is moved closer to the centerline the attained index is more or less the same for both vessels. Vessel I gives slightly better results when LBH3 is placed close to the hull side, but overall the development corresponds.

The development of the attained index for Vessel I and II, arrangement C, is quite similar to arrangement B. The attained index for Vessel I is higher than for Vessel II when LBH3 is close to the hull, but as the LWTB is moved towards the centerline the difference evens out.

Vessel III and IV – Longitudinally Vs. transversally divided machinery room

When comparing Vessel III and IV the attained index is considerably higher for Vessel IV, compared to Vessel III, for all placements of LBH3. But the development of the total attained index is corresponding for both arrangements.

The arrangement of Vessel III stands out from the rest by the longitudinally divided machinery room. As seen from the results, this has a considerable influence on the attained index. When comparing the S-factor diagrams for Vessel III and IV, with LBH3 at approximately the same placement, the difference is evident. As seen in Figure 5-29 and Figure 5-30 the S_i -factors in the machinery area are significantly lower for the longitudinally divided machinery room. The longitudinally divided machinery area causes unsymmetrical damage cases that causes the ship to heel more than 15 degrees. There are therefore more damages where the ship heels more than 15 degrees for Vessel III than IV, due to the machinery room configuration. This is one of the reasons that the total attained index for Vessel IV is significantly better than for Vessel III.

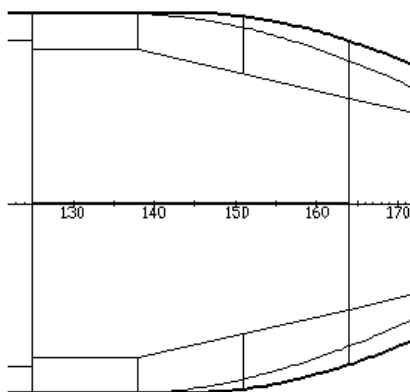


Figure 5-27: Vessel III with longitudinally divided machinery room

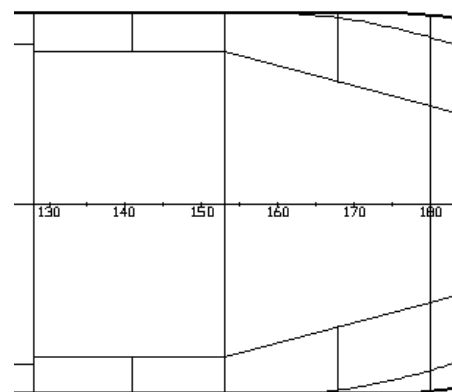


Figure 5-28: Vessel IV with transversally divided machinery room

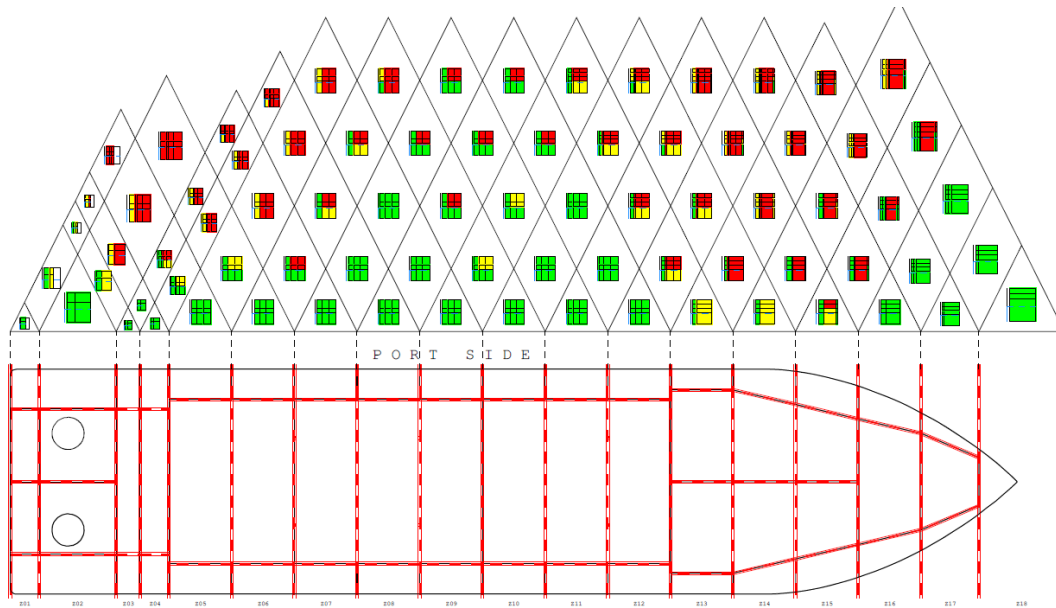


Figure 5-29: S-fac diagram Vessel III, arrangement B, LBH3 at $0.14 \cdot B$ m from the centerline

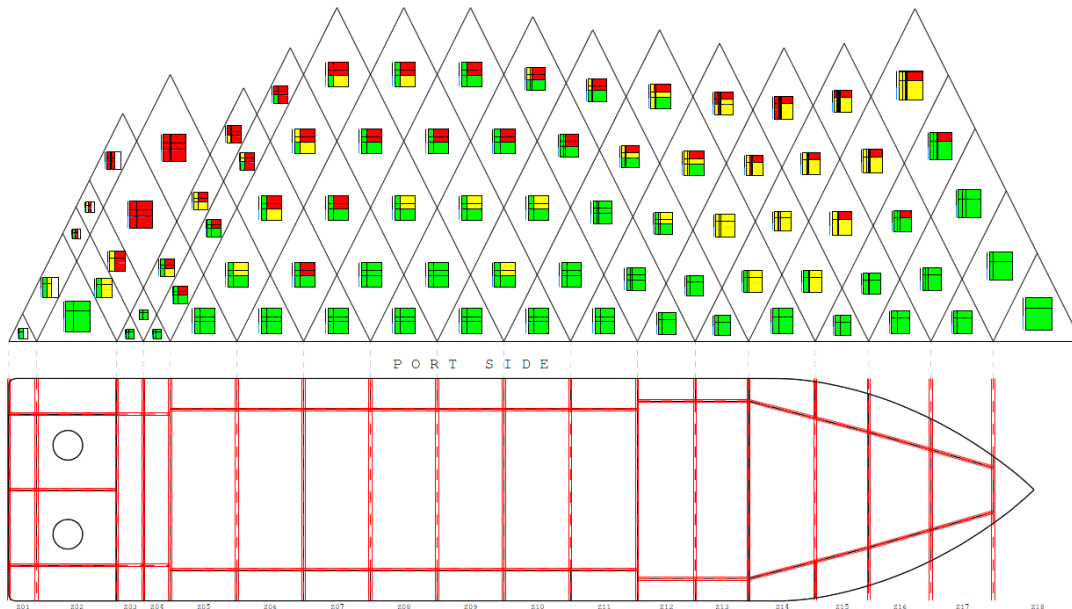


Figure 5-30: S-fac diagram Vessel IV, arrangement B, LBH3 at $0.14 \cdot B$ m from the centerline

Another factor that influences the total attained index when comparing Vessel III and IV is the difference in residual stability. The scaling of the hull influences the residual stability of the vessels. The flare angle of the vessels increases with the size of the vessels due to the way the hulls were scaled, which results in more residual stability for the largest vessels. The residual stability will improve the damage stability properties of a vessel, which will also improve the attained index. The effects from residual stability will be furthered discussed in the next subchapter. A combination of the residual stability and the unsymmetrical damages in the machinery room are contributing to the difference in the total attained index for Vessel III and IV with arrangement B and C.

5.2 The attained index for different loading conditions

Why is the attained index larger for D_s than for D_l and D_p for Vessel III and IV?

It can be seen from Figure 4-6 through Figure 4-9 that the attained index for Vessel III and IV is larger for the deepest subdivision draughts. Why these vessels sustain damages better when they are fully loaded compared to lightly or partially loaded?

The factors that will change when these vessels have a deeper loading condition are the S_i -factors and the V_i -factors. The P_i -factor will remain the same for the included damage cases for all loading conditions, since the arrangement remains the same for all loading conditions.

To explain why the attained index is higher for D_s than D_p and D_l the S-factor diagrams can be helpful. To analyze why the S_i -factor is varying for the different loading conditions, a damage case from Vessel III, arrangement C, is investigated. The one zone damage case is shown with a red circle in the S-factor diagrams below. Figure 5-31, Figure 5-32 and Figure 5-33 shows the S-factor diagrams for the three different loading conditions. When taking a closer look at the diagrams there are more cases that are yellow or red for D_l than for the D_s and D_p . As mentioned in Chapter 3.2.2, the squares represents different damage cases. Red squares indicates that the S_i -factor is zero, and yellow means that S_i is between zero and one for the particular damage case.

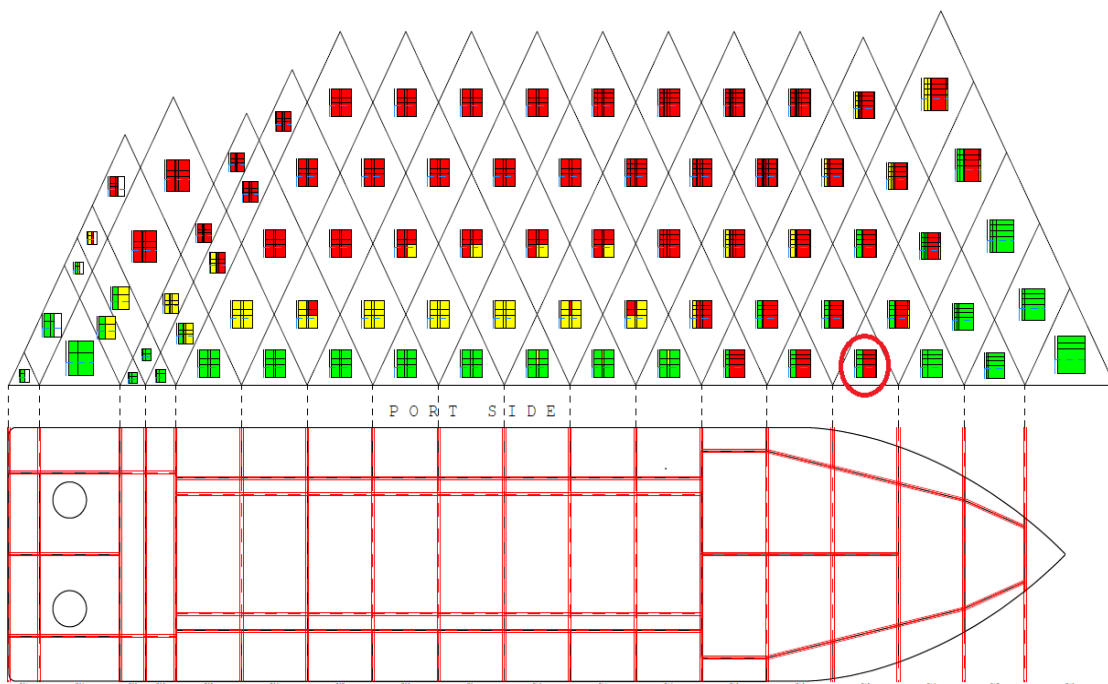


Figure 5-31: S-factor diagram for D_l condition, Vessel III, arrangement C

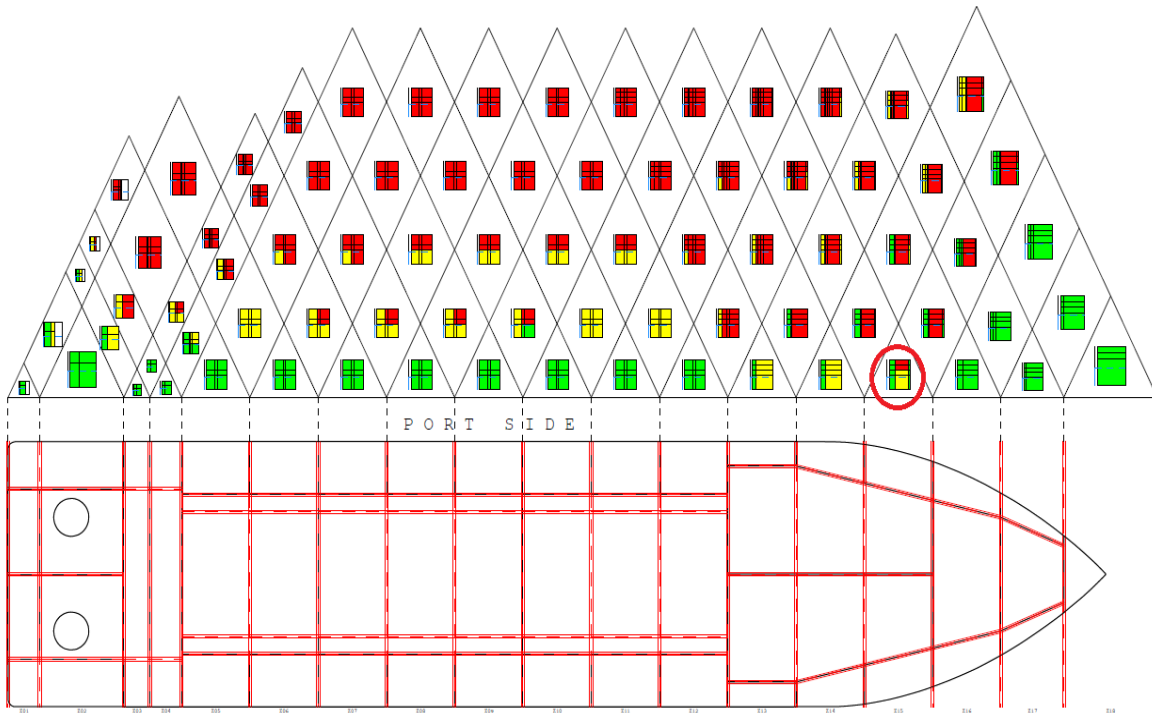


Figure 5-32: S-factor diagram for D_p condition, Vessel III, arrangement C

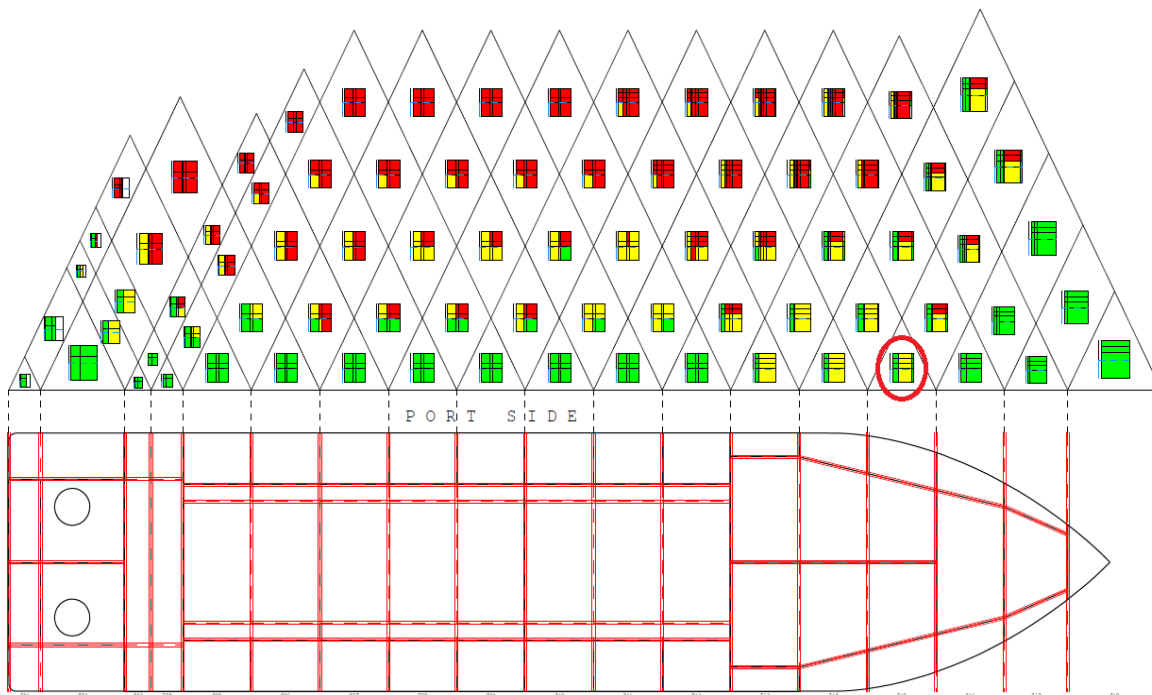


Figure 5-33: S-factor diagram for D_s condition, Vessel III, arrangement C

The damage cases in zone 15 can be seen in the figures on the next page in an enlarged version. Since the square is yellow for damage case 15.2.2-1 for D_p and D_s , the S_i -factor is between 0 and 1. And the S_i -factor for D_I is 0, since the square for the damage case is red. This damage cases is between 2nd and 1st deck that penetrates into the engine control room, which causes a heeling moment. Since no openings are included, the machinery room and

engine control room was modeled as one compartment. Even though the damage is between 2nd and 1st deck the whole engine room and control room compartment will be flooded as seen in Figure 5-40.

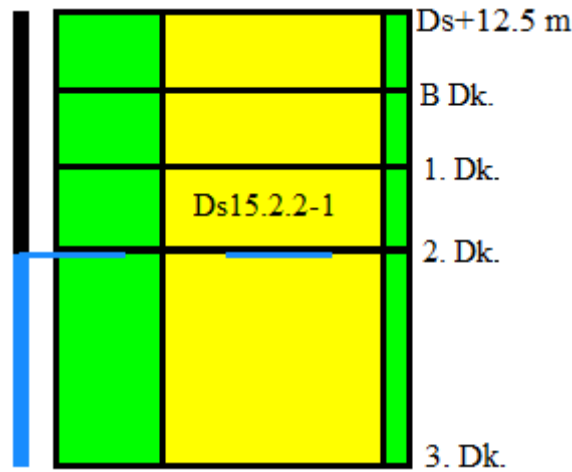


Figure 5-34: S_i -factor for D_s

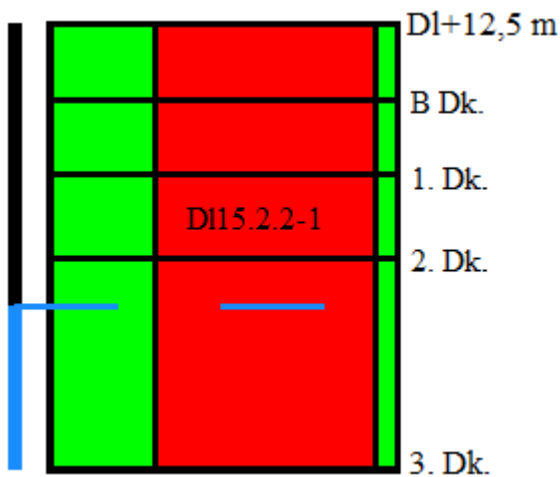


Figure 5-35: S_i -factor for D_i



Figure 5-36: S_i -factor for D_p

Table 5-3: Results for damage case 15.2.2-1

Case	Draught [m]	Trim [m]	Heel [Deg.]	GZmax [m]	Range [Deg.]	GM	S_i -factor
D_s	9.268	2.415	10.1	0.48	38	2.5	0.7826
D_p	8.344	2.461	14.4	0.27	27.1	1.8	0.2738
D_i	7.035	2.634	17.5	0.12	23.4	1.8	0

The results for each damage case displayed in Table 5-3, was computed using NAPA. As seen from the values, it is the heeling angle which is influencing the S_i -factor. By implementing the results, displayed in Table 5-3, into Eq. 17, it can be seen that the $\left[\frac{GZ_{max}}{0.12} \cdot \frac{Range}{16}\right]^{\frac{1}{4}}$ part of

the equation will equal 1 for all the loading conditions. $K, \sqrt{\frac{\theta_{\max} - \theta_e}{\theta_{\max} - \theta_{\min}}}$, will consequently determine the S_i -factor, which again is determined from the equilibrium heeling angle after a damage. Figure 5-37, Figure 5-38 and Figure 5-39 displays the GZ-curves for the loading conditions. Parts of the results in Table 5-3, such as the equilibrium heeling angle, GZmax and range are found using these GZ-curves.

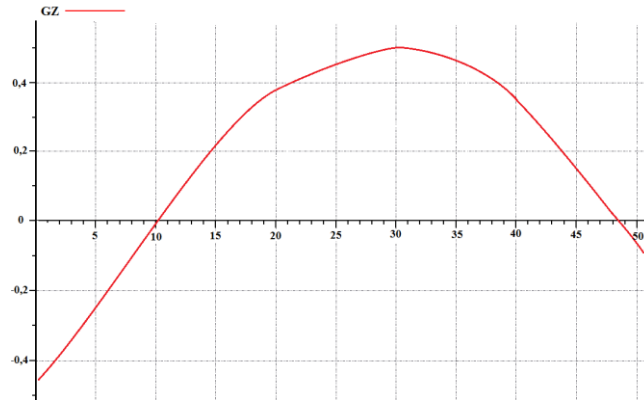


Figure 5-37: GZ-curve for D_s after damage

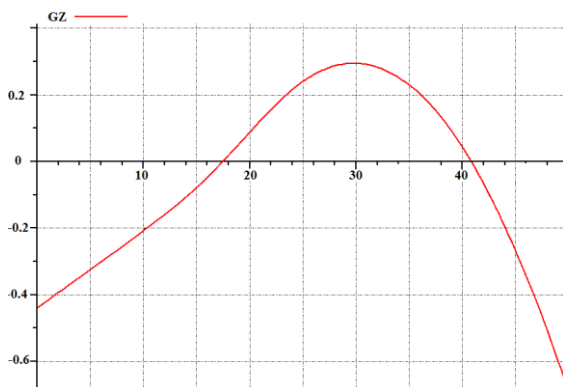


Figure 5-38: GZ-curve for D_1 after damage

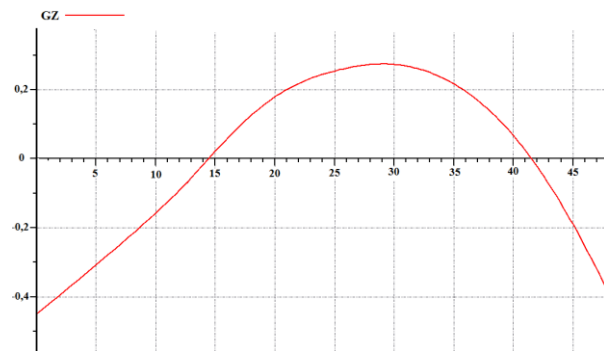


Figure 5-39: GZ-curve for D_p after damage

But why does the vessel heel more in the D_p and D_1 loading conditions than in D_s ? To explain why the vessel heels more in the lighter loading conditions it is helpful to look at the floating position for the different damage cases. We know from Eq. 22 that the GZ value is dependent on GM and the residual stability MS:

$$GZ = GM \cdot \sin \varphi + MS(\varphi) \tag{Eq. 22}$$

φ : Heeling angle

MS: Residual stability

(Amdahl, et al., 2011)

Since the GM value is the same for the D_p and D_l condition it has to be the residual stability that governs the GZ value. The residual stability is determined based on the form of the vessel. As long as the area moment of inertia remains the same for the waterline plane, $MS(\varphi)$ remains constant. If the area moment of inertia, I (m^4), increases due to heeling of a vessel, $MS(\varphi)$ will increase accordingly (Amdahl, et al., 2011). We will not go into details about the derivation of MS, since that is not within the scope of this thesis.

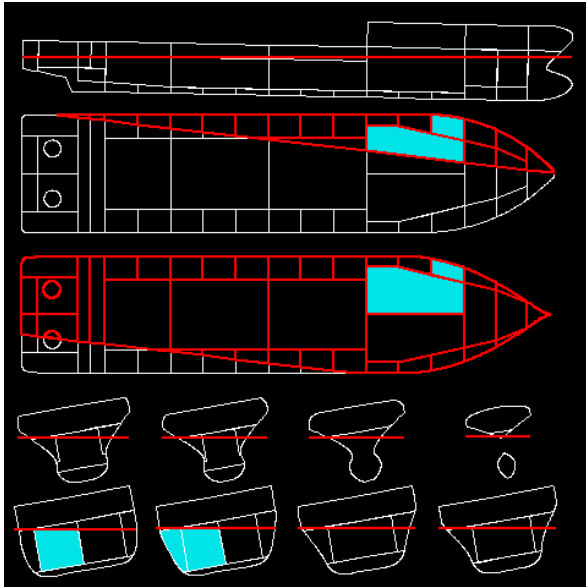


Figure 5-40: D_s floating condition

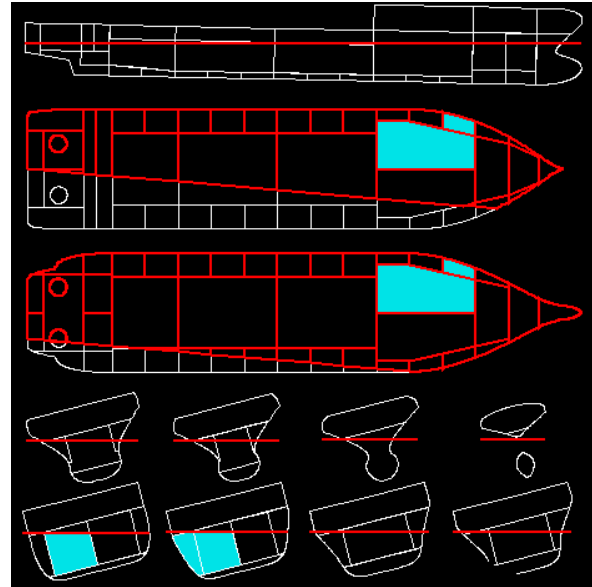


Figure 5-41: D_p floating condition

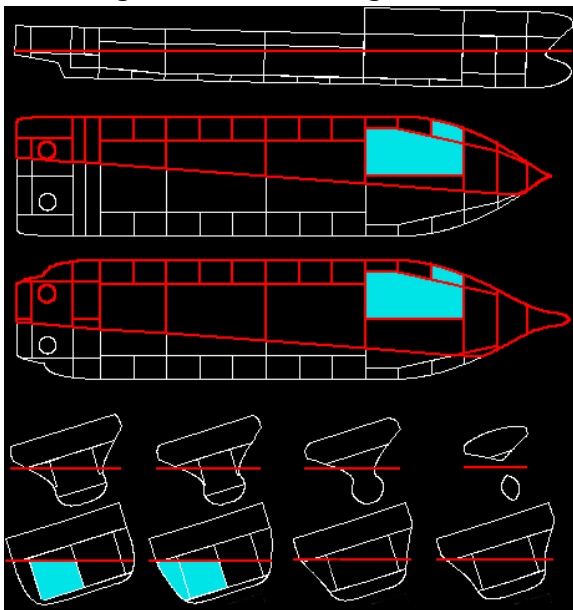


Figure 5-42: D_l floating condition

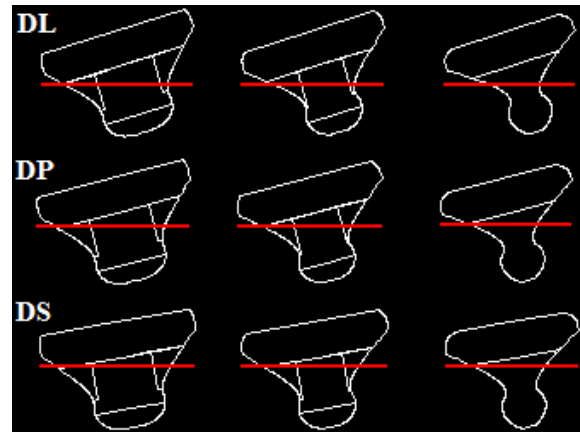


Figure 5-43: Floating position for D_l , D_p and D_s

Figure 5-40, Figure 5-41 and Figure 5-42 displays the different floating conditions for the three loading conditions. By examining the different floating positions, the change in the area moment of inertia for the three loading conditions can be seen. The change in waterline plane area is not the same when the vessel heels for the different loading conditions. It is important to look at the hydrostatic properties of the forward part of the vessel when analyzing the residual stability. The flare angle, illustrated in Figure 5-44, will influence the

residual stability, because the area moment of inertia will not increase proportionally for all loading conditions. The flare angle increases for every deck, and the area moment of inertia will therefore increase accordingly. Figure 5-43 shows where the waterline for the different loading conditions are. As seen from the figure, the deepest loading conditions has a waterline where the flare angle is large. When the ship starts to heel, due to a damage, the area of the water plane will increase faster for deeper loading conditions. The rise in water plane area will influence the residual stability, thus increasing the ship stability, which is why the heel angle will be smaller for the deepest loading conditions.

Since the residual stability is the determining parameters for many of the damage cases, the residual stability will influence the results. When the ship is in a deeper loading condition, the residual stability will increase. This is why the attained index is larger for the deepest loading conditions for Vessel III and IV. But why is this not the case for Vessel I and II?

As mentioned earlier, the hull form was scaled from the smallest vessel. Since the vessels were scaled all the measures were increased proportionally. Some measurements were not authentic to the reference vessels due to the way the hull was scaled. One example is the flare angle in the forward part of the vessel. The scale factor for the OCV's were larger, leading to a larger deviation from an authentic vessel. The flare angle of the OCV's were therefore large, which is why the residual stability has a larger impact on the damage stability properties for these vessels. This could be the reason why the attained index for D_s is greater than D_p and D_l for the largest vessels.

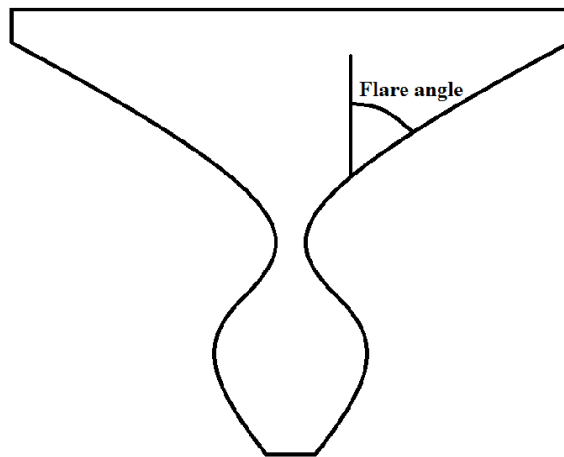


Figure 5-44: Cross section of bow illustrating the flare angle

6 Conclusion

Introduction

This study has analyzed how the attained index changes when the transverse position of the LWTB is changed for four vessels with two arrangement configurations. One of the objectives was to find out if it is possible to maximize the attained index by moving the LWTB. Calculations were conducted for four vessels, to see if the attained index developed equally with different ship sizes and arrangement configurations. Since it is common to introduce U-tanks to maximize the attained index, the study has analyzed how much the attained index will increase when U-tanks are introduced.

The first subchapter will describe the limitations and uncertainties for the thesis. The following subchapter will conclude how we can interpret the results and how this knowledge can be used by designers. The final subchapter will describe further works that can be conducted in the future to further understand how changes in the arrangement affects the attained index.

6.1 Limitations

Uncertainties and limitations will influence the results of the study, and the following subchapters will discuss the impact on the results of these uncertainties.

Passengers

When calculating the S_i -factor for the damage cases, a moment from passenger movement is taken into account. As mentioned in Eq. 16, S_i is calculated as follows:

$$S_i = \text{minimum}[S_{\text{intermediate},i} \text{ OR } (S_{\text{final},i} \cdot S_{\text{mom},i})]$$

$S_{\text{mom},i}$ is calculated based on the maximum moment from passengers, wind force or by survival crafts being lowered. The survival craft momentum has to be manually calculated based on the weight and placement of the craft. As the placement of survival crafts would vary according to vessel types the survival craft moment was not included. The moment from passengers is calculated as follows:

$$M_{\text{passengers}} = (0.075 \cdot N_p) \cdot (0.45 \cdot B)$$

N_p = Maximum number of passengers permitted

B = Ship beam

The aim of the study was to get as generic results as possible. Since the number of personnel varies according to the ship owners requests, passengers were left out of the calculations. An attained index was calculated for Vessel I and IV with passengers, to check how large the influence from passengers would be.

Table 6-1: Comparison of vessels with and without passengers

<i>Vessel</i>	<i>A_{Total} without passengers</i>	<i>A_{Total} with passengers</i>	<i>Passengers</i>
<i>Vessel I, arrC, LBH3 at 0.09*B m</i>	<i>0.64808</i>	<i>0.64818</i>	<i>50</i>
<i>Vessel I, arrC, LBH3 at 0.12*B m</i>	<i>0.65224</i>	<i>0.65264</i>	<i>50</i>
<i>Vessel IV, arrC, LBH3 at 0.04*B m</i>	<i>0.73094</i>	<i>0.73094</i>	<i>120</i>
<i>Vessel IV, arrC, LBH3 at 0.08*B m</i>	<i>0.73483</i>	<i>0.73483</i>	<i>120</i>

As seen from the results in Table 6-1, the influence of passengers are negligible for both placements of LBH3 for Vessel I and IV. As long as the influence of passengers remains the same for different placements of LBH3, the passengers does not influence the results. Passengers didn't affect the attained index for the studied placements of LBH3 for Vessel I and IV, but it is important to keep in mind that the effect of passengers has not been analyzed for all vessels, with all placements of the longitudinal bulkhead.

6.1.1 Stability

GM values

The assessment of choosing the GM values can be found in the method section of the thesis. As mentioned earlier the values chosen for GM will significantly influence the results of the attained index. GM is one of the elements that has the greatest influence when calculating the S_i -factor, and will vary according to ship type and operations that are expected to be executed. Since the GM values are varying for different vessels, it is uncertain how the attained index will develop for other GM values. The further work section will discuss how it would be possible to find out how much the GM values influences the total attained index.

Hull form affecting the residual stability

Since the hulls were scaled to obtain the dimensions for the larger vessels, the hull forms were not authentic for Vessel II, III and IV. As the vessels were scaled, the flare angle of the larger vessels were large, which affected the residual stability. It is uncertain how much the residual stability affected the development of A_{Total} when LBH3 was relocated for the different arrangements.

6.1.2 Arrangement

Splitting of wing tanks

For vessels with U-tank configuration, the wing tanks are placed on top of the U-tank as seen in Figure 6-1. For arrangements without U-tanks, the wing tanks were divided horizontally as seen in Figure 6-2. The splitting of the wing tank for arrangements without U-tanks, is not common practice in the industry (Fykse, 2015). The splitting was done without sufficient investigation of the common practice in the industry. Since the aim was to design as authentic vessels as possible, the wing tank splitting conflicts with the reference vessels. If the wing tank were not divided, damages to the wing tank would be larger. When larger wing tanks are damaged it will cause the vessel to heel more. More heeling reduces the S_i -

factor which again reduces the total attained index. Since the wing tanks are divided for arrangement C, the longitudinal bulkhead can be moved closer to the centerline before wing tank damages are critical.

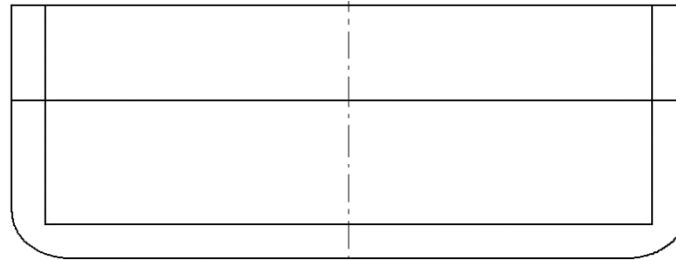


Figure 6-1: U-tank configuration, arrangement B

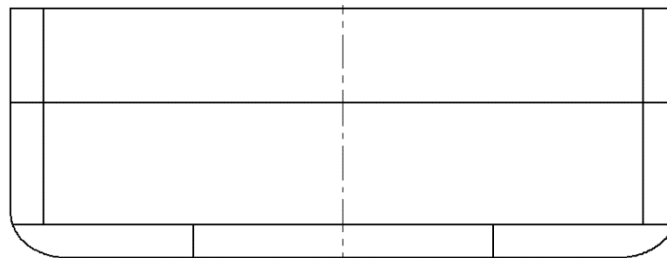


Figure 6-2: Longitudinally divided double bottom with no U-tanks, arrangement C

U-tanks in the whole mid-ship area

U-tanks limits the amount of unsymmetrical damages, which is favorable for the attained index. A designer will try to fit as many U-tanks as possible, to limit unsymmetrical damages. But there are certain limitations. For example an OCV will need anti-heeling tanks to counteract the heeling moment in lifting operations. The vessels with arrangement B has U-tanks in the entire mid-ship area, which is favorable. The study aimed to design the vessels as authentic as possible, but also to be as generic as possible. Due to the generic aspect, U-tanks were configured in the entire mid-ship section. This would limit the uncertainty of the placement and size of anti-heeling tanks, as this will vary extensively according to the crane capacity and operation. The size and placement of miscellaneous tanks in the double bottom would also vary according to ship type and operation specifications. Since the vessels in this study has U-tanks in the entire mid ship section, it is uncertain if the development of the attained index would be the same as for authentic vessels. The effect of introducing U-tanks are therefore not as favorable as presented in Figure 5-26: *Percent change between arrangement B and C.*

Openings

Openings such as doors, ventilation and vertical escapes are usually implemented in the NAPA model to account for water intrusion and flow between compartments. Since the placements of openings would vary according to vessel types, no opening were included. Instead of modeling compartments separately and introducing openings such as doors, ventilations, escape routes, etc. the compartments that were assumed to be connected by unprotected openings, were modeled as one compartment.

In hindsight, openings for ventilation of the tanks could have been included. Openings could have been placed above the main deck in the aft corner, mid-ship and on the aft side of the superstructure. These areas would most likely have ventilations for all vessel types and could have had an influence on the final results. But the decision was made, together with Ketil Fykse, to neglect any openings in order to minimize the runtime in NAPA.

Size of cargo area

As the study aims get as generic results as possible, the cargo area in the mid-ship section had limited subdivision, because different ship types has different subdivision in this area. As PSVs usually have cargo tanks, such as liquid mud, these vessels have more subdivisions in the center area of the ship. OCV's usually has some kind of storage for pipes and possibly a winch room, depending on crane size, in the center area of the vessel. As the volumes of the different compartments influences the results, it is uncertain how the attained index would develop for an authentic PSV or OCV. The sizes of the cargo tanks were not evaluated thoroughly, and had a large influence on the results. Damage cases that penetrated the cargo area were critical for the survivability of the smallest vessels. It is not normal that damage cases that penetrates the LWTB are critical for most damage cases for authentic OCV's and PSV's. It is difficult to predict the development of the attained index if the compartments inside the LWTB were smaller. If damages to the center cargo tanks would not be critical, it would not be as favorable to move the longitudinal bulkhead for vessels with U-tanks. This is because the S_i -factor would not increase for damages to smaller compartments in the center. For vessels with no U-tanks the attained index would not increase by moving the LWTB closer to the center. If the S_i -factor can't be increased for the center compartment damages by moving the LWTB, it would not be favorable to move the bulkhead closer to the centerline.

6.2 Contributions

The goal of the study was to get generic results that could be applied for all vessel types. As different vessel types has different subdivision in the mid ship area, it is hard to make generic conclusions that can be applied for all offshore vessels. Is it really possible to get generic results that can be applied to all vessel types when dealing with probabilistic damage stability calculations?

As mentioned in the introduction, probabilistic damage stability calculations requires a detailed general arrangement in order to be conducted. All vessels are different, and small modifications to the arrangement will influence the results. This study experienced difficulties dealing with a methodology that requires all details, when analyzing how the attained index develops for all offshore vessels, with different arrangement configurations. The following subchapters will conclude how changes in the arrangement affects the total attained index for the vessels in the dissertation. The conclusions are based on the results from the vessels and cannot be applied for offshore vessels in general.

Correlation between ship sizes

The results of the development of attained index for all vessels in the study with the different placements of the LWTB can reveal if there is a correlation between different ship sizes. From the results it can be concluded that the overall development of the attained index corresponded for different vessel sizes with U-tanks.

The development of the attained index for the vessels without U-tanks did not correspond as well as for vessels with U-tanks. The attained index increased for some of the vessels as the LWTB was moved from the hull towards the centerline for the first movements. As the LWTB was moved further towards the centerline, the development of the attained index corresponded for all four vessels.

Development of the attained index for offshore vessels with U-tanks, arrangement B

The attained index increased as the longitudinal bulkhead was moved towards the centerline for vessels with U-tank configuration. Damages to the U-tanks would not cause the vessel to heel over. This is because the water will flow down in the double bottom and create a symmetrical damage. U-tank and upper wing tank damages were therefore not critical when the longitudinal bulkhead was placed relatively close to the hull side. Damages to the center compartments were critical for most placements of the LWTB, due to the large volumes of the center compartments.

Since probability of damages to the center tanks decreased as the bulkhead was moved inwards, the total attained index increased. The attained index can therefore be increased by moving the LWTB closer to the centerline for vessels with large center compartments and U-tanks.

Development of the attained index for offshore vessels without U-tanks, arrangement C

The attained index increased for some of the vessels as the LWTB was moved for the first steps from the hull towards the centerline. The correlation between the development of the attained index and the different ship sizes did not correspond when the LWTB was placed relatively close to the hull. This makes it problematic to conclude how to maximize the attained index for vessels without U-tanks.

When the wing tanks were damaged for vessels without U-tanks, the vessel would heel over. The further the LWTB was moved from the hull, the larger the volumes of the wing tanks, leading to a larger heeling moment. When the LWTB was moved close to the centerline, wing tank damages would result in a low S_i -factor and the total attained index would decrease accordingly. The attained index will be maximized when damages to the wing tanks are not critical for the survivability of the vessel.

Maximizing the attained index for offshore vessels in general

Based on the results presented in this report it is not possible to give an exact value of the optimal placement of the longitudinal bulkhead to maximize the attained index. But the study presents sufficient information, regarding the development of the attained index, so that a designer can know which factors that are affecting the attained index.

Figure 6-3 shows an approach that designers can use, when placing the LWTB, to maximize the attained index for offshore vessels. A Naval Architect can use the flowchart in Figure 6-3 to find out which factors that will influence the results for the total attained index. The development of the total attained index for the different vessels are not corresponding well enough to conclude with exact values for the best placement of the LWTB, but the factors affecting the results are the same for all vessels.

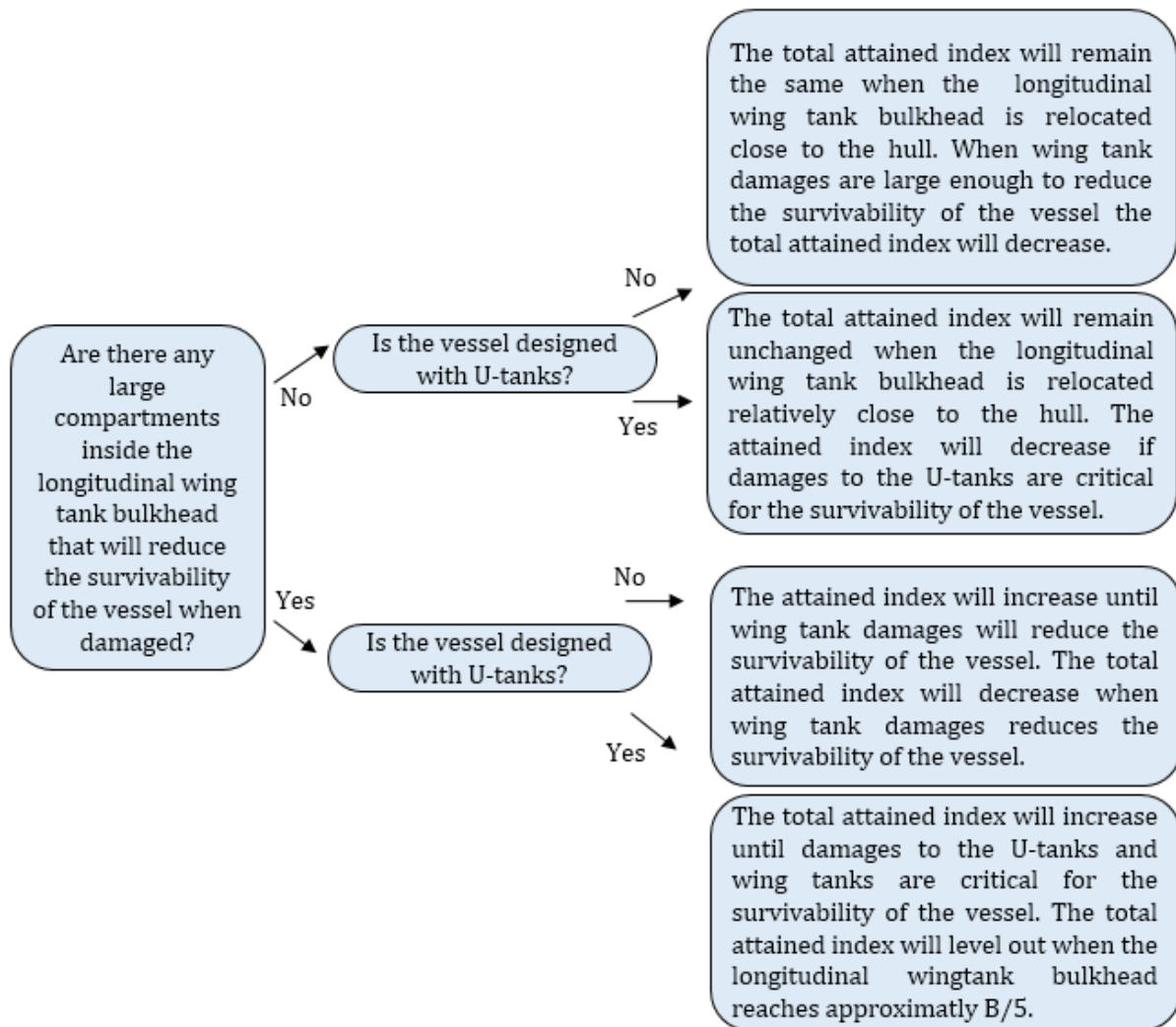


Figure 6-3: Flowchart to maximizing the attained index for offshore vessels

6.3 Further work

6.3.1 Limit uncertainties of results for vessels in the study

There are many uncertainties connected to the vessels in this study. This subchapter will focus on how the method of the study could be improved to get more reliable results.

Design of vessels

The study aims to get generic results that could be applied for all vessel types. As the internal subdivision of the vessels vary according to the ship type, the development of the attained index would vary according to the internal arrangement. To limit the uncertainties of the development of the attained index, the design of each vessel should be as authentic as possible.

Hull form

The hull forms used for the vessels in this study was scaled from the smallest vessel to have similar hydrostatics for the different vessel. This had a larger impact on the results than expected. It is uncertain if the results would have been the same if authentic hull forms were used for all vessels. Existing vessel hulls should be remodeled with the same main dimensions as in the study. The arrangement should be the same as in the study and probabilistic damage stability calculations should be rerun for all placements of the longitudinal bulkhead to verify the results. This would show how much the residual stability influences the results.

Openings

As the effect of openings is uncertain for this study, it should be further analyzed. Since openings are related to tank configuration, openings could have been introduced to the existing arrangement. The effect of openings should be included to check how much it could influence the results. All openings does not have to be introduced, but openings in the aft corners, the mid ship sections and at the aft side of the superstructures would be enough to verify the effect of openings.

Passengers

As the effect of passengers is uncertain it should be further analyzed. Some conditions were checked by introducing passengers, and the results showed that they had no effect. But it is uncertain if they would affect other arrangement types. In order to minimize the uncertainty of the effect of passengers, more runs with passengers should be conducted and compared with the existing results.

Stability

The initial stability of the vessels influences the results dramatically. In order to see how the GM values affects the results, varying the GM values would clarify how large the effect of GM values would be. This would be very time consuming, but would create a broader understanding of the influence of the initial stability.

6.3.2 New aspects that could be analyzed on the existing vessels

Probabilistic damage stability is very complicated and multiple factors influences the results. There are numerous aspects that could be further analyzed to find out how the attained index is influenced.

Arrangement

The distance between the transversal bulkheads has not been analyzed in this study. The distance was based on the damage extent according to regulation 9, *Damage extent* = $1/3 * L^{2/3}$. The designers are free to place the transversal bulkheads wherever they like. And the effect of different placements of the transversal bulkheads could be analyzed.

The results could be compared to the results for Mr. Ravn's PhD thesis. As this could reveal if the development of the attained index for different arrangement configurations are the same as for Ro-Ro vessels and offshore vessels.

Deck heights influences the V_i -factor for the damage cases. Analyzing how the V_i -factor impacts the results of the attained index for different vessel types would be valuable information for a Naval Architect.

Vessel III in the study has a longitudinally divided machinery area. This was conducted to compare the see how much this would influence the results. But as there were no vessels with the same dimensions with a transversal divided machinery room, the results are uncertain. In order to see how much the attained index is affected by a longitudinally divided machinery room, stability calculations could be conducted for two vessels with the same size.

Loading conditions

This study has not analyzed how the attained index develops for the different loading conditions for all the vessels. The development can be seen in the figures in chapter 4.1, but has not been furthered analyzed. For some of the vessels the attained index for one loading condition develops very differently from another loading condition for the same vessel and arrangement. In order to get a deeper understanding of the development of the total attained index, the development of the attained index for the different loading conditions could be furthered analyzed.

6.3.3 Studying one vessel type

As probabilistic damage stability is very dependent on details, it is not possible to find accurate results that will apply for all vessel types and sizes. In order to find results that can be directly applicable when designing a new ship, the vessels in the study has to be similar to the new vessel. As the volumes of the internal subdivisions influences the results for the development of the attained index when the LWTB is moved, it is important that the volumes of the internal compartments are as authentic as possible. The study shows that the development of the attained index varies according to the volumes of the internal tanks. In order to get results that are more reliable, the arrangement subdivisions should be more specific for one vessel type. By studying one vessel type, one could find out if it is possible to create a rule of thumb for the placement of the longitudinal bulkhead to maximize the attained index for this ship type.

7 Bibliography

- Amdahl, J., Endal, A., Fuglerud, G., Hultgreen, L. R., Minsaas, K., Rasmussen, M., . . . Vallan, H. (2011). *TMR4100- Marinteknikk intro, TMR4105- Marin Teknikk 1*. Trondheim: Marinteknisk senter, NTNU.
- Baltsersen, J. P., & Erichsen, H. (2007). *Presentation of Probabilistic Damage Stability regulations, New SPS Code and MARPOL Regulation 12A*. Retrieved December 12, 2014, from Skipstekniskskapselskab.dk:
<http://www.skibstekniskskapselskab.dk/public/dokumenter/Skibsteknisk/Download%20materiale/2007/5%20nov%2007/Den%205%20nov%20jens%20Peter%20%26%20Henrik%20E.pdf>
- Evangelos K., B., Apostolos D., P., & Zaraphonitis, G. (2004, July). Optimization of Arrangements of Ro-Ro Passenger Ships with Generic Algorithms. *Ship Technonogy Research*, 51(3), 99-105.
- Fykse, K. (2014). Global Dicipline Leader Stability, Wärtsilä Ship Design, Telephone and email communication.
- Fykse, K. (2015). Global Disipline Leader Stability, Wärtsilä Ship Design. Telephone and email conversations.
- Hjort, G. (2014, November). Email correspondance, Principal Surveyor Stability DNV GL.
- IMO. (1966). SOLAS, International Convention on Load Lines, Article 2 Definitions. International Maritime Organisation.
- IMO. (2006a). SOLAS Chapter II-1, Part B-1 Stability. International Maritime Organization.
- IMO. (2006b). SOLAS Chapter II-1, Part B-2, Regulation 12. International Maritime Organisation.
- IMO. (2008a). Resolution MSC.281(85) - Explanatory notes to the SOLAS Chapter II-1, Part B. International Maritime Organization.
- IMO. (2008b). SOLAS, Chapter II-1 Construction-structure, Subdivision and stability, Machinery and electrical installations, Part A General, Regulation 2 Defenitions. Internatinal Maritime Organization.
- IMO. (2008c). Resolution MSC.266(84) - Code of safety for special purpose ships, 2008.
- Lützen, M. (2001, Desember). *PhD thesis: Ship Collision Damage*. Lyngby, Denmark: Department of Mechanical Engineering, TUD.
- NAPA. (2011). NAPA online manual, Probabilistic damage (PROB).
- NAPA. (2015, April 21). *NAPA -Solutions for Design and Operation of Ships*. Retrieved from <https://www.napa.fi/About-NAPA>

Bibliography

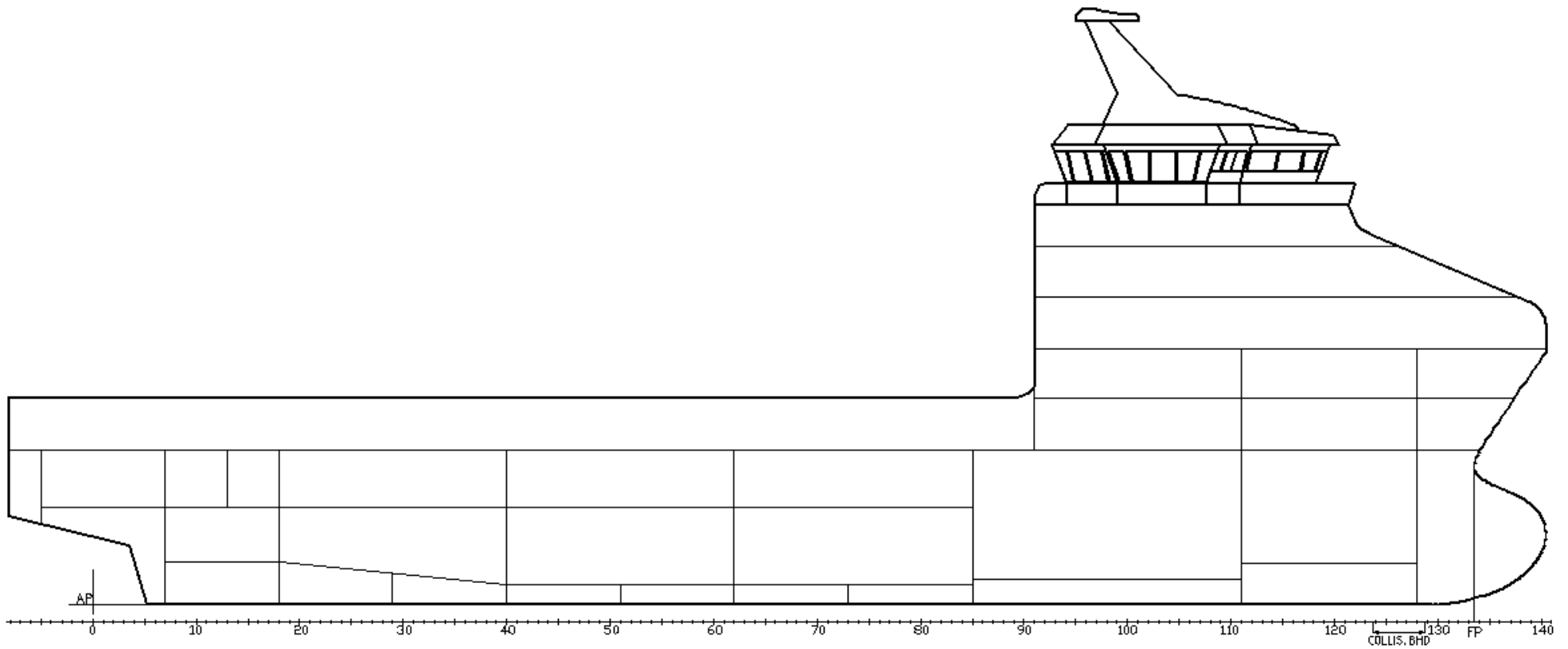
- Olufsen, O., & Hjort, G. (2013, June 17). An introduction to revised chapter II-1 of SOLAS-74. Horten: DNV.
- Papanikolaou, A., & Eliopoulou, E. (2007). On the development of the new harmonised damage stability regulations for dry cargo and passenger ships. *Reliability Engineering and System Safety*.
- Patterson, C., & Ridley, J. (2014). *Ship Stability, Powering and Resistance*. London: Adlard Coles Nautical an imprint of Bloomburrry Publishing Plc.
- Puisa, R., Tsakalakis, N., & Vassalos, D. (2012). Reducing Uncertainty in Subdivision Optimization. *Journal of Shipping and Ocean Engineering*, 18-27.
- Puustinen, O. (2012). Workshop 7, FAQ in NAPA Damage Stability. NAPA.
- Ravn, E. S. (2003, February). *PhD thesis: Probabilistic Damage Stability of Ro-Ro Ships*. Technical University of Denmark.
- Vickovic, V. (2015). Email communication with Naval Architect at Wärtsilä Ship Design.

Appendix A

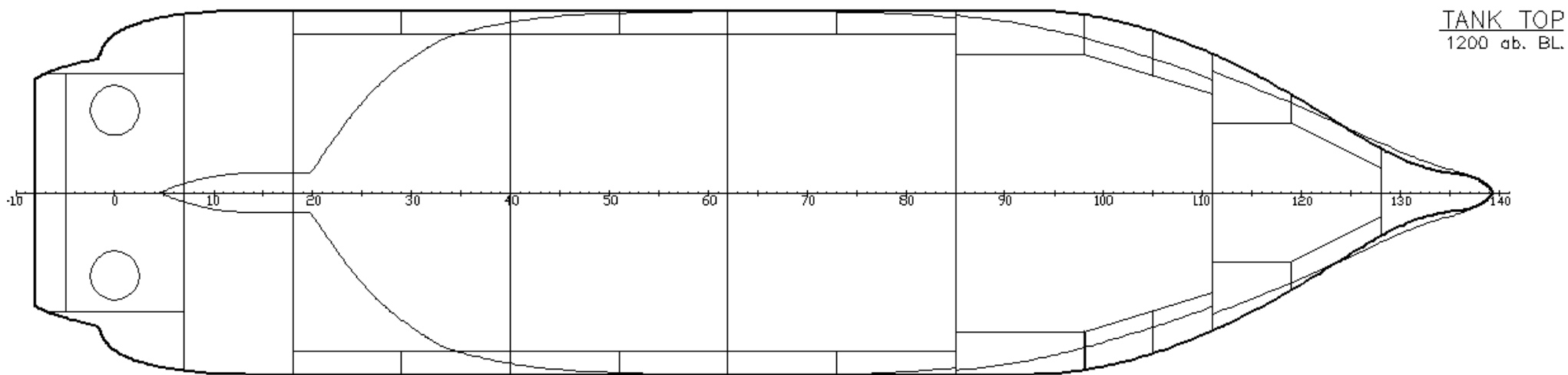
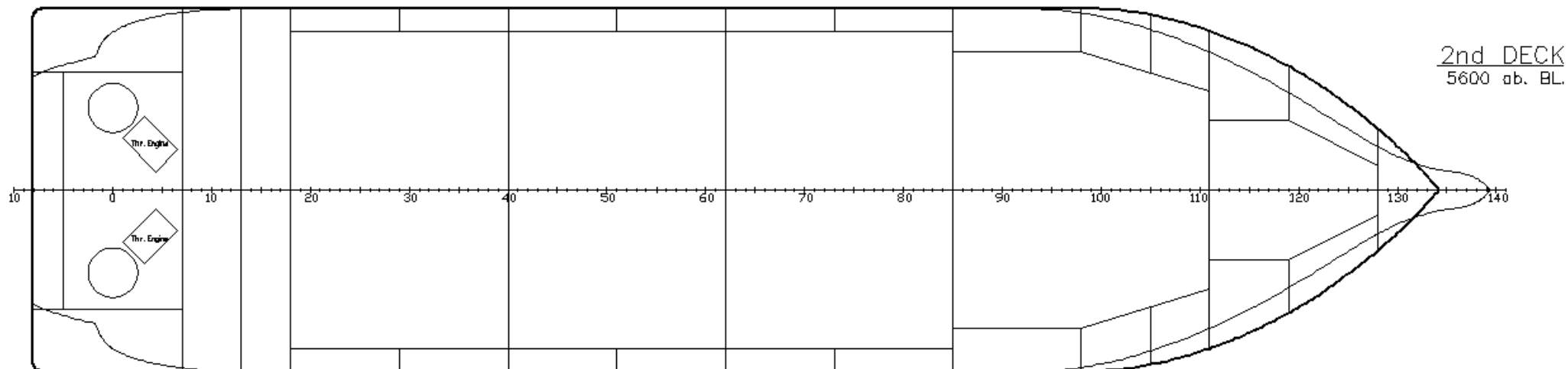
General arrangement Vessel I

Arrangement B/C

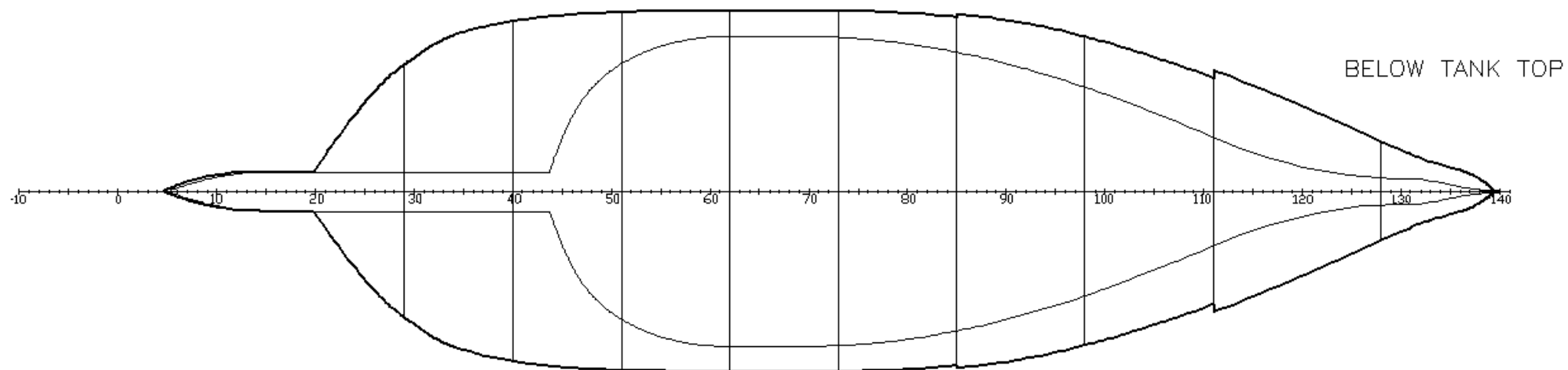
Frame space 600 mm



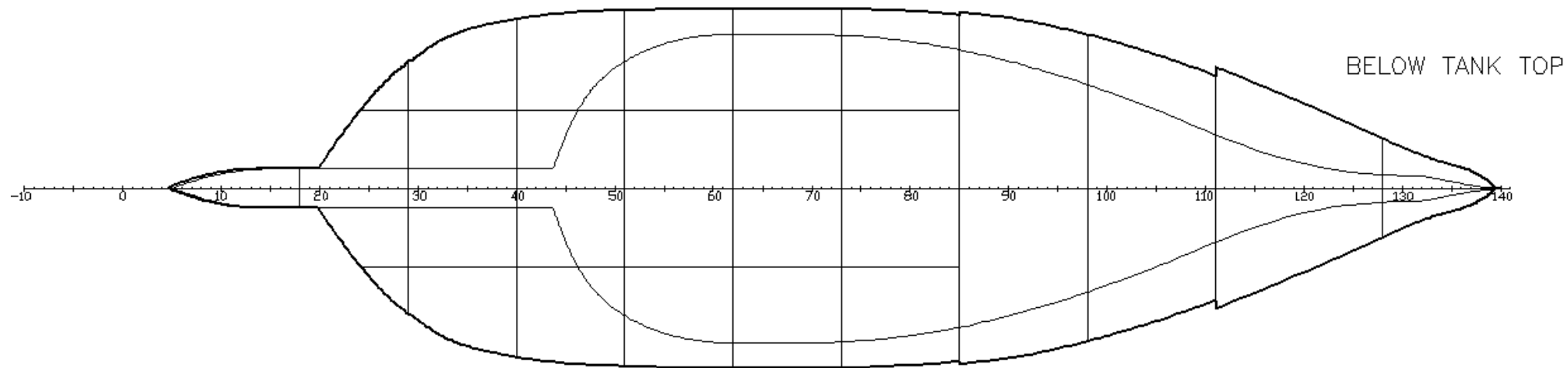
Arrangement B/C



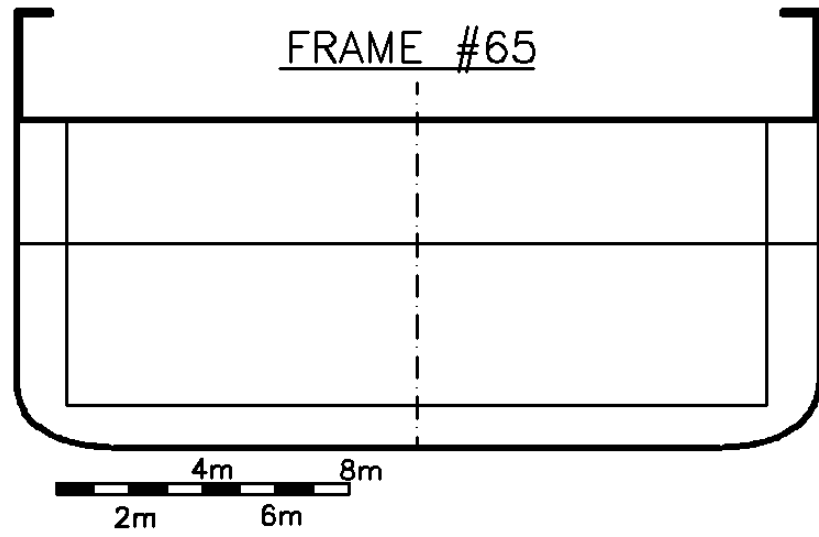
Arrangement B



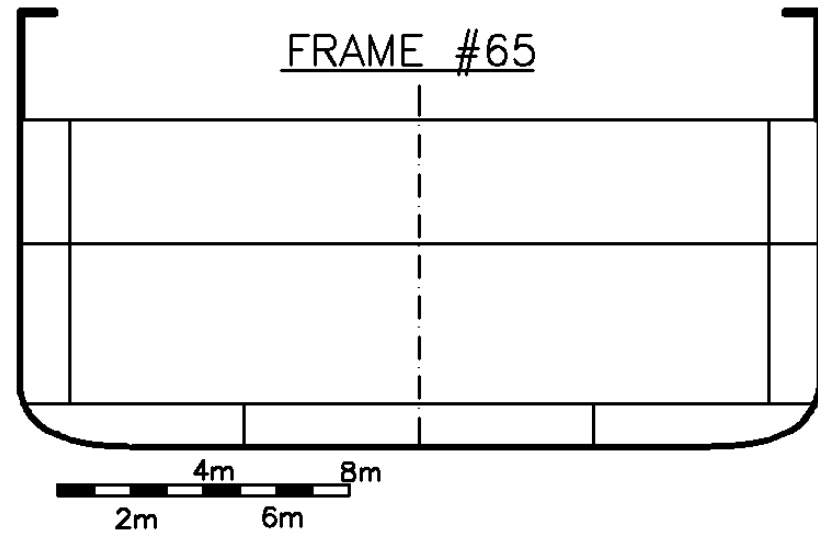
Arrangement C



Arrangement B



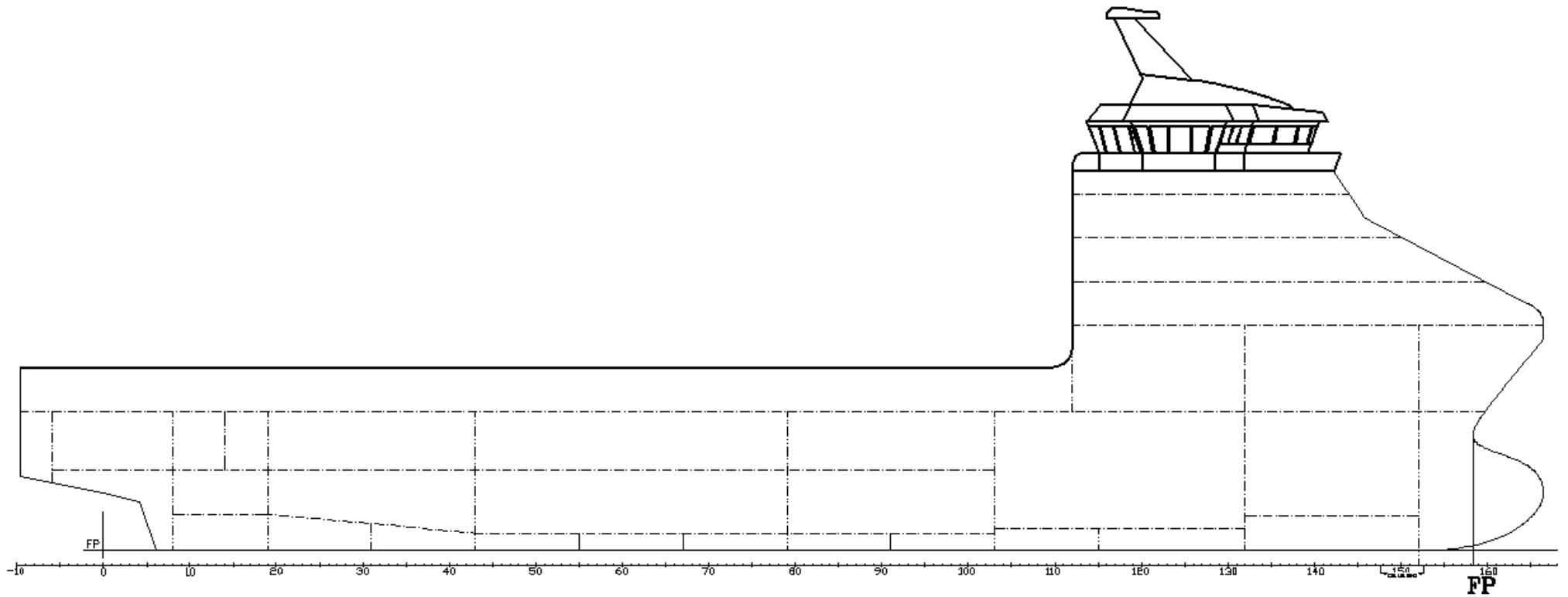
Arrangement C



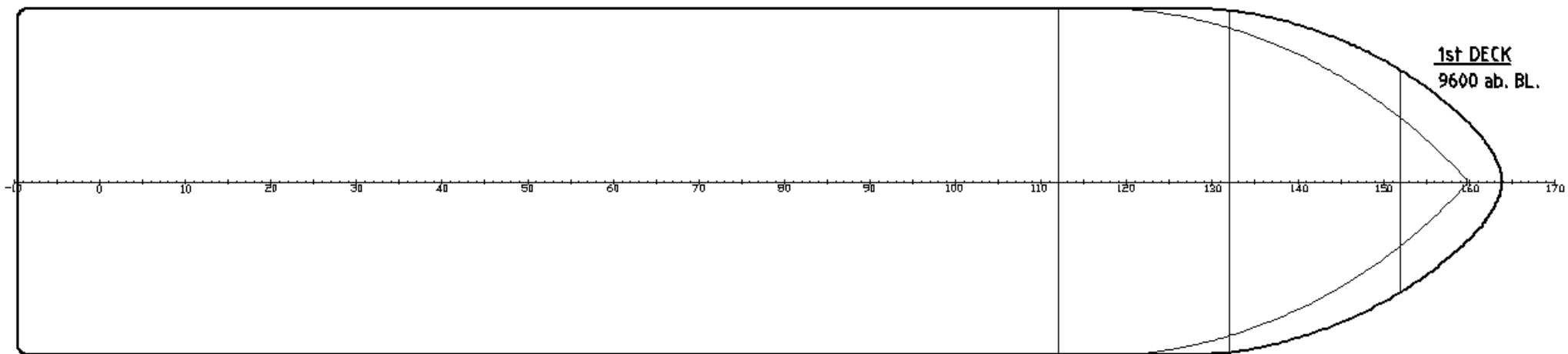
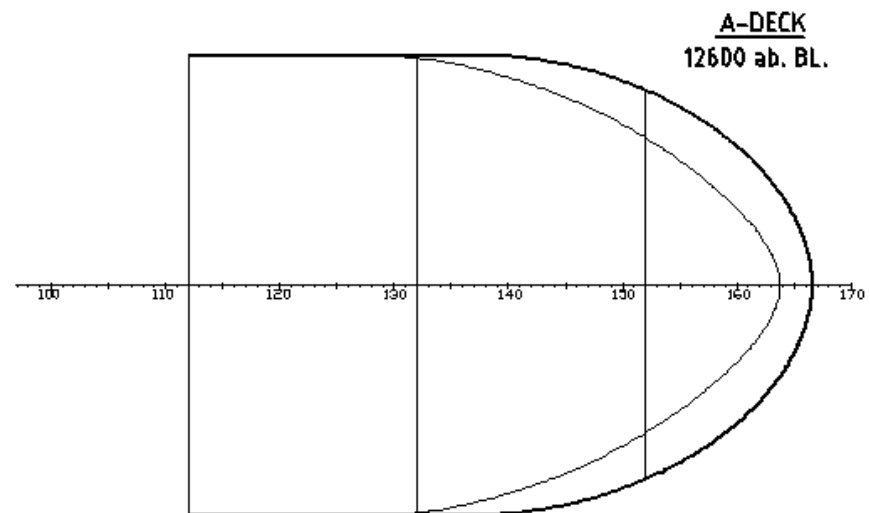
General arrangement Vessel II

Arrangement B/C

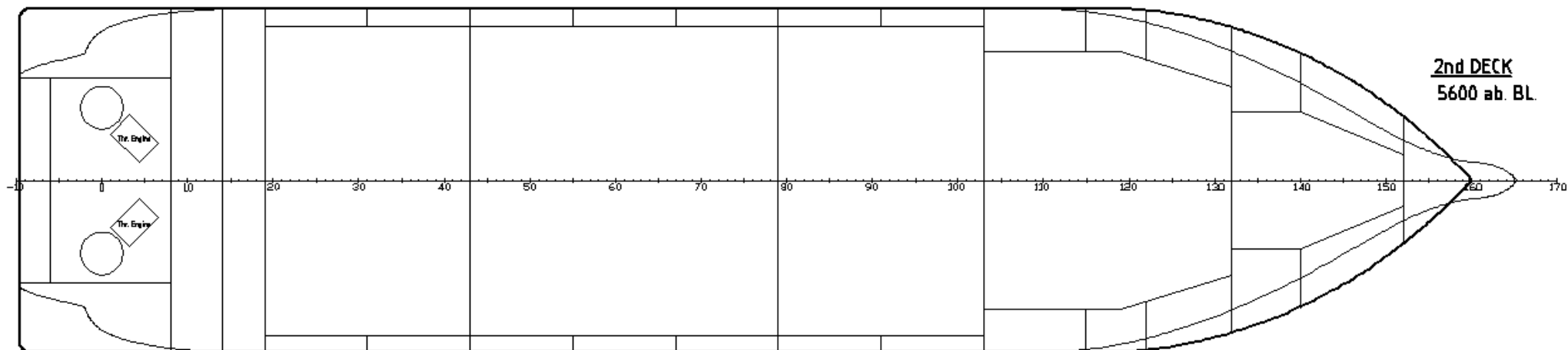
Frame space 600 mm



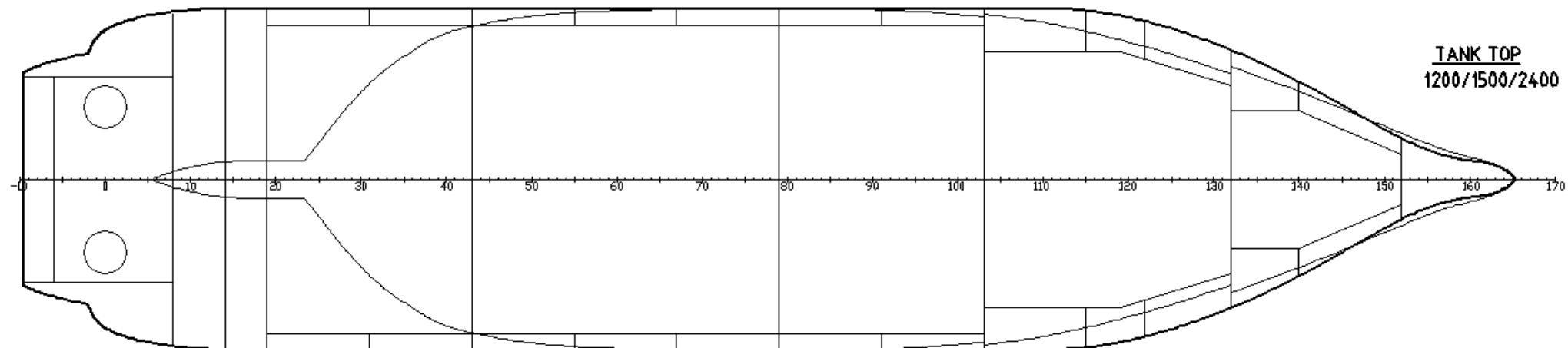
Arrangement B/C



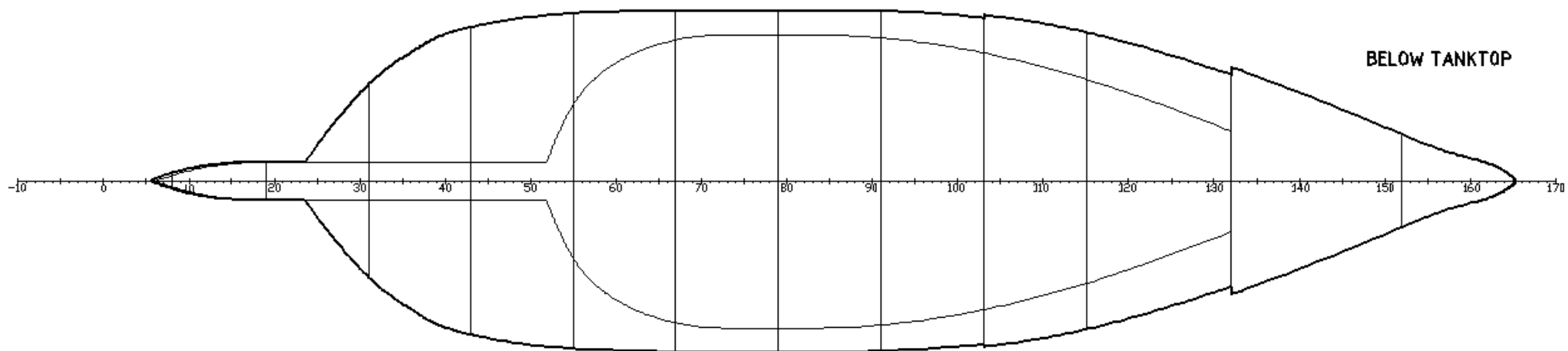
Arrangement B/C



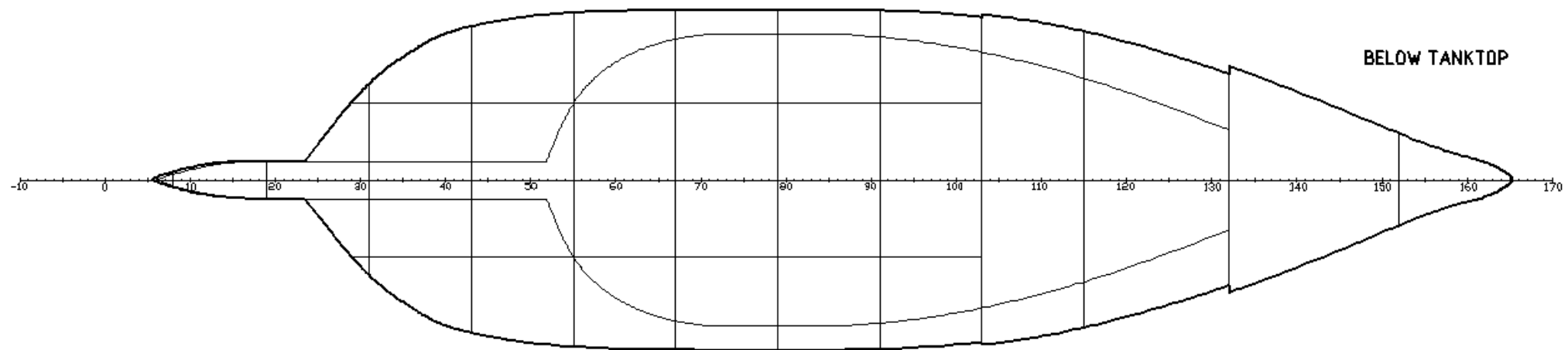
Arrangement B/C



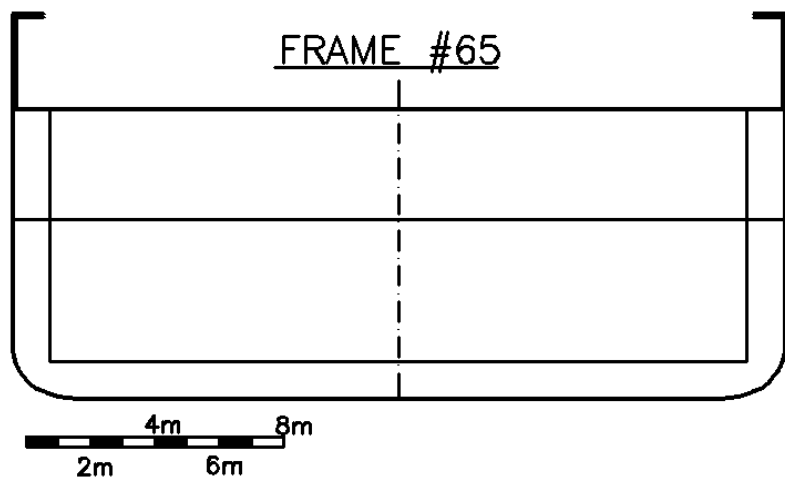
Arrangement B



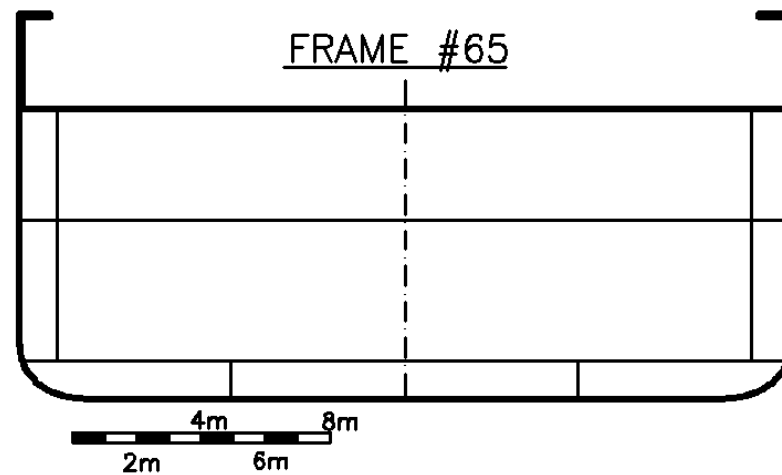
Arrangement C



Arrangement B



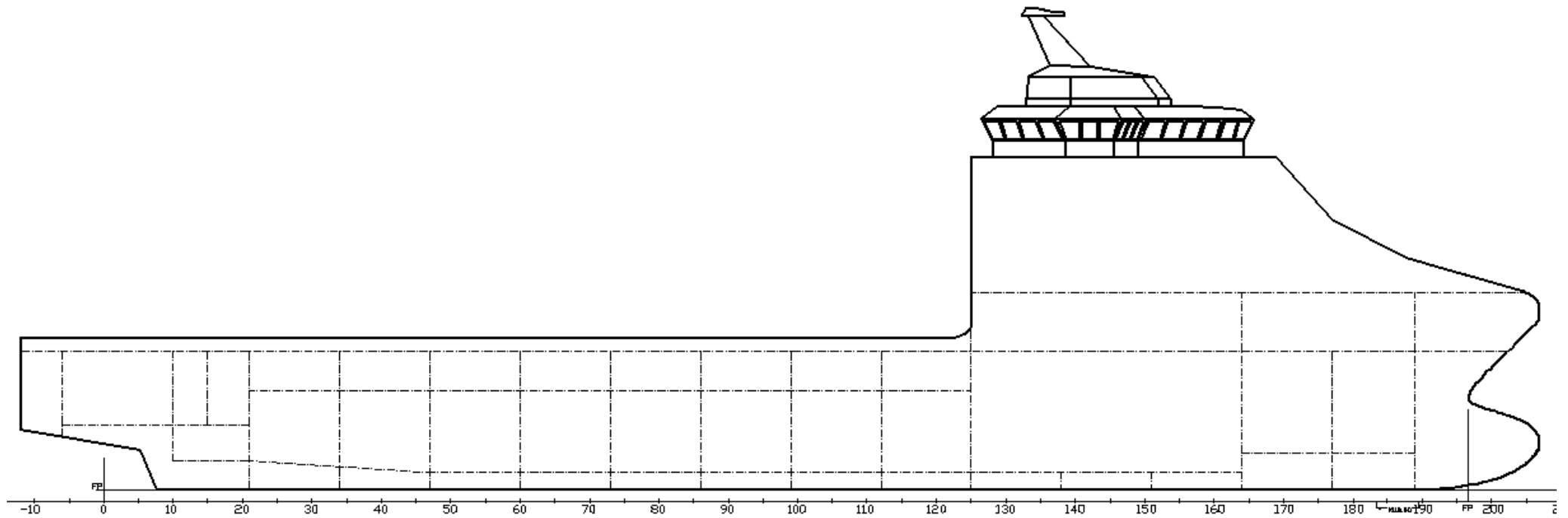
Arrangement C



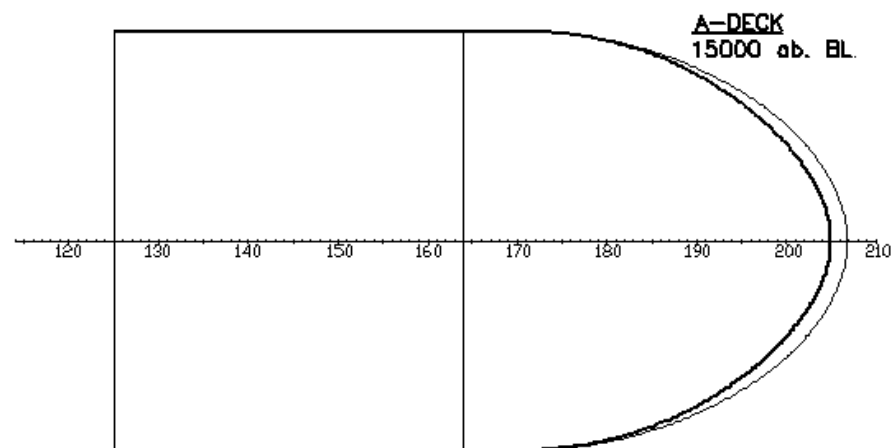
General arrangement Vessel III

Arrangement B/C

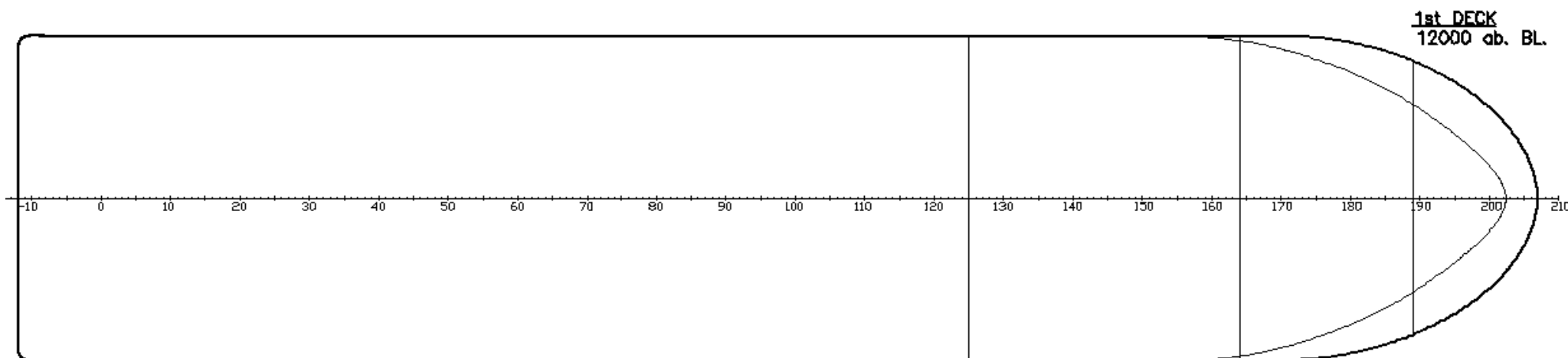
Frame space 600 mm



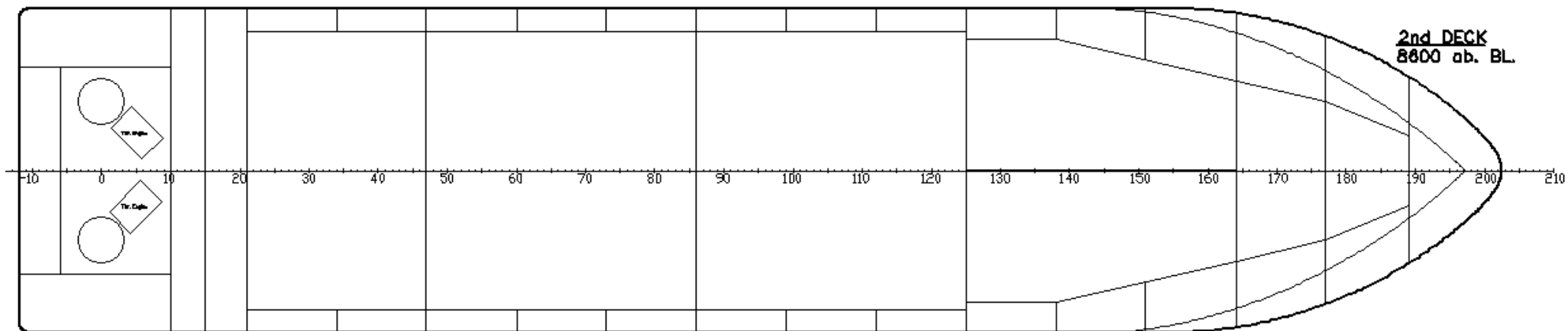
Arrangement B/C



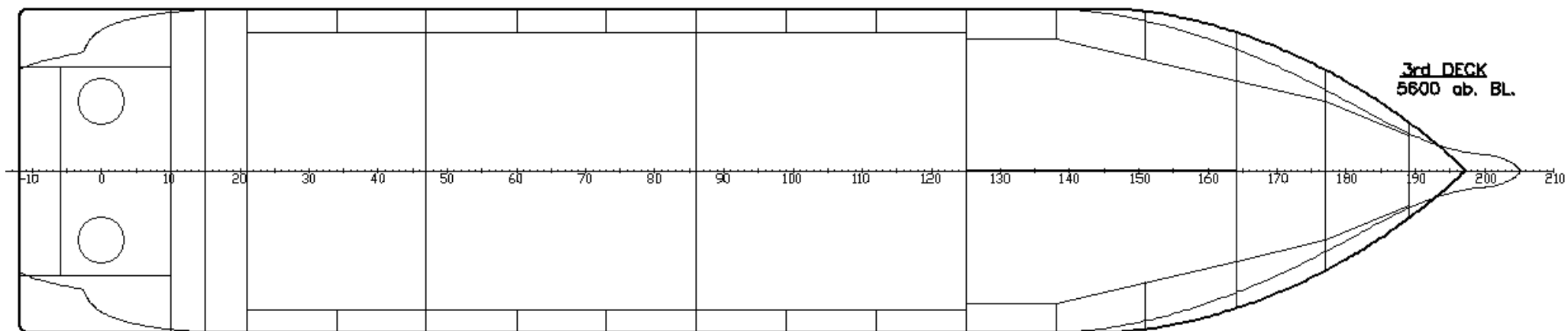
Arrangement B/C



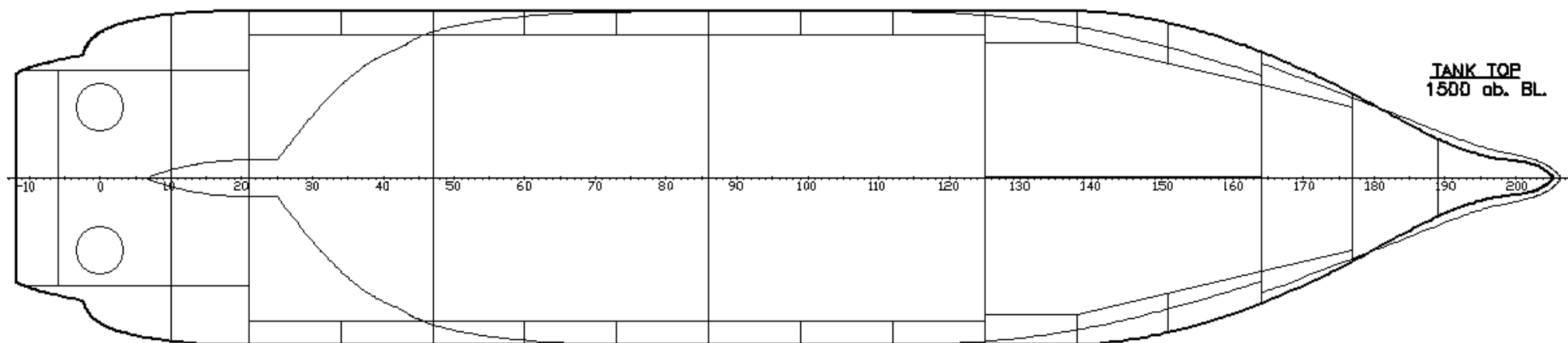
Arrangement B/C



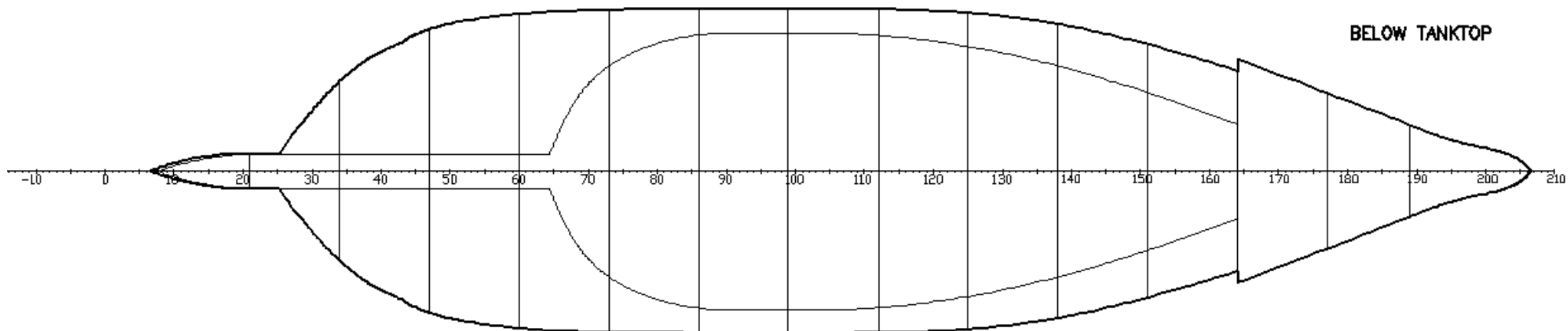
Arrangement B/C



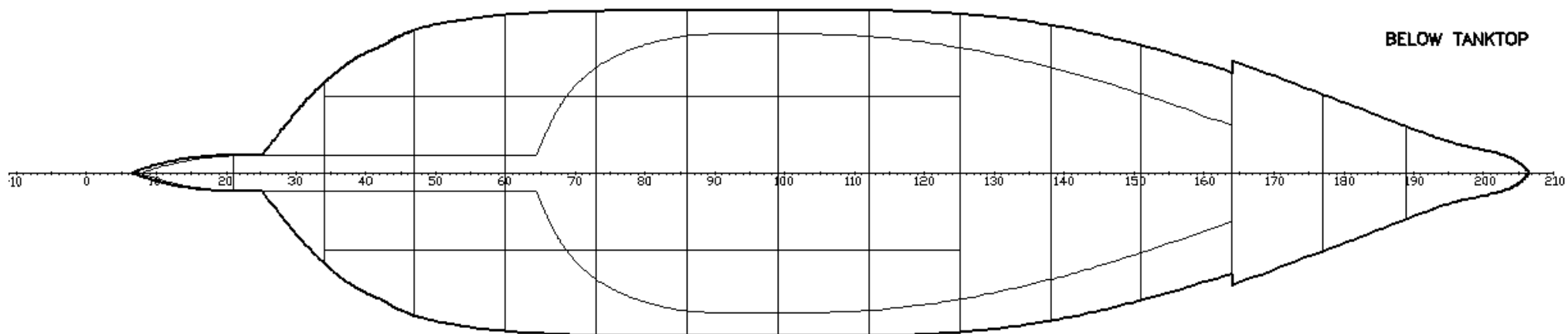
Arrangement B/C



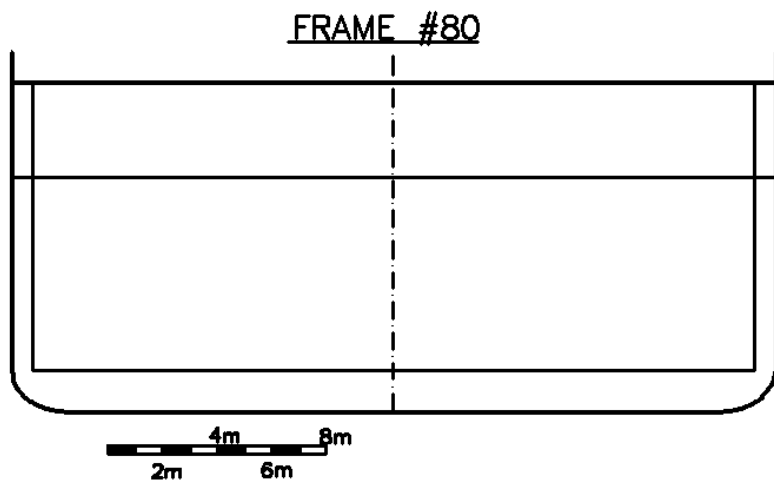
Arrangement B



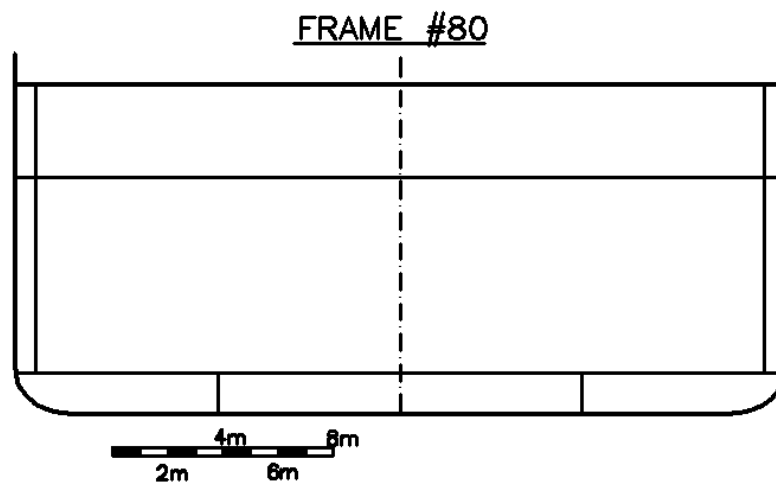
Arrangement C



Arrangement B



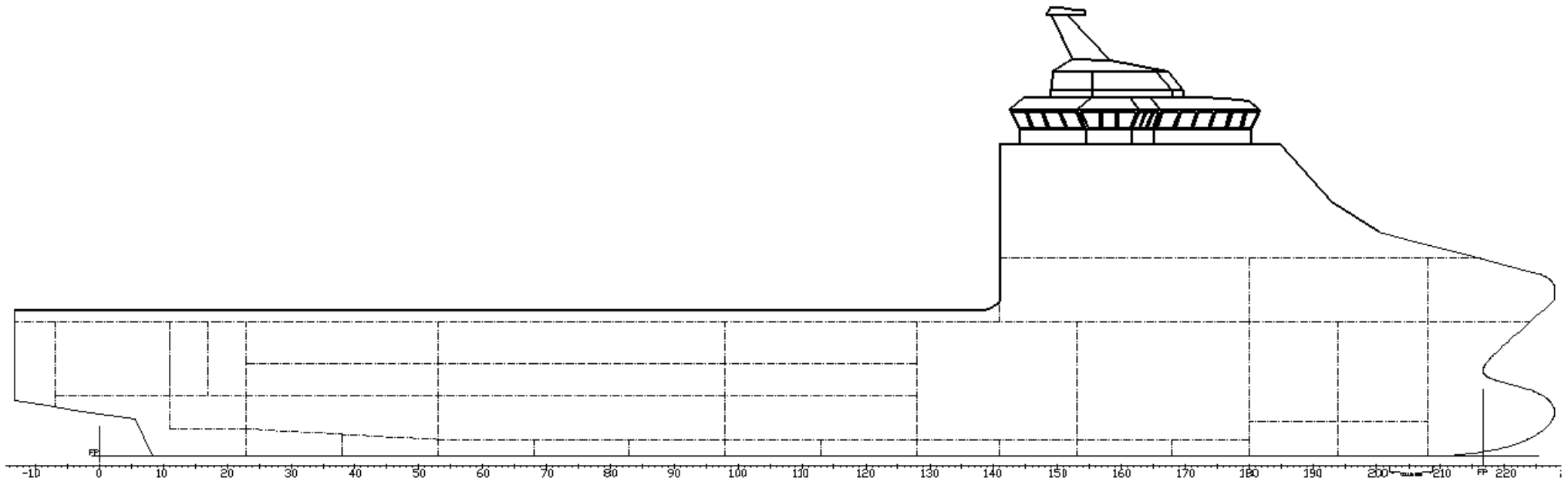
Arrangement C



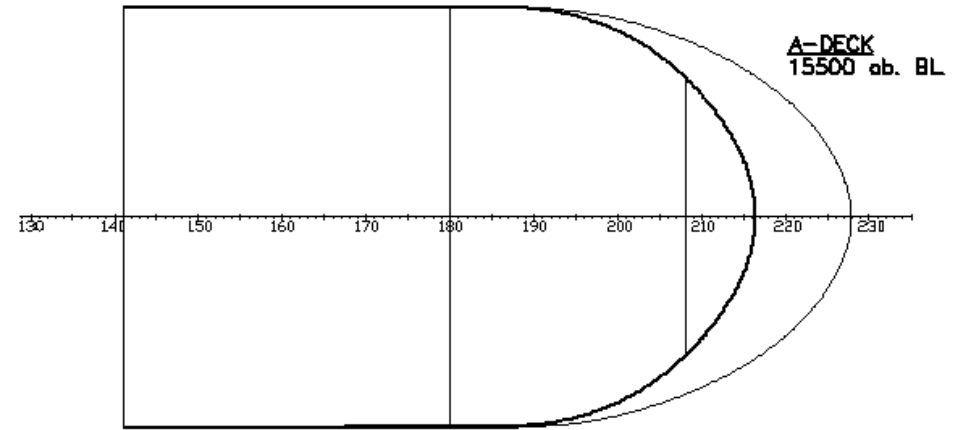
General arrangement Vessel IV

Arrangement B/C

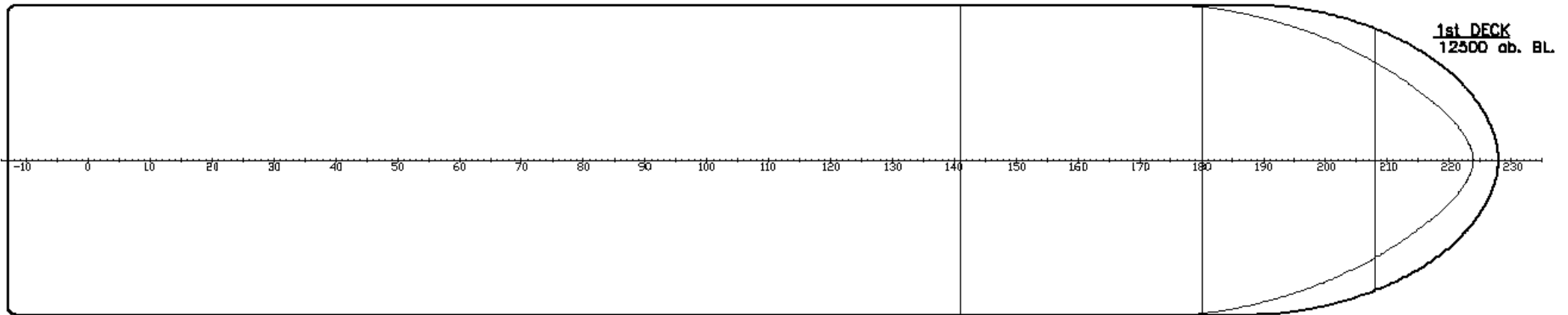
Frame space 600 mm



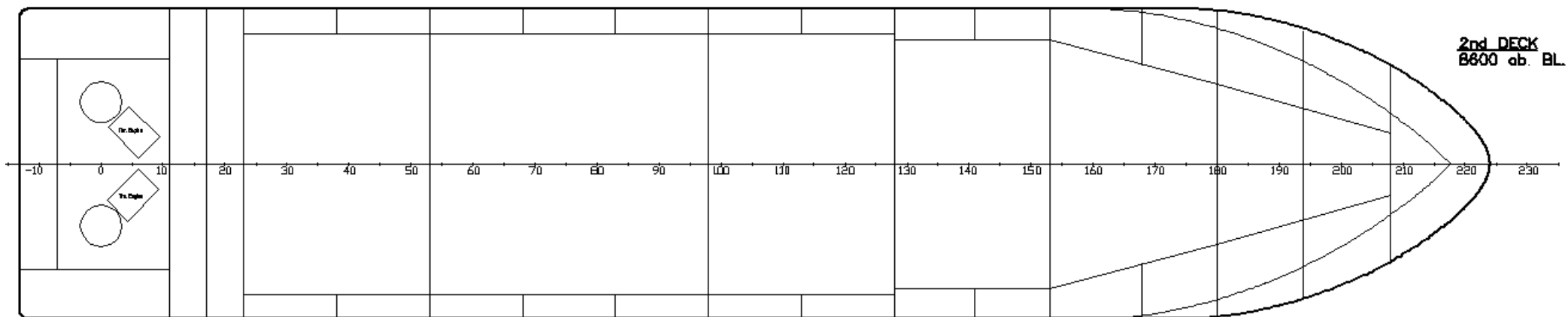
Arrangement B/C



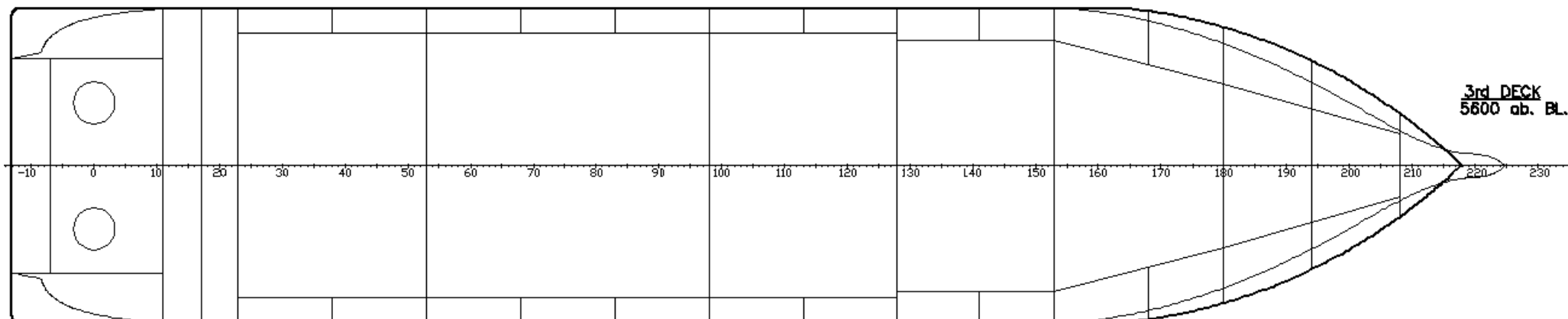
Arrangement B/C



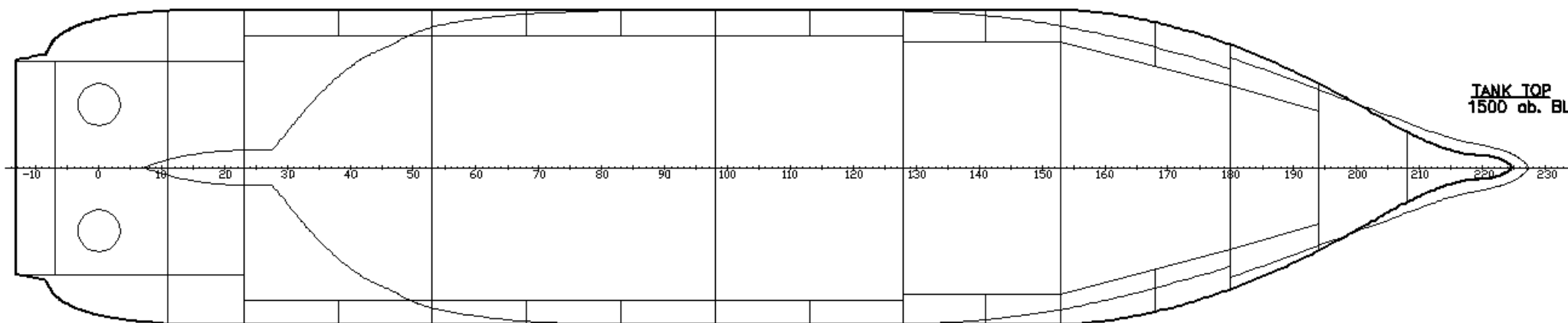
Arrangement B/C



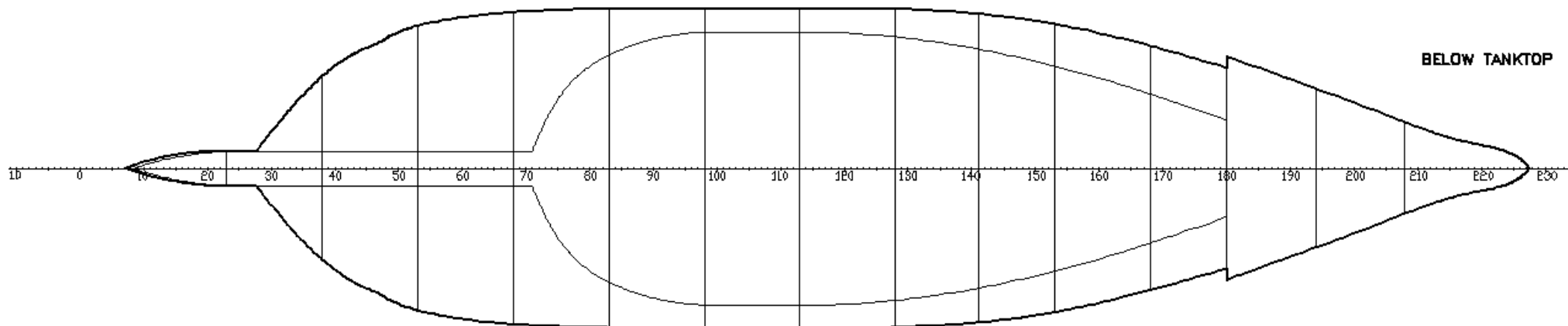
Arrangement B/C



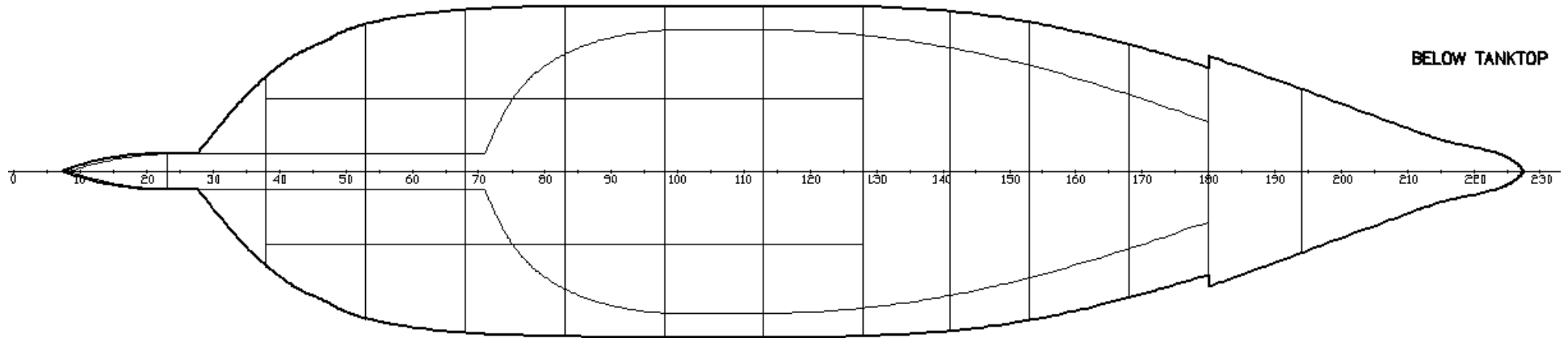
Arrangement B/C



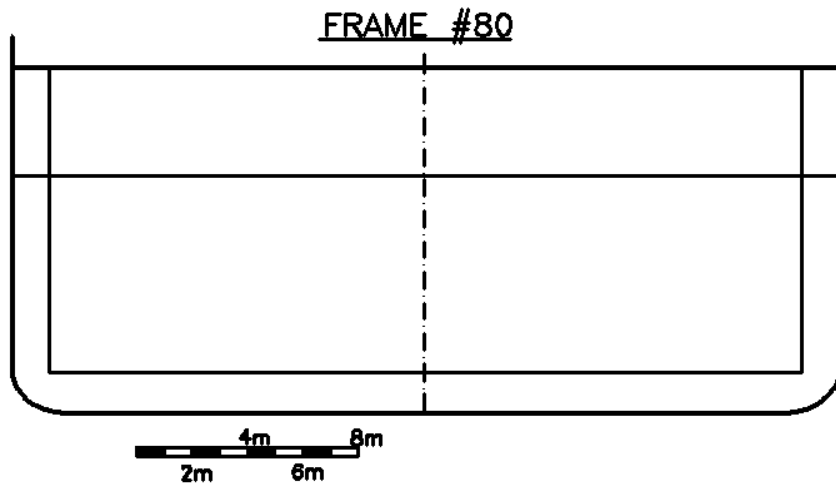
Arrangement B



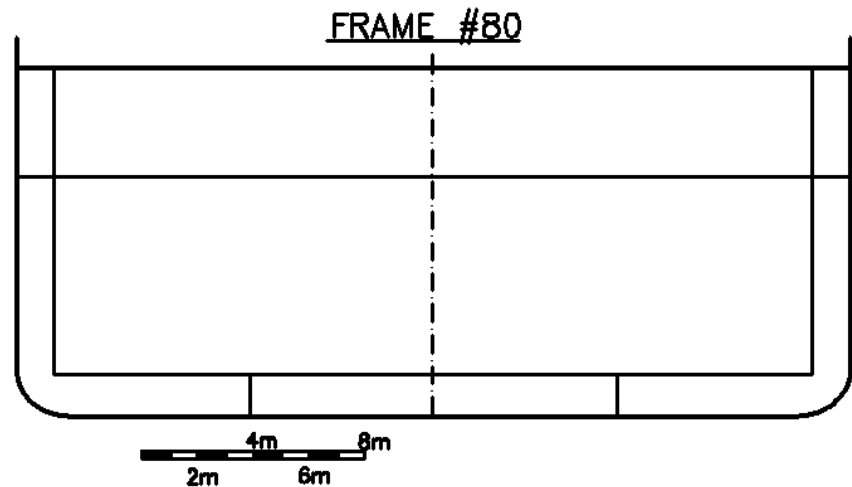
Arrangement C



Arrangement B

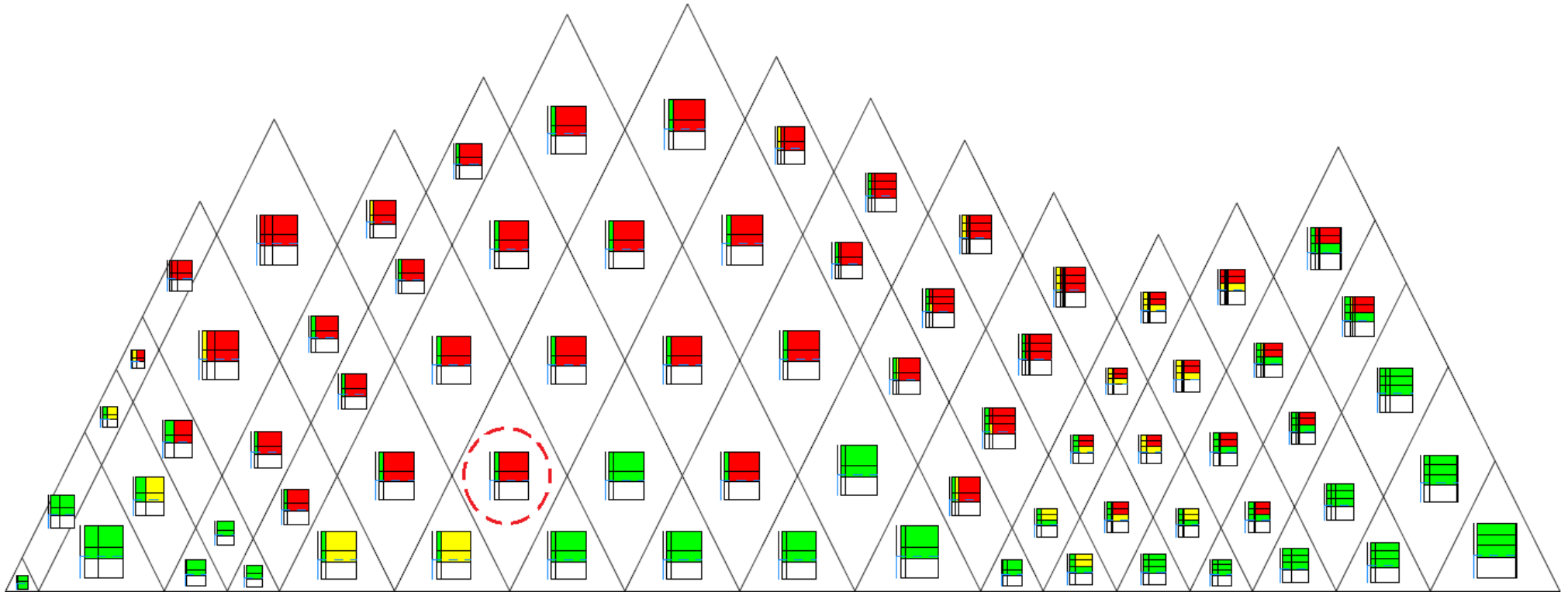


Arrangement C

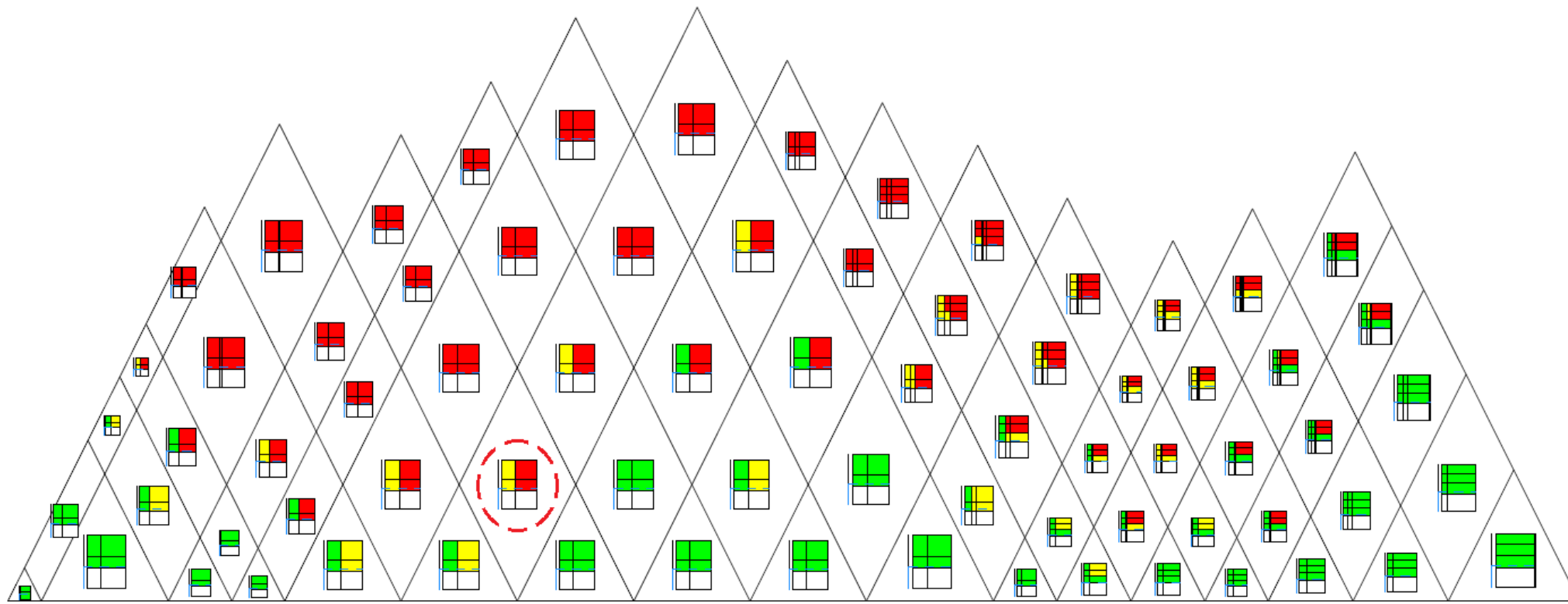


Appendix B

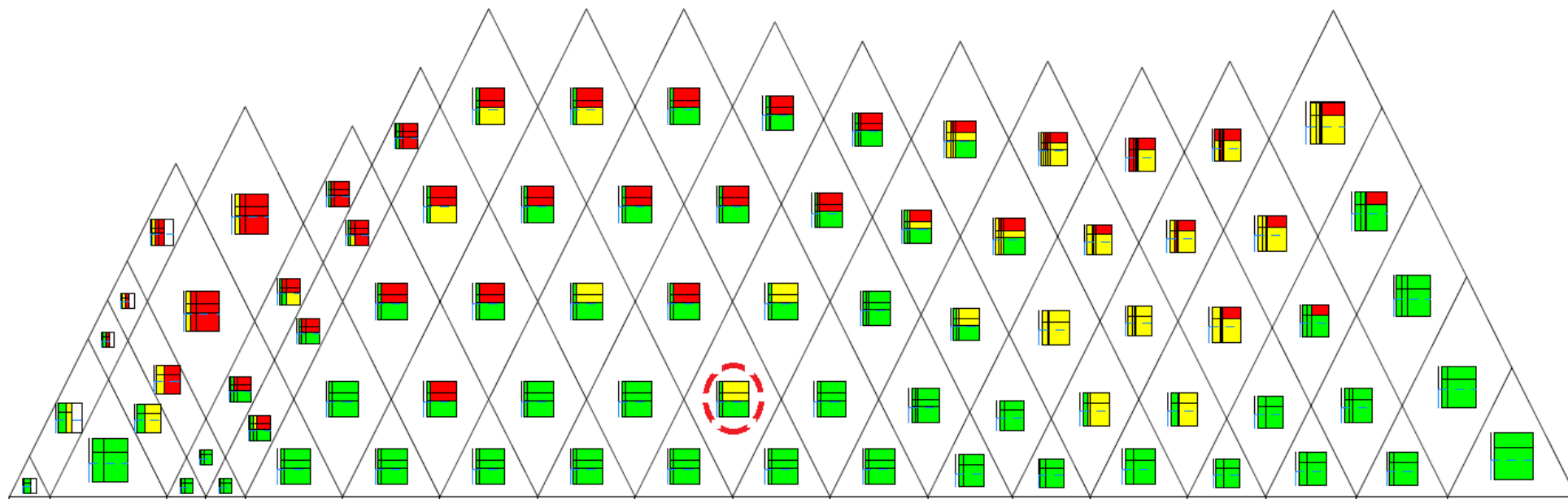
S-factor diagrams



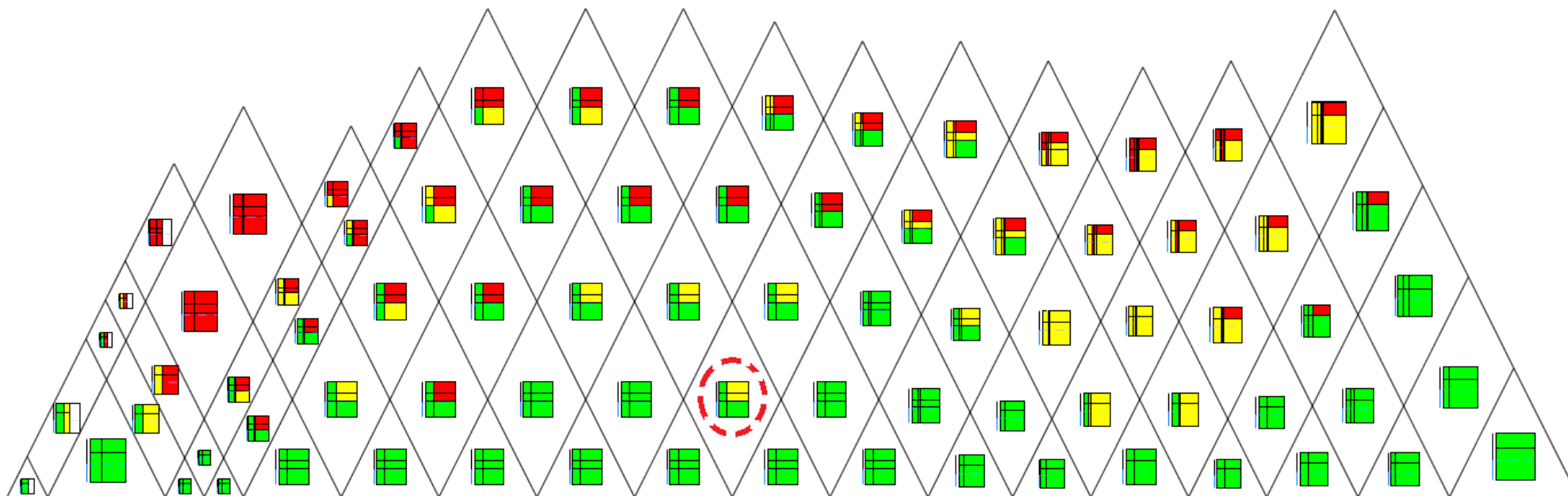
S-factor diagram for Vessel I, arrangement B, D_p , LBH3 at $0.06 \cdot B$ from the hull



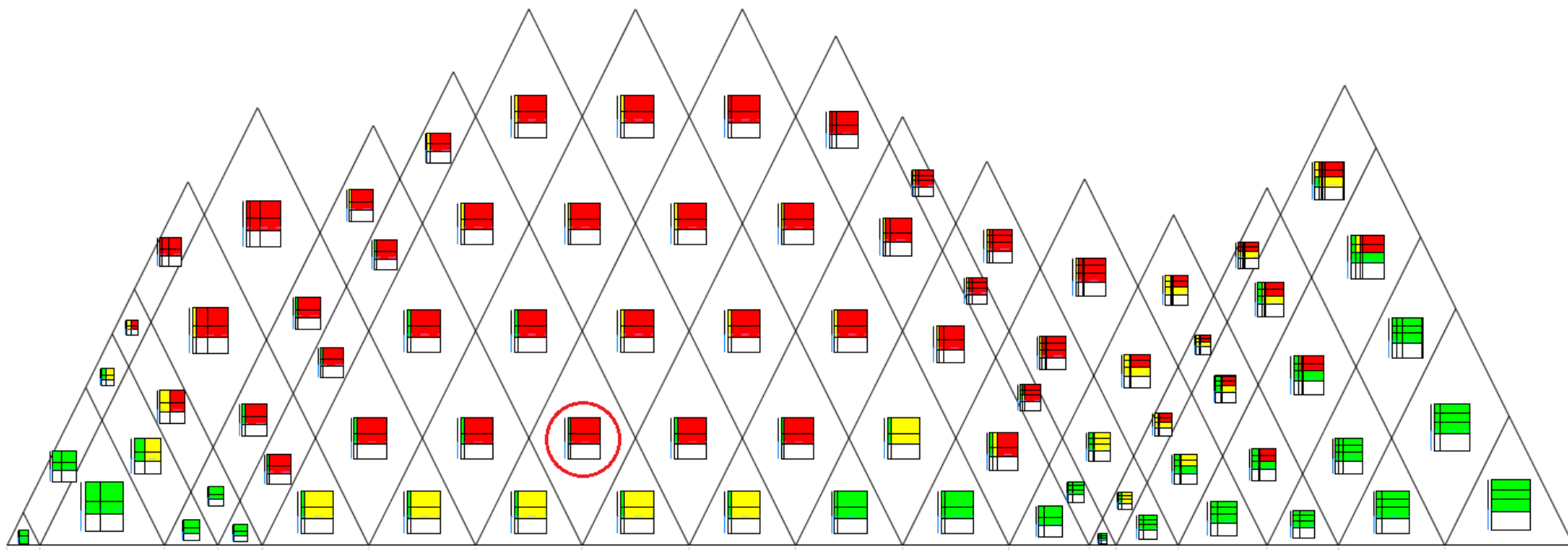
S-factor diagram for Vessel I, arrangement B, D_p , LBH3 at $0.2 \cdot B$ from the hull



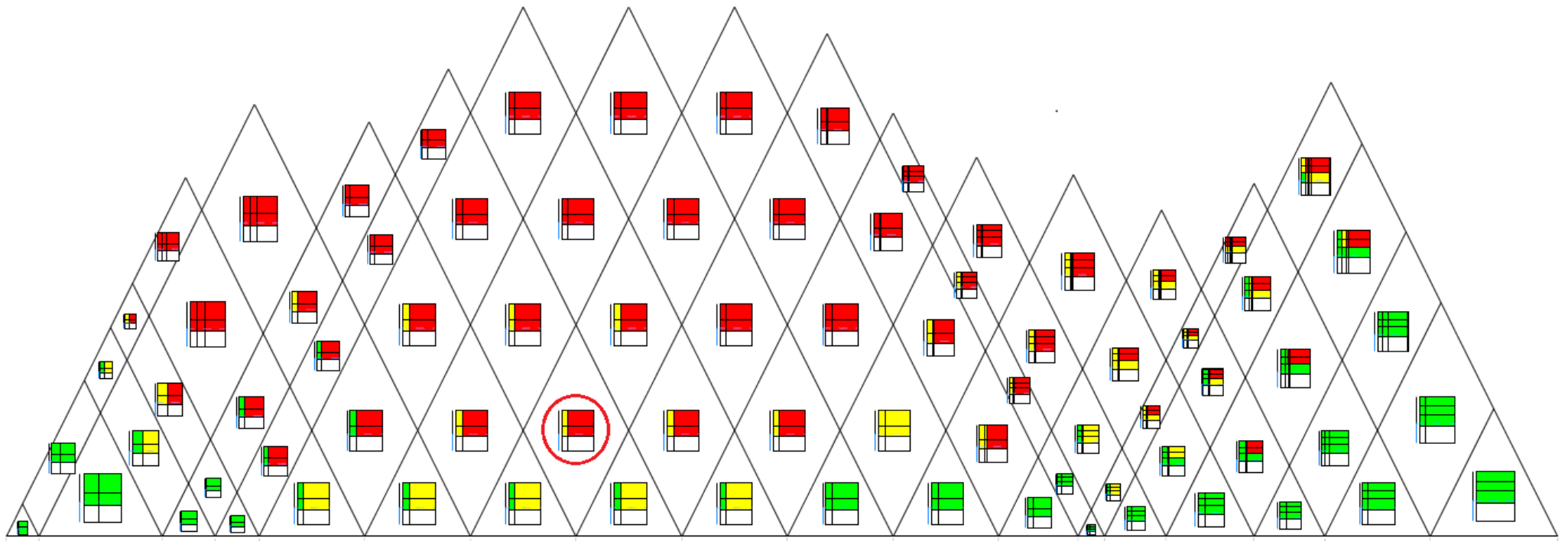
S-fac diagram, Vessel IV, arrangement B, D_p , with LBH3 at $0.06 \cdot B$ m from the hull



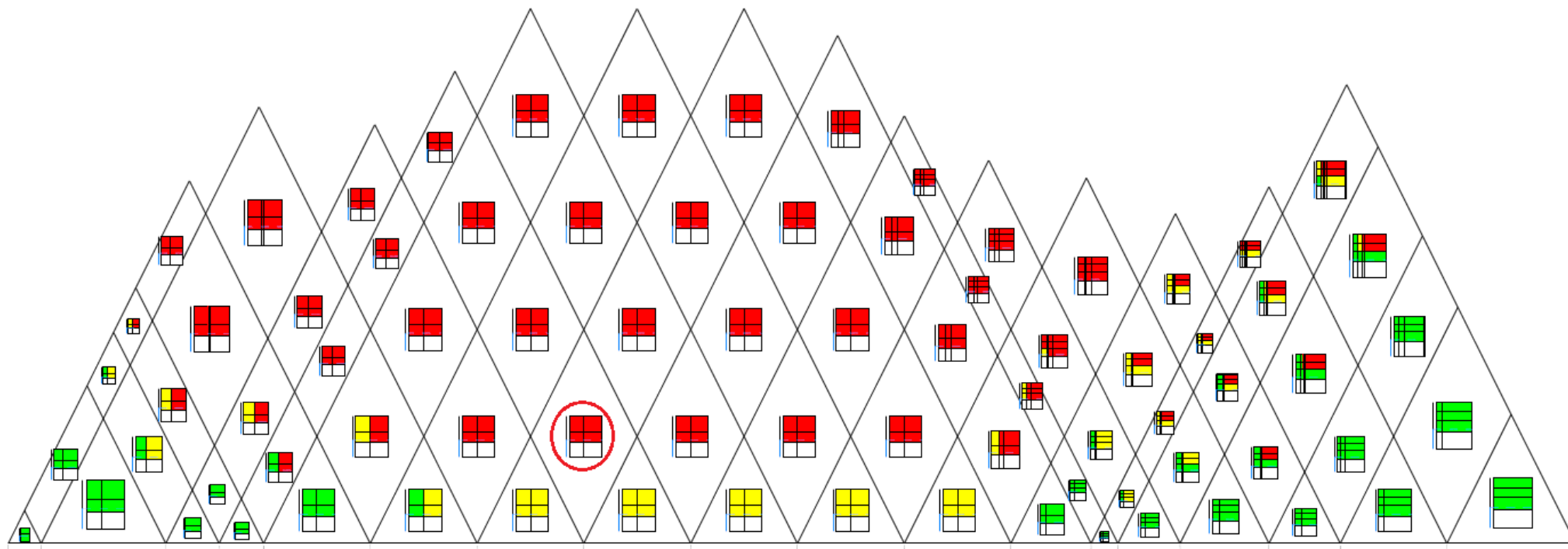
S-factor diagram, Vessel IV, arrangement B, D_p , with LBH3 at $0.14 \cdot B$ m from the hull



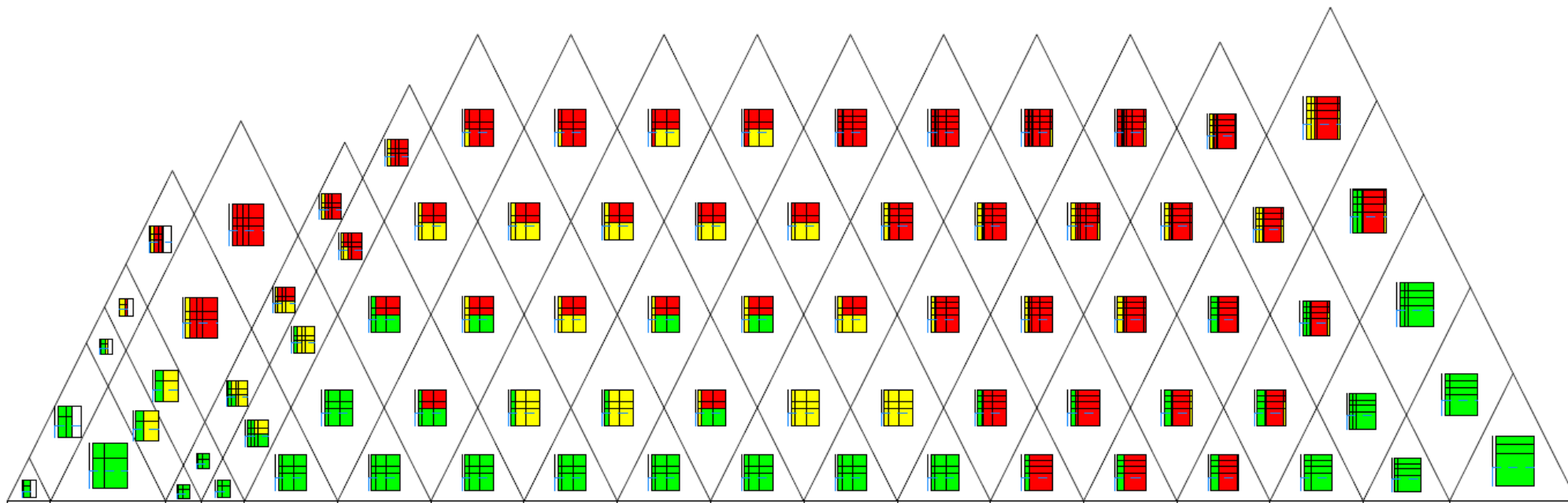
S-factor diagram for Vessel II, D_p, arrangement C, LBH3 at 0.05*B m from the hull



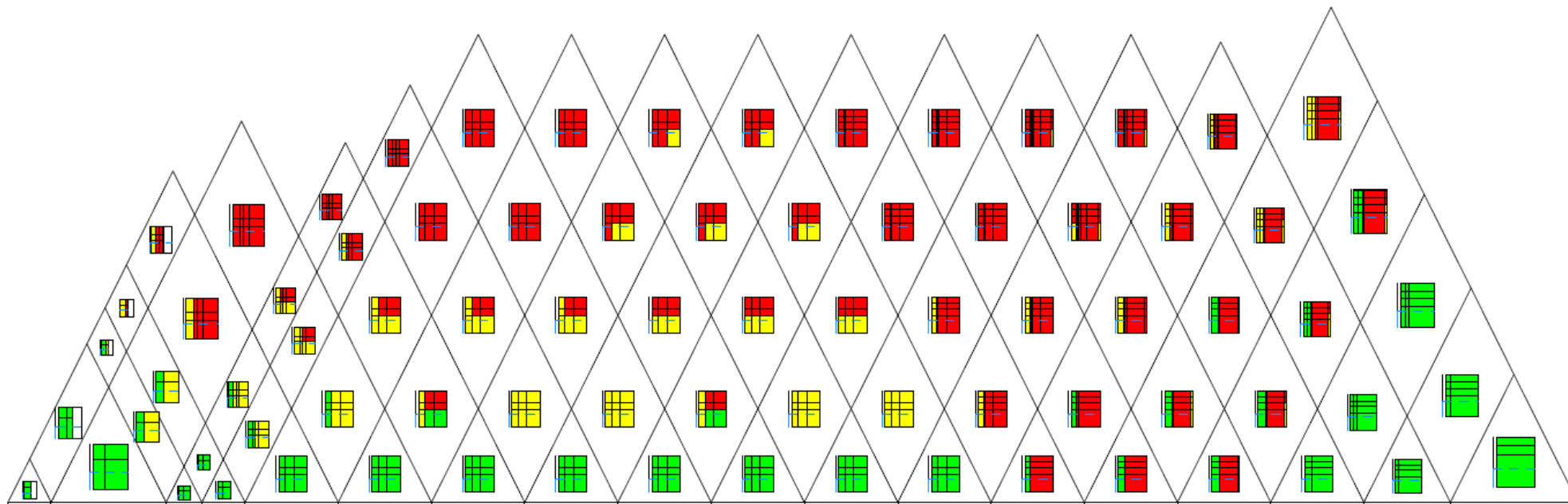
S-factor diagram for Vessel II, D_p , arrangement C, LBH3 at $0.1 \cdot B$ m from the hull



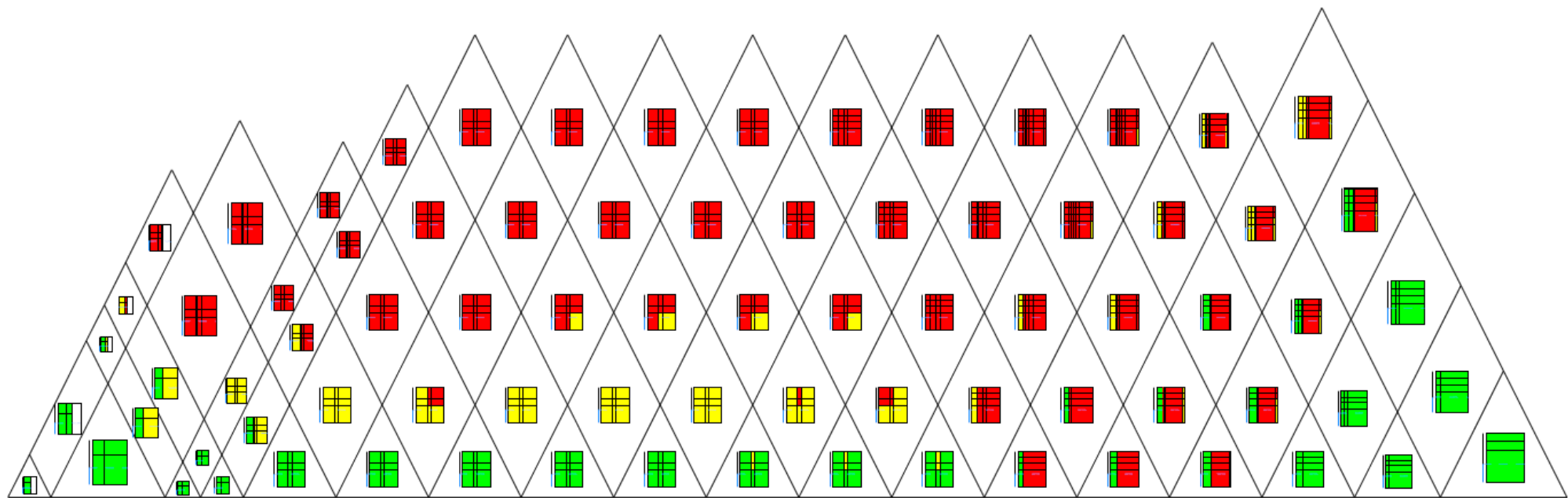
S-factor diagram for Vessel II, D_p , arrangement C, LBH3 at $0.225 \cdot B$ m from the centerline



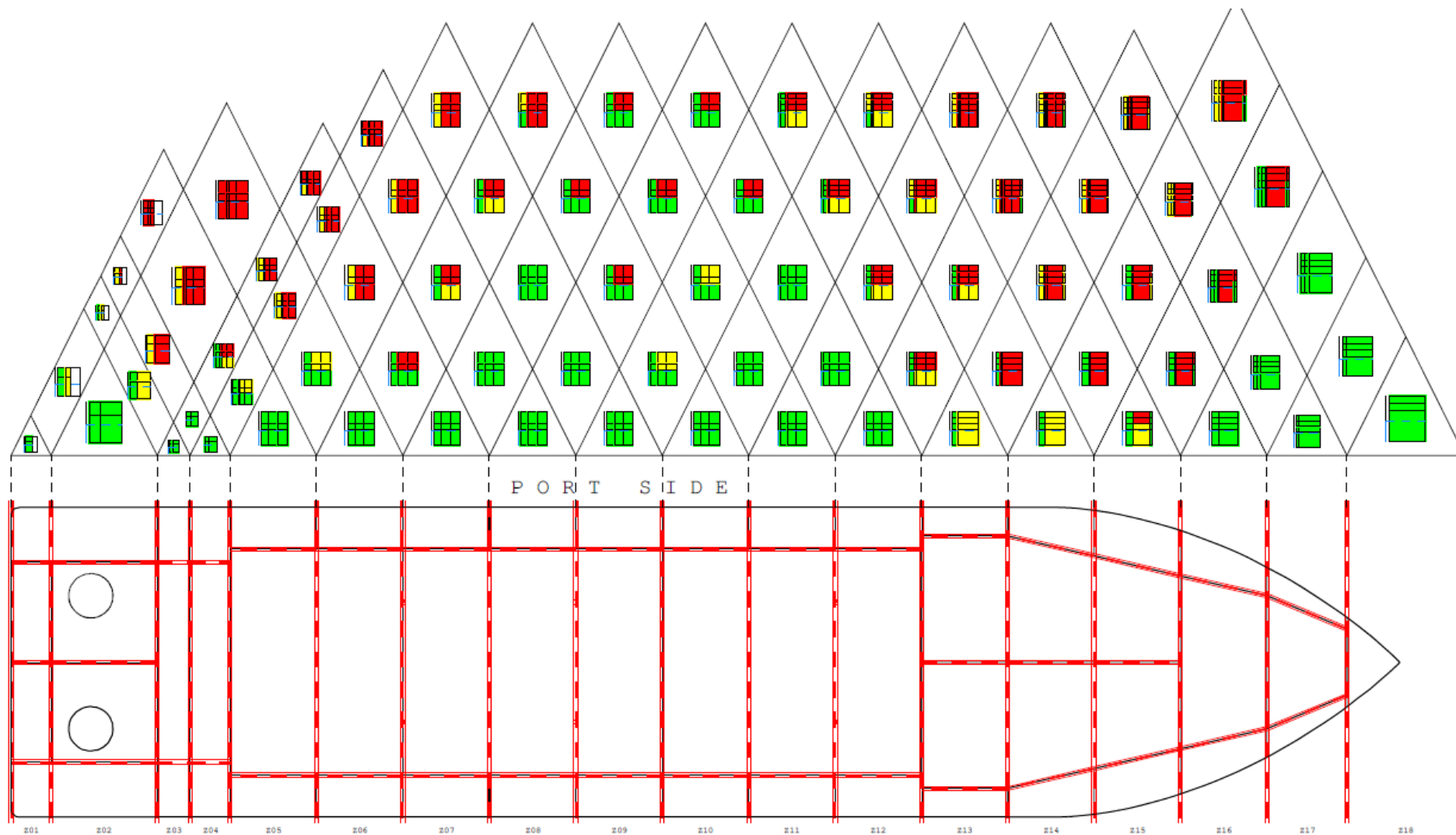
S-factor diagram Vessel III, D₁, arrangement C, LBH3 at 0.07*B m from hull



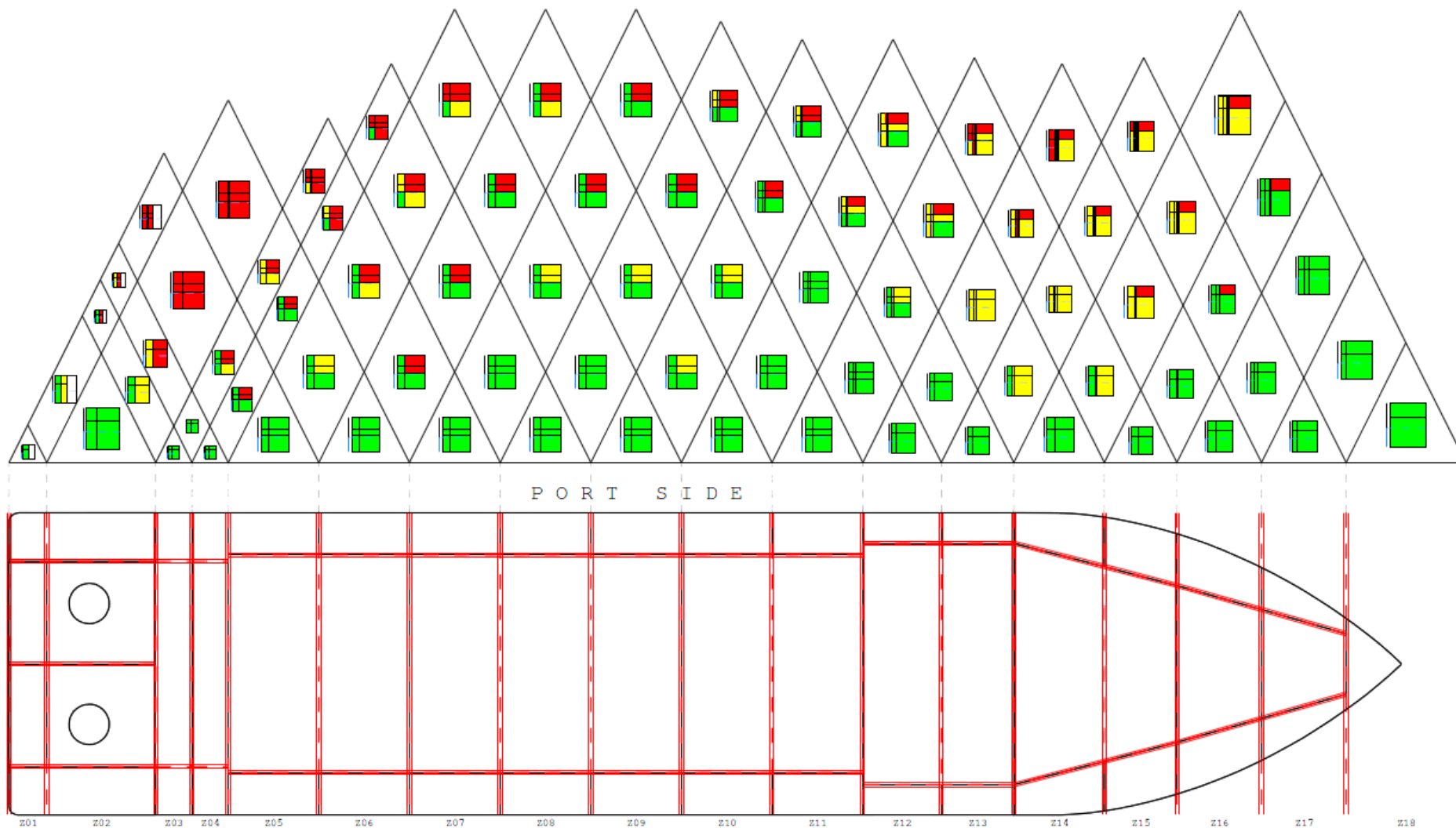
S-factor diagram Vessel III, D₁, arrangement C, LBH3 at 0.11*B m from hull



S-factor diagram Vessel III, D₁, arrangement C, LBH3 at 0.2*B from hull



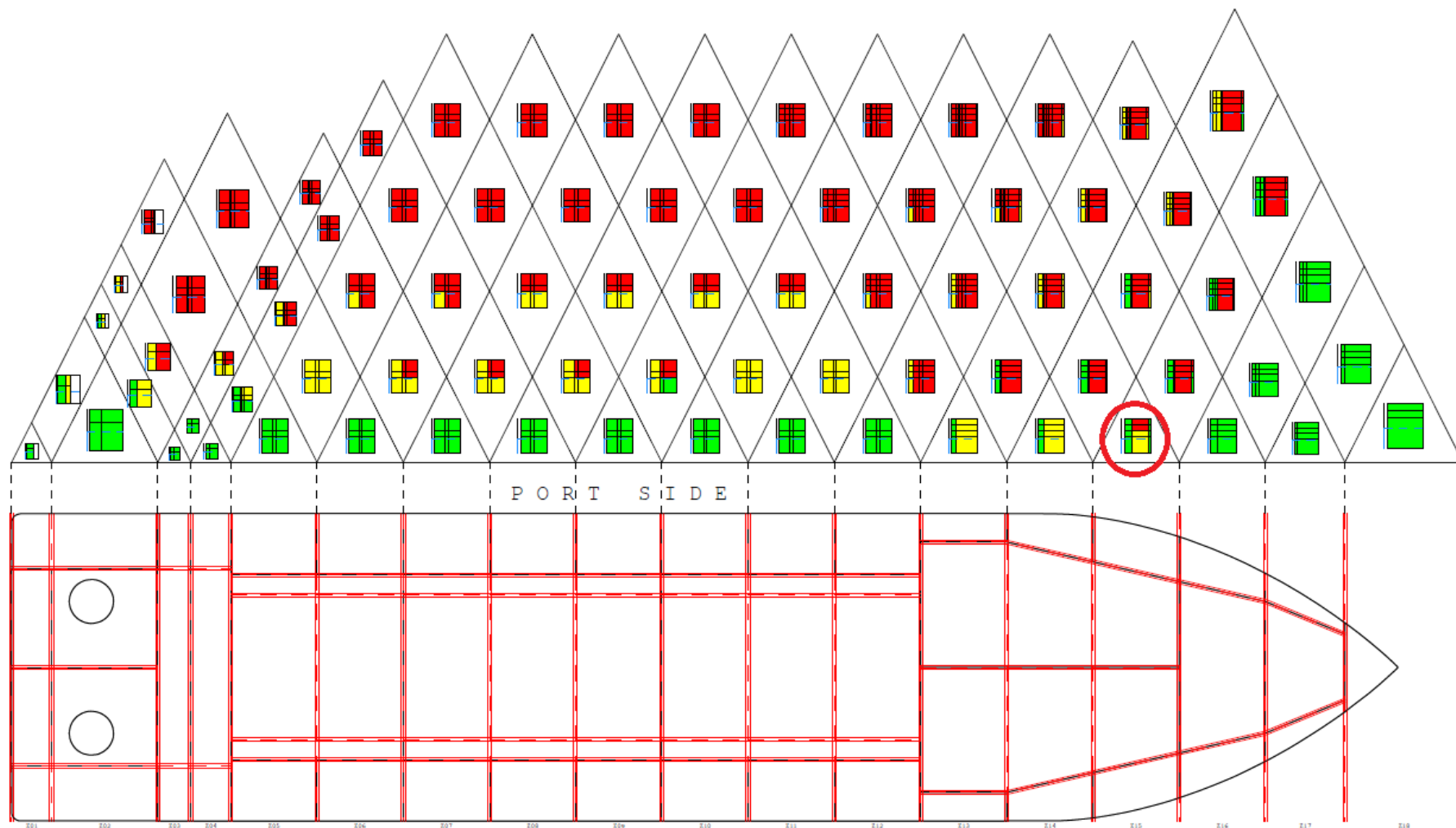
S-factor diagram Vessel III, arrangement B, LBH3 at 0.14*B m from the centerline



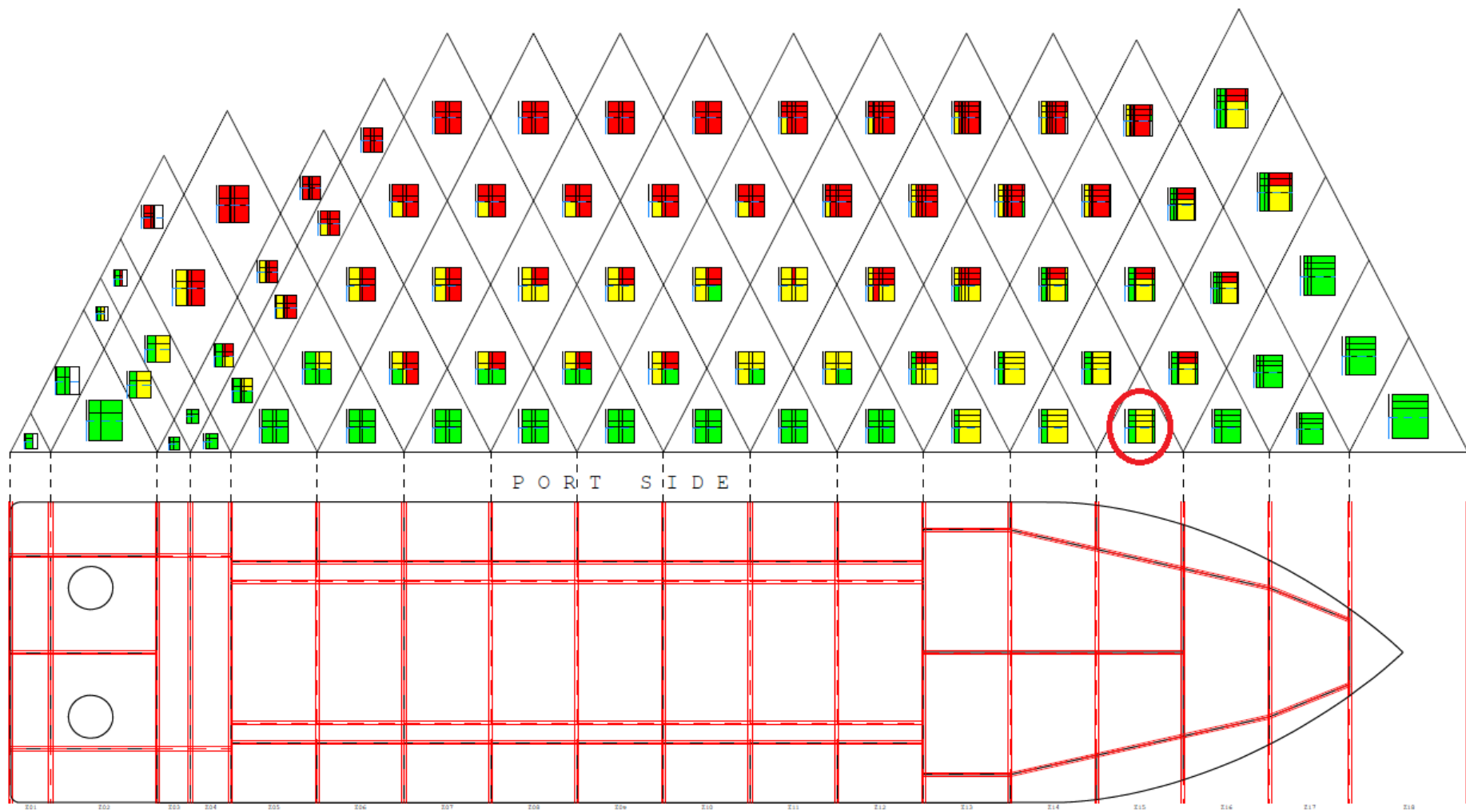
S-factor diagram Vessel IV, arrangement B, LBH3 at $0.14 \cdot B$ m from the centeline



S-factor diagram for D₁ condition Vessel III, arrangement C



S-factor diagram for D_p condition Vessel III, arrangement C



S-factor diagram for D_s condition Vessel III, arrangement C

Appendix C

Electronic files

- Probabilistic damage stability calculations for all vessels with all placements of the LWTB
- Tank plan for the four vessels with the two different arrangement configurations
- AutoCAD drawings of the four vessels

The electronic files can be found by searching for the thesis at: <https://daim.idi.ntnu.no/soek/>